



저작자표시-비영리-변경금지 2.0 대한민국

이용자는 아래의 조건을 따르는 경우에 한하여 자유롭게

- 이 저작물을 복제, 배포, 전송, 전시, 공연 및 방송할 수 있습니다.

다음과 같은 조건을 따라야 합니다:



저작자표시. 귀하는 원저작자를 표시하여야 합니다.



비영리. 귀하는 이 저작물을 영리 목적으로 이용할 수 없습니다.



변경금지. 귀하는 이 저작물을 개작, 변형 또는 가공할 수 없습니다.

- 귀하는, 이 저작물의 재이용이나 배포의 경우, 이 저작물에 적용된 이용허락조건을 명확하게 나타내어야 합니다.
- 저작권자로부터 별도의 허가를 받으면 이러한 조건들은 적용되지 않습니다.

저작권법에 따른 이용자의 권리는 위의 내용에 의하여 영향을 받지 않습니다.

이것은 [이용허락규약\(Legal Code\)](#)을 이해하기 쉽게 요약한 것입니다.

[Disclaimer](#)

藥學博士 學位論文

**Protective effects of 17-oxo-docosahexaenoic acid
and taurine chloramine on experimentally
induced inflammation and carcinogenesis**

실험적으로 유도된 염증 및 암화 모델에서
17-oxo-docosahexaenoic acid 및
taurine chloramine 의 보호 효과 및 기전 연구

2023 年 2 月

서울대학교 大學院

藥學科 醫藥生命科學專攻

金 晟 燾

**Protective effects of 17-oxo-docosahexaenoic acid
and taurine chloramine on experimentally
induced inflammation and carcinogenesis**

실험적으로 유도된 염증 및 암화 모델에서
17-oxo-docosahexaenoic acid 및
taurine chloramine 의 보호 효과 및 기전 연구

指導教授 徐 榮 俊

이 論文을 藥學博士 學位論文으로 提出함
2022 年 11 月

서울大學校 大學院
藥學科 醫藥生命科學專攻
金 晟 燾

金晟燾의 藥學博士 學位論文을 認准함
2022 年 12 月

委員長 이 정 원 (印)

副委員長 Marc Diederich (印)

委 員 서 영 준 (印)

委 員 차 혁 진 (印)

委 員 나 혜 경 (印)

**Protective effects of 17-oxo-docosahexaenoic acid
and taurine chloramine on experimentally
induced inflammation and carcinogenesis**

by

Seong Hoon Kim

A thesis submitted in partial fulfillment of the requirements
for the degree of

DOCTOR OF PHILOSOPHY

(Pharmacy: Pharmaceutical bioscience major)

under the supervision of Professor Young-Joon Surh

at the

College of Pharmacy,
Seoul National University

February 2023

ABSTRACT

Protective effects of 17-oxo-docosahexaenoic acid and taurine chloramine on experimentally induced inflammation and carcinogenesis

SEONG HOON KIM

**Under the supervision of Professor Young-Joon Surh
at the College of Pharmacy, Seoul National University**

Taurine protects tissues from oxidative damage and inflammation through up-regulation of anti-oxidant and anti-inflammatory gene expression and accelerates the biological and structural repair of damaged tissues. During the oxidative burst, hydrogen peroxide (H_2O_2) is produced, which is converted to highly reactive hypochlorous acid (HOCl) by the myeloperoxidase activity of the activated neutrophils in the presence of chloride ion. HOCl has bactericidal activity, but at the site of acute inflammation, but it can also be detrimental to host. At the inflamed site, taurine reacts with residual HOCl, resulting in the formation of taurine chloramine (TauCl). From previous studies, TauCl is known to inhibit the production of pro-inflammatory

mediators of tissue damage, such as chemokines and cytokines in various cells and tissues.

In this study, I investigated the protective effect of TauCl against colitis caused by 2,4,6-trinitrobenzene sulfonic acid (TNBS). TauCl administration attenuated oxidative stress as assessed by 4-hydroxy-2-nonenal (4-HNE) production and expression/production of pro-inflammatory factors such as tumor necrosis factor- α , interleukin- 6, and cyclooxygenase-2 (COX-2). TauCl also inhibited the activation of two key transcription factors, NF κ B and STAT3 mediating pro-inflammatory signaling. Specifically, the protective effects of TauCl against oxidative stress and inflammation in the colon of TNBS-treated mice were associated with increased activation of Nrf2 and upregulation of its target genes and proteins.

To further elucidate the protective role of TauCl under inflammatory conditions, an experimentally induced murine dermatitis model was employed. Excessive exposure to solar radiation, especially ultraviolet rays, causes extensive photodamage, a major cause of dermatitis and skin cancer. Upon irradiation of ultraviolet B (UVB) at an intensity of 180 mJ/cm² induced oxidative damage and cell death in the epidermis of mice. These symptoms were alleviated through the topical application of TauCl. In addition, the UVB-induced expression of pro-inflammatory cytokines was lower in the skin of TauCl treated mice than that of the vehicle-treated control group.

The anti-inflammatory effects of TauCl are related to the inhibition of STAT3 signaling with concomitant activation of Nrf2 and induction of

antioxidant enzymes such as heme oxygenase-1 and NAD(P)H:quinone oxidoreductase 1. Taken together, these results suggest that TauCl exerts protective effects against colitis and dermatitis through the upregulation of Nrf2-dependent cytoprotective gene expression while downregulation of proinflammatory signaling mediated by NFκB and STAT3.

Docosahexaenoic acid (DHA) is one of the prototype omega-3 (ω -3) polyunsaturated fatty acids and has been reported to inhibit inflammatory and carcinogenic processes. 17-Oxo-DHA is an electrophilic fatty acid metabolite, produced from DHA via a series of steps involving COX-2 and dehydrogenase in activated macrophages. 17-Oxo-DHA was found to play an important role in UVB-induced dermatitis and photocarcinogenesis. In the present study, it was confirmed that UVB-induced phosphorylation of Tyr705, which is essential for the activation of STAT3, was inhibited by topically applied 17-oxo-DHA in mouse skin *in vivo*. Topical application of 17-oxo-DHA reduced the expression of oxidative stress markers in UVB-irradiated mouse skin. These protective effects were associated with the inhibition of inflammatory cytokines and acceleration of the resolution of inflammation through activation of Nrf2 and concurrent upregulation of anti-inflammatory and antioxidant proteins.

Macrophages play an essential role in the resolution of inflammation by exerting the phagocytic activity. Treatment with 17-oxo-DHA enhanced the engulfment of dead epidermal cells by macrophages. These effects were attributable to increased expression of the scavenger receptor, CD36 induced

by Nrf2. In conclusion, 17-oxo-DHA inhibits oxidative stress and inflammation as well as enhances the efferocytosis activity of macrophages to accelerate the resolution phase. These effects were associated with elevated expression of antioxidant and anti-inflammatory/proresolving proteins via the activation of the Nrf2 signal pathway. Thus, 17-oxo-DHA is an endogenous molecule with the potential as a therapeutic agent to alleviate inflammatory symptoms.

Keywords

Taurine Chloramine (TauCl); 17-Oxo-docosahexaenoic acid (17-oxo-DHA); Nuclear factor erythroid 2-related factor 2 (Nrf2); Signal transducer and activator of transcription 3 (STAT3); Efferocytosis

Student Number: 2016-21798

TABLE OF CONTENTS

Abstract	i
Table of Contents	v
List of Figures	viii
List of Tables	xii
List of Abbreviations	xiii

Chapter I

Taurine Chloramine and 17-Oxo-Docosahexaenoic Acid as Novel Endogenous Proresolving and Anti-inflammatory Substances with Chemopreventive Potential	1
1. Introduction	2
2. NF- κ B and STAT3 as two representative proinflammatory signaling molecules	4
3. Taurine chloramine	6
4. 17-Oxo-docosahexaenoic acid (17-Oxo-DHA)	8
5. Regulation of the Nrf2 signaling pathway by taurine chloramine and 17-oxo-DHA.....	9
6. References	14
Statement of Purpose	21

Chapter II

Protective Effects of Taurine Chloramine on Experimentally

Induced Colitis: NFκB, STAT3, and Nrf2 as Potential Targets 22

1. Abstract -----	23
2. Introduction -----	25
3. Materials and Methods -----	28
4. Results -----	36
5. Discussion -----	52
6. References -----	56

Chapter III

Topically Applied Taurine Chloramine Protects Against UVB-

induced Oxidative Stress and Inflammation in Mouse Skin - 60

1. Abstract -----	61
2. Introduction -----	63
3. Materials and Methods -----	65
4. Results -----	73
5. Discussion -----	86
6. References -----	90

Chapter IV

Protective Effects of an Electrophilic Metabolite of

Docosahexaenoic Acid on UVB-induced Oxidative Cell Death,

Dermatitis, and Carcinogenesis ----- 99

1. Abstract ----- 100

2. Introduction ----- 102

3. Materials and Methods ----- 105

4. Results ----- 117

5. Discussion ----- 152

6. References ----- 157

Conclusion ----- 166

Abstract in Korean ----- 167

LIST OF FIGURES

Chapter I

- Fig. 1-1. Differences between acute and chronic inflammation. -----10
- Fig. 1-2. NF- κ B signaling: Canonical and noncanonical pathways. -----11

Chapter II

- Fig. 2-1. Effects of TauCl on inflammatory damage in the colon of TNBS-treated mice. -----39
- Fig. 2-2. Attenuation of TNBS-induced colonic cell death, MPO activity, and oxidative damage by administration of TauCl. -----40
- Fig. 2-3. Effects of TauCl administration on expression of proinflammatory cytokines and COX-2 in mouse colonic mucosa. -----42
- Fig. 2-4. Inhibitory effects of TauCl on TNBS-induced p65 phosphorylation and nuclear localization of NF κ B. -----44
- Fig. 2-5. Inhibitory effects of TauCl on phosphorylation of STAT3 and its target protein expression in the colonic tissue of TNBS-treated mice. -----46
- Fig. 2-6. Upregulation of antioxidant signaling molecules induced by TauCl administration in mouse colon. -----48
- Fig. 2-7. Induction of Keap1 degradation and nuclear translocation of Nrf2 by TauCl in mouse colon. -----50

Fig. 2-8. Molecular mechanisms by which TauCl protects against
experimentally induced colitis. -----51

Chapter III

Fig. 3-1. UVB-induced oxidative stress and apoptotic cell death were
ameliorated in TauCl-treated mouse skin. -----76

Fig. 3-2. The expression of UVB-induced inflammatory enzymes was
attenuated by topical application of TauCl. -----78

Fig. 3-3. TauCl application inhibited UVB-induced expression of pro-
inflammatory cytokines and enzymes in mouse skin. -----79

Fig. 3-4. Topically applied TauCl attenuated UVB-induced
phosphorylation of STAT3 in mouse skin. -----80

Fig. 3-5. UVB-induced phosphorylation of STAT3 was diminished in
TauCl-treated mouse skin. -----81

Fig. 3-6. The Nrf2-mediated expression of antioxidant enzymes was
elevated in TauCl-treated mice. -----83

Fig. 3-7. A proposed molecular mechanism underlying the protective
effects of TauCl against UVB-induced dermatitis. -----85

Chapter IV

- Fig. 4-1. Protective effects of topically applied 17-oxo-DHA on UVB-induced inflammation and oxidative stress in mouse skin. --124
- Fig. 4-2. Enhanced nuclear translocation of Nrf2 and its target protein expression in 17-oxo-DHA treated mice. -----127
- Fig. 4-3. Attenuation of UVB-induced STAT3 phosphorylation in mouse skin treated with 17-oxo-DHA. -----129
- Fig. 4-4. 17-Oxo-DHA-mediated acceleration of the resolution of UVB-induced inflammation in mouse skin. -----131
- Fig. 4-5. Nrf2-mediated enhancement of efferocytosis activity of macrophages by 17-oxo-DHA. -----133
- Fig. 4-6. Effects of pharmacologic and genetic inhibition of Nrf2 on effecrocytic activity of macrophages. -----135
- Fig. 4-7. Protective effects of 17-oxo-DHA against UVB-induced tumor development in hairless mouse skin. -----138
- Fig. 4-8. Attenuation of long-term UVB-induced oxidative skin damage in 17-oxo-DHA treated mice. -----140
- Fig. 4-9. Mass spectrometric analysis of covalent modification of STAT3 by 17-oxo-DHA. -----142
- Fig. 4-10. A schematic representation of the molecular mechanism underlying protective effects of 17-oxo-DHA against UVB-induced dermatitis and skin carcinogenesis. -----145

Supplementary Fig. 1. The changes in inflammatory severity for 7 days
after UVB irradiation. -----147

Supplementary Fig.2 Attenuation of UVB-induced inflammation and
apoptosis in mouse skin by topically applied 17-oxo-DHA. -149

Supplementary Fig.3 Cleavage information of 17-oxo-DHA was acquired
by DIMS analysis. -----150

LIST OF TABLES

Chapter I

Table 1-1. Effects of taurine chloramine on the anti-inflammation pathway----12

Table 1-2. Effects of 17-oxo-DHA on the anti-inflammation pathway. -----13

Table 1-3. Effects of 17-oxo-DHA on the antioxidant pathway. -----13

LIST OF ABBREVIATIONS

- TauCl, Taurine chloramine
- PUFA, polyunsaturated fatty acid
- DHA, docosahexaenoic acid
- 17-oxo-DHA, 17-oxo-docosahexaenoic acid
- WT, wild-type
- NADPH, nicotinamide adenine dinucleotide phosphate
- H₂O₂, hydrogen peroxide
- UVB, ultraviolet B
- TNBS, 2,4,6-trinitrobenzene sulfonic acid
- CD, crohn's disease
- UC, ulcerative colitis
- IBD, inflammatory bowel disease
- MPO, myeloperoxidase
- LO, lipoxygenase
- STAT3, signal transducer and activator of transcription 3
- Nrf2, nuclear factor erythroid-related factor 2
- Keap1, Kelch-like ECH-associated protein 1
- ARE, antioxidant response element
- ROS, reactive oxygen species
- DAI, disease activity index

4-HNE, 4-hydroxynonenal

MDA, malondialdehyde

8-oxo-dG, 8-hydroxy-2'-deoxyguanosine

COX-2, cyclooxygenase-2

iNOS, inducible nitric oxide synthase

HO-1, heme oxygenase-1

NQO1, NAD(P)H:quinone oxidoreductase-1

Trx, thioredoxin

BMDM, bone marrow-derived macrophage

M-CSF, macrophage colony-stimulating factor

SPM, specialized pro-resolving mediator

H&E, hematoxylin and eosin

TUNEL, terminal deoxynucleotidyl transferase dUTP nick-end labeling

IHC, immunohistochemical analysis

DAPI, 4',6-diamidino-2-phenylindole

DTT, dithiothreitol

PMSF, phenylmethyl sulfonylfluoride

EDTA, ethylenediaminetetraacetic acid

HEPES, 4-(2-hydroxyethyl)-1-piperazineethanesulfonic acid

NP-40, Nonidet P-40

SDS, sodium dodecyl sulfate

PAGE, polyacrylamide gel electrophoresis

PVDF, polyvinylidene difluoride

TBST, tris-buffered saline containing 0.1% tween 20

ECL, enhanced chemiluminescent

RT-PCR, reverse transcription-polymerase chain reaction analysis

qPCR, quantitative real-time polymerase chain reaction

M-MLV, Moloney murine leukemia virus

NF- κ B, nuclear factor kappa B

DMEM, Dulbecco's modified Eagle's medium

FBS, fetal bovine serum

MEM, minimum essential medium

PBS, phosphate-buffered saline

SD, standard deviation

SE, standard error

Chapter I

Taurine Chloramine and 17-Oxo-docosahexaenoic Acid

as Novel Endogenous Proresolving and Anti-

inflammatory Substances with Chemopreventive

Potential

1. Introduction

Inflammation is an immediate host response to microbial infection and mechanical injury, ultimately aimed to restore the tissue function and structure [1, 2]. This response is referred to as the innate-adaptive immune response which represents a major essential element of the host's defense system [3, 4]. Innate immunity serves as the first line of defense against noxious stimuli. It provides the necessary signals to direct the adaptive immune system to initiate a response after recognizing an external harmful substance [5]. In addition to the innate immune responses, the inflammatory response is accompanied by the infiltration of adaptive immune cells that convey specific immune responses to antigens by T cells and B cells which are differentiated into plasma cells with specific antibody production [6].

In contrast to acute or physiological inflammation which is health beneficial, prolonged inflammation leads to undesirable consequences, which are implicated in the pathogenesis of various chronic diseases. In addition to the accumulation of monocyte-derived macrophages and lymphocytes, this long-term reaction to an inflammatory stimulus is characterized by changes in wound healing functions, such as the proliferation of fibroblasts and blood vessels. The therapeutic strategy of chronic inflammation is hence important in the management of autoimmune diseases including, rheumatoid arthritis, atherosclerosis, asthma, psoriasis, and cancer. [7-9].

Acute inflammation is an essential protective response to injury or infection, and its timely initiation and resolution are critical for restoring tissue homeostasis [10]. The response is a coordinated effort of multiple cell types that work together to eliminate pathogens and promote tissue repair (Fig. 1). The process can be divided into two phases: initiation and resolution. The involvement and regulation of intrinsic mechanisms are essential for this type of self-limiting inflammatory response [11]. Acute inflammation requires constant activation of the adaptive immune system, so it is vital to precisely reinforce the resolution of inflammation [12-14].

Chemoprevention is defined as a pharmacological approach used to inhibit, retard, or even reverse the multi-stage carcinogenesis. Many fruit- and vegetable-derived substances, collectively termed phytochemicals, have anti-inflammatory and antioxidant properties which contribute to their chemopreventive potential [15], and various *in vitro/in vivo* studies have been conducted to assess their chemopreventive effects [16-19]. Many natural compounds have shown the ability to potentiate cellular antioxidant and anti-inflammatory defense, which is mainly mediated by Nrf2, without cytotoxic effects in a normal state. Although activation of anti-inflammatory as well as antioxidant signaling by Nrf2 [20-22] has been extensively investigated, its involvement in resolution of inflammation remains poorly understood.

A series of endogenous proresolving mediators, including resolvins and maresins, have been identified [23] and their therapeutically applicable forms

have been or are being developed. By accelerating the resolution of inflammation beyond simple inhibition of a chronic inflammatory process, these endogenous fire extinguishers may exert cancer chemopreventive effects as well. In this thesis, I investigated the chemoprotective and chemopreventive effects of two endogenously formed antioxidant and anti-inflammatory substances, taurine chloramine and 17-oxo-docosahexaenoic acid in relation to the resolution of inflammation.

2. NF- κ B and STAT3 as two representative proinflammatory signaling molecules

NF- κ B is a redox-sensitive transcription factor that regulates inflammatory responses and immune processes. NF- κ B is composed of five functional members, including NF- κ B1 (p50), NF- κ B2(p52), RelA (p65), RelB, and c-Rel. Under normal physiologic conditions, NF- κ B is kept inactive in the cytoplasm by binding to I κ B protein [24, 25]. The activation of NF- κ B involves two pathways: the canonical and noncanonical (**Fig. 2**). The canonical pathway responds to proinflammatory stimuli such as tumor necrosis factor-alpha (TNF α) and interleukin 1 β (IL-1 β). The activation of the I κ B kinase (IKK) complex, consisting of IKK α , IKK β catalytic subunits and IKK γ regulatory subunit, triggers phosphorylation of I κ B and its subsequent degradation through ubiquitination, leading to nuclear translocation of NF- κ B. In contrast, the non-canonical NF- κ B pathway is activated through IKK α -

mediated processing of the inactive p100 protein into its active form p52.

IKK α is a crucial component of this pathway [26].

Signal transducer and activator of transcription 3 (STAT3) is a member of the STAT family and involved in the proinflammatory responses in various disease including brain injury [27], dermatitis [28], colitis [29], and even cancer [30, 31]. Activation of STAT3 proceeds through overexpression or sustained induction of growth factor receptors and cytokine receptors related to the Janus kinase family and is referred to as the intrinsic pathway. In addition, the extrinsic pathway is activated through these receptors and non-receptor tyrosine kinases by environmental factors such as stress, ultraviolet rays, and various infections [32]. The activated tyrosine kinases in both intrinsic and extrinsic pathways phosphorylate STAT3 on tyrosine kinase 705. This results in the formation of a dimer that translocates to the nucleus and regulates gene expression. STAT3 upregulates genes encoding proteins involved in cell cycle progression (e.g., Cyclin D1) and survival (e.g., survivin), and also those associated with cancer-promoting inflammation, such as IL-6 and COX-2 [33, 34]. Therefore, inhibition of STAT3 activation is recognized as an important preventive/therapeutic approach in the management of inflammation-associated cancer, while reducing the severity of apoptosis and restoring tissue homeostasis.

3. Taurine chloramine

Taurine is one of the most abundant free amino acids in the body, accounting for about 0.1% of body weight in most mammals [35]. Taurine was initially considered an inactive endpoint metabolite of a simple sulfur-containing amino acid, but later studies revealed that it has diverse physiological functions [36-38]. It is known to be involved in osmotic pressure regulation, membrane stabilization, reproduction, and detoxification and also has anti-inflammatory and protective effects against oxidative stress and cytotoxicity [39-42].

When inflammation occurs due to external stimuli or oxidative stress, the primary defense proceeds through neutrophils which accumulate in the inflamed sites, engulf invading microorganisms, and kills them with oxidizing agents and bactericidal proteins [43, 44]. Neutrophils that swallow the invading microorganism activate nicotinamide adenine dinucleotide phosphate (NADPH) oxidase to form a superoxide anion (O_2^-), which is then converted to hydrogen peroxide (H_2O_2) by superoxide dismutase. Hydrogen peroxide also has a strong sterilization ability. It is converted into substances with more vital sterilization ability, such as hypochlorite ($HOCl/OCl^-$) in the presence of chloride ion by myeloperoxidase (MPO) overexpressed in the activated neutrophils [43, 45, 46].

Though $HOCl$ can fight microbial infection due to its bactericidal and other cytotoxic activities, its excessive production can also be detrimental to the

host. Taurine, as a trap for excessive HOCl, forms taurine chloramine, which is more stable and less toxic than HOCl. Notably, taurine chloramine has a strong anti-inflammatory as well as antioxidant activity [47, 48, 62]

The accumulation of taurine chloramine in neutrophils is increased within an acceptable range upon inflammation. These results suggest that inhibition of oxidative stress by taurine chloramine in activated phagocytic cells such as neutrophils and macrophages may result from its inhibitory effect on the assembly of functional NADPH oxidase, which may then serve as a self-limiting protective mechanism. Thus, the generation of taurine chloramine plays an essential role in the cytoprotective effects of phagocytic cells against inflammatory damage by inhibiting secondary oxidative damage by ROS and hypochlorite. According to previous studies, taurine chloramine released from apoptotic neutrophils at inflamed sites increases efferocytic activity via upregulation of Nrf2-mediated HO-1 expression. Especially, treatment of macrophages with carbon monoxide, the byproduct of HO-1 catalyzed reaction, also enhanced the taurine chloramine-induced phagocytosis [49, 50]. All these results suggest that taurine chloramine has pronounced pro-resolving and anti-inflammatory effects (**Table 1**), and has a therapeutic potential as a regulator of inflammatory disorders.

4. 17-Oxo-docosahexaenoic acid (17-Oxo-DHA)

Dietary omega-3 polyunsaturated fatty acids (n-3 PUFAs) are known to alleviate various inflammatory disorders, including cardiovascular and asthma [51-53]. Docosahexaenoic acid (C22:6, DHA), one of the representative omega-3 fatty acids, is converted to a hydroxy and ketone derivative, 17-oxo-DHA by COX-2 and dehydrogenase activities, which protects cells from oxidative stress and inflammatory damage [54]. 17-Oxo-DHA and other electrophilic fatty acid metabolites can directly react with proteins through Michael reaction to modulate their activity [55].

As previously mentioned, 17-oxo-DHA is an endogenous electrophilic α,β -unsaturated ketone derivative of DHA produced by activated macrophages. The efficacy of 17-oxo-DHA has been evaluated against chronic diseases and inflammatory responses (**Table 2**). This substance induces expression of an anti-inflammatory enzyme, HO-1 in mouse skin *in vivo* and cultured murine epidermal cells [56] through activation of Nrf2. In exploring the proresolving effects of 17-oxo-DHA, I found the association between Nrf2 and CD36 by using Nrf2 knockout and wildtype mice. In addition, 17-oxo-DHA treatment enhanced the efferocytic activity of bone marrow-derived macrophages by increasing the expression of CD36 (S.-H. Kim & Y.-J. Surh, unpublished observation). Based on these findings, I extended the work to a long-term *in vivo* experiment to evaluate the chemopreventive effects of 17-oxo-DHA on inflammation-associated carcinogenesis.

5. Regulation of the Nrf2 signaling pathway through taurine chloramine and 17-oxo-DHA

Under normal conditions, the redox-sensitive transcription factor Nrf2 binds to Keap1 to form a structural complex in the cytoplasm. When cells are exposed to various internal/external stimuli and stresses, cysteine thiol residues present in Keap1 undergo oxidative modification, which promotes the dissociation of Nrf2 [57, 58]. Nrf2 released from Keap1 translocates to the nucleus and binds to a DNA sequence known as an antioxidant element (ARE). This binding increases the expression of Nrf2 target proteins such as HO-1, NADPH:quinone oxidoreductase and thioredoxin [59-61].

It was confirmed that taurine chloramine and 17-oxo-DHA promote the nuclear translocation of Nrf2 and increase the expression of antioxidant and anti-inflammatory enzymes and other cytoprotective proteins [56]. The treatment with taurine chloramine upregulates cytoprotective gene expression through Nrf2 activation in mouse skin and colon [62, 63]. In addition, an increase in Nrf2 expression was confirmed in TauCl treated macrophages. This contributed to resolution of inflammation through phagocytosis [50].

Previous studies demonstrated the molecular mechanisms underlying Nrf2-mediated induction of cytoprotective effects upon 17-oxo-DHA treatment [56]. In addition, compared to the non-electrophilic precursor DHA, 17-oxo-DHA is a more potent activator of Nrf2 in inducing expression of antioxidant/anti-inflammatory proteins (**Table3**).

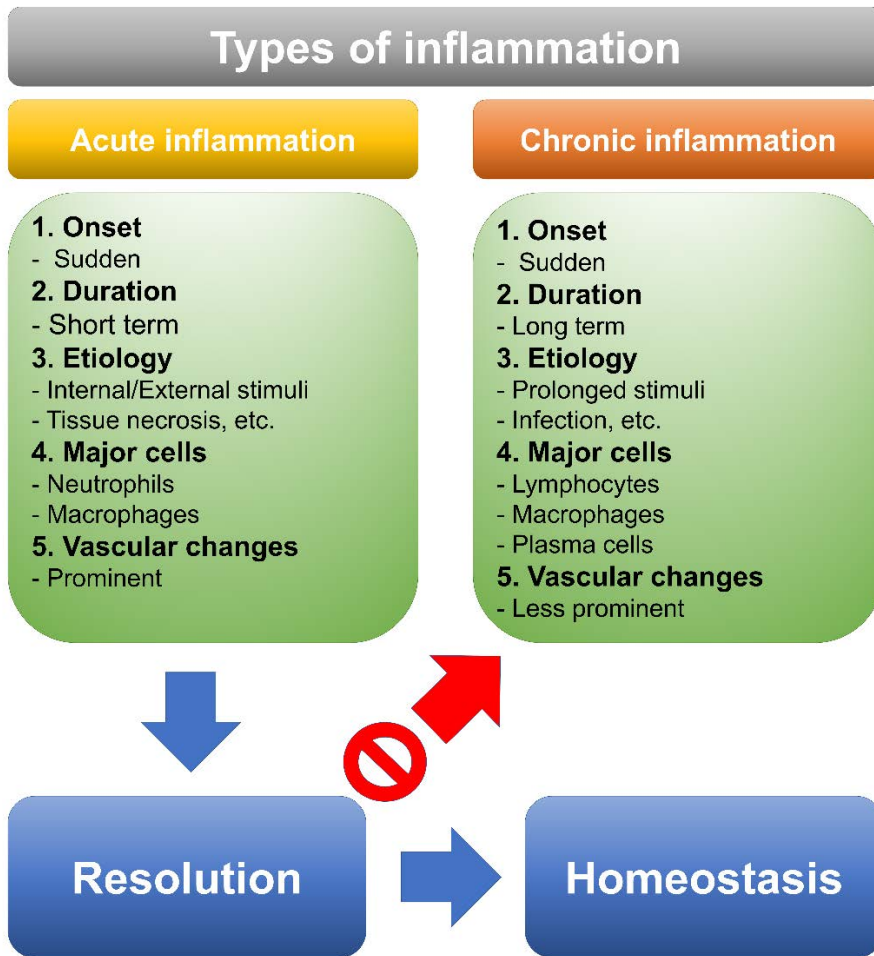


Figure 1-1. Differences between acute and chronic inflammation.

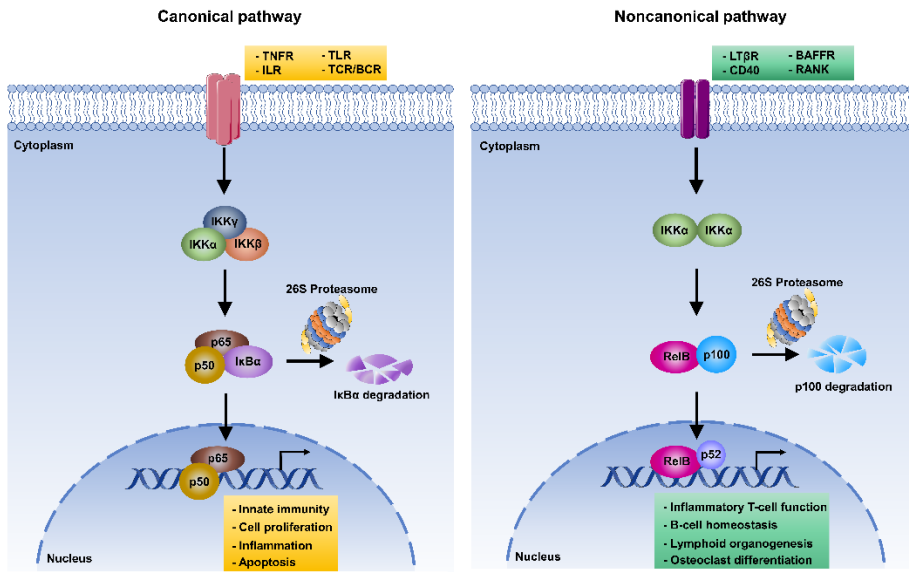


Figure 2-1. NF- κ B signaling: Canonical and noncanonical pathways.

Table 1 Effects of taurine chloramine on the anti-inflammation pathway

Cell and Tissue	Stimuli	Effects	References
Lymphocytes (Isolated from rats)	Concanavalin A	↓ The expression level of TNF α	[64]
Murine macrophages (RAW 264.7, Primary)	Zymosan A	↑ Phagocytic activity	[65]
Mouse bone marrow cells	Lipopolysaccharide (LPS)	↓ LPS-induced TNF α , IL-1 β	[66]
Murine macrophages (RAW 264.7)	Zymosan, IFN- γ	↓ Production of NO and TNF α	[67]
Human adipose tissue	Lipopolysaccharide (LPS),	↓ Induction of IL-6, TNF α , and IL-8	[68]
Mouse lung tissue	Lipopolysaccharide (LPS)	↓ LPS-induced IL-6	[69]
Mouse lung tissue	Lipopolysaccharide (LPS)	↓ LPS-induced IL-6, TNF α	[70]
Mouse skin tissue	Ultraviolet B (UVB)	↓ The expression of COX-2, iNOS and proinflammatory cytokines	[63]
Mouse colon tissue	2,4,6-Trinitrobenzene sulfonic acid (TNBS)	↓ Production of COX-2 and activation of STAT3	[62]
Mouse arthritis model	Bovine type II collagen	↓ Infiltration of inflammatory cells and synovial cells	[71]

Table 2 Effects of 17-oxo-DHA on the anti-inflammation pathway

Cell	Stimuli	Effects	References
Human macrophages (THP-1)	Cigarette smoke extract (CSE)	↓ CSE-induced TNF α , IL-1 β ↓ CSE-induced ROS generation	[72]
Bronchial epithelial cell (16HBE)	Lipopolysaccharide (LPS)	↓ LPS-induced TNF α , IL-1 β	[72]
Human macrophages (THP-1)	Lipopolysaccharide (LPS),	↓ LPS-induced TNF α , IL-1 β	[66]
Human macrophages (THP-1)	Ca ²⁺ ionophore	↓ Production of 5-HETE and LTB ₄	[73]

Table 3 Effects of 17-oxo-DHA on the antioxidant pathway

Model of studies	Cell and Tissue	Effects	References
Cell culture studies	Human non-small cell lung cancer (NSCLC) cell lines	↓ Cell proliferation ↑ Induction of apoptosis and expression of caspase-8, caspase-3/7	[74]
	Mouse epidermal cell (JB6 Cl 41)	↑ Regulation of Nrf2 and Nrf-mediated signaling	[56]
Animal studies	SKH1- <i>Hr^{hr}</i> mice	↑ Nuclear translocation of Nrf2 and induction of Nrf-mediated proteins	[56]

6. References

1. Chovatiya, R. and R. Medzhitov, *Stress, inflammation, and defense of homeostasis*. Mol Cell, 2014. **54**(2): p. 281-8.
2. Mittal, M., et al., *Reactive oxygen species in inflammation and tissue injury*. Antioxid Redox Signal, 2014. **20**(7): p. 1126-67.
3. Holgate, S.T., *Innate and adaptive immune responses in asthma*. Nat Med, 2012. **18**(5): p. 673-83.
4. Schleimer, R.P., et al., *Epithelium: at the interface of innate and adaptive immune responses*. J Allergy Clin Immunol, 2007. **120**(6): p. 1279-84.
5. Newton, K. and V.M. Dixit, *Signaling in innate immunity and inflammation*. Cold Spring Harb Perspect Biol, 2012. **4**(3).
6. Sun, L., et al., *Innate-adaptive immunity interplay and redox regulation in immune response*. Redox Biol, 2020. **37**: p. 101759.
7. Leuti, A., et al., *Bioactive lipids, inflammation and chronic diseases*. Adv Drug Deliv Rev, 2020. **159**: p. 133-169.
8. Watson, N., et al., *Chronic inflammation - inflammaging - in the ageing cochlea: A novel target for future presbycusis therapy*. Ageing Res Rev, 2017. **40**: p. 142-148.
9. Medzhitov, R., *Origin and physiological roles of inflammation*. Nature, 2008. **454**(7203): p. 428-35.
10. Meizlish, M.L., et al., *Tissue Homeostasis and Inflammation*. Annu Rev Immunol, 2021. **39**: p. 557-581.
11. Serhan, C.N., *Resolution phase of inflammation: novel endogenous anti-inflammatory and proresolving lipid mediators and pathways*. Annu Rev Immunol, 2007. **25**: p. 101-37.
12. Feehan, K.T. and D.W. Gilroy, *Is Resolution the End of Inflammation?* Trends Mol Med, 2019. **25**(3): p. 198-214.
13. Panigrahy, D., et al., *Resolution of inflammation: An organizing principle in biology and medicine*. Pharmacol Ther, 2021. **227**: p. 107879.

14. Coussens, L.M. and Z. Werb, *Inflammation and cancer*. Nature, 2002. **420**(6917): p. 860-7.
15. Surh, Y.J., *Cancer chemoprevention with dietary phytochemicals*. Nat Rev Cancer, 2003. **3**(10): p. 768-80.
16. Lange, N.F., P. Radu, and J.F. Dufour, *Prevention of NAFLD-associated HCC: Role of lifestyle and chemoprevention*. J Hepatol, 2021. **75**(5): p. 1217-1227.
17. Kucuk, O., *Chemoprevention of prostate cancer*. Cancer Metastasis Rev, 2002. **21**(2): p. 111-24.
18. Soria, J.C., et al., *Chemoprevention of lung cancer*. Lancet Oncol, 2003. **4**(11): p. 659-69.
19. Xie, X., et al., *Cancer metastasis chemoprevention prevents circulating tumour cells from germination*. Signal Transduct Target Ther, 2022. **7**(1): p. 341.
20. Harris, I.S. and G.M. DeNicola, *The Complex Interplay between Antioxidants and ROS in Cancer*. Trends Cell Biol, 2020. **30**(6): p. 440-451.
21. Sporn, M.B. and K.T. Liby, *NRF2 and cancer: the good, the bad and the importance of context*. Nat Rev Cancer, 2012. **12**(8): p. 564-71.
22. Kobayashi, E.H., et al., *Nrf2 suppresses macrophage inflammatory response by blocking proinflammatory cytokine transcription*. Nat Commun, 2016. **7**: p. 11624.
23. Serhan, C.N., *A search for endogenous mechanisms of anti-inflammation uncovers novel chemical mediators: missing links to resolution*. Histochem Cell Biol, 2004. **122**(4): p. 305-21.
24. Vallabhapurapu, S. and M. Karin, *Regulation and function of NF-kappaB transcription factors in the immune system*. Annu Rev Immunol, 2009. **27**: p. 693-733.
25. Liu, T., et al., *NF-kappaB signaling in inflammation*. Signal Transduct Target Ther, 2017. **2**: p. 17023-.
26. Sun, S.C., *The non-canonical NF-kappaB pathway in immunity and inflammation*. Nat Rev Immunol, 2017. **17**(9): p. 545-558.

27. Seton-Rogers, S., *STAT3 on the brain*. Nat Rev Cancer, 2018. **18**(8): p. 468-469.
28. Boos, A.C., et al., *Atopic dermatitis, STAT3- and DOCK8-hyper-IgE syndromes differ in IgE-based sensitization pattern*. Allergy, 2014. **69**(7): p. 943-53.
29. Sugimoto, K., *Role of STAT3 in inflammatory bowel disease*. World J Gastroenterol, 2008. **14**(33): p. 5110-4.
30. Hillmer, E.J., et al., *STAT3 signaling in immunity*. Cytokine Growth Factor Rev, 2016. **31**: p. 1-15.
31. Zou, S., et al., *Targeting STAT3 in Cancer Immunotherapy*. Mol Cancer, 2020. **19**(1): p. 145.
32. Yu, H., D. Pardoll, and R. Jove, *STATs in cancer inflammation and immunity: a leading role for STAT3*. Nat Rev Cancer, 2009. **9**(11): p. 798-809.
33. Johnson, D.E., R.A. O'Keefe, and J.R. Grandis, *Targeting the IL-6/JAK/STAT3 signalling axis in cancer*. Nat Rev Clin Oncol, 2018. **15**(4): p. 234-248.
34. Gong, J., et al., *Combined targeting of STAT3/NF-kappaB/COX-2/EP4 for effective management of pancreatic cancer*. Clin Cancer Res, 2014. **20**(5): p. 1259-73.
35. Ripps, H. and W. Shen, *Review: taurine: a "very essential" amino acid*. Mol Vis, 2012. **18**: p. 2673-86.
36. De Luca, A., S. Pierno, and D.C. Camerino, *Taurine: the appeal of a safe amino acid for skeletal muscle disorders*. J Transl Med, 2015. **13**: p. 243.
37. Muhling, J., et al., *Effects of propofol and taurine on intracellular free amino acid profiles and immune function markers in neutrophils in vitro*. Clin Chem Lab Med, 2002. **40**(2): p. 111-21.
38. Howard, D. and D.F. Thompson, *Taurine: an essential amino acid to prevent cholestasis in neonates?* Ann Pharmacother, 1992. **26**(11): p. 1390-2.
39. Qaradakhhi, T., et al., *The Anti-Inflammatory Effect of Taurine on Cardiovascular Disease*. Nutrients, 2020. **12**(9).

40. Baliou, S., et al., *Protective role of taurine against oxidative stress (Review)*. Mol Med Rep, 2021. **24**(2).
41. Qiu, T., et al., *Taurine attenuates arsenic-induced pyroptosis and nonalcoholic steatohepatitis by inhibiting the autophagic-inflammasomal pathway*. Cell Death Dis, 2018. **9**(10): p. 946.
42. Seidel, U., P. Huebbe, and G. Rimbach, *Taurine: A Regulator of Cellular Redox Homeostasis and Skeletal Muscle Function*. Mol Nutr Food Res, 2019. **63**(16): p. e1800569.
43. Liew, P.X. and P. Kubes, *The Neutrophil's Role During Health and Disease*. Physiol Rev, 2019. **99**(2): p. 1223-1248.
44. Teng, T.S., et al., *Neutrophils and Immunity: From Bactericidal Action to Being Conquered*. J Immunol Res, 2017. **2017**: p. 9671604.
45. Winterbourn, C.C., A.J. Kettle, and M.B. Hampton, *Reactive Oxygen Species and Neutrophil Function*. Annu Rev Biochem, 2016. **85**: p. 765-92.
46. Pase, L., et al., *Neutrophil-delivered myeloperoxidase dampens the hydrogen peroxide burst after tissue wounding in zebrafish*. Curr Biol, 2012. **22**(19): p. 1818-24.
47. Kim, C. and Y.N. Cha, *Taurine chloramine produced from taurine under inflammation provides anti-inflammatory and cytoprotective effects*. Amino Acids, 2014. **46**(1): p. 89-100.
48. Seol, S.I., et al., *Taurine Protects against Postischemic Brain Injury via the Antioxidant Activity of Taurine Chloramine*. Antioxidants (Basel), 2021. **10**(3).
49. Kim, W., et al., *Taurine Chloramine Stimulates Efferocytosis Through Upregulation of Nrf2-Mediated Heme Oxygenase-1 Expression in Murine Macrophages: Possible Involvement of Carbon Monoxide*. Antioxid Redox Signal, 2015. **23**(2): p. 163-77.
50. Kim, S.H., et al., *Taurine chloramine potentiates phagocytic activity of peritoneal macrophages through up-regulation of dectin-1 mediated by heme oxygenase-1-derived carbon monoxide*. FASEB J, 2018. **32**(4): p. 2246-2257.

51. Horrocks, L.A. and Y.K. Yeo, *Health benefits of docosahexaenoic acid (DHA)*. Pharmacol Res, 1999. **40**(3): p. 211-25.
52. Ghasemi Fard, S., et al., *How does high DHA fish oil affect health? A systematic review of evidence*. Crit Rev Food Sci Nutr, 2019. **59**(11): p. 1684-1727.
53. Kiecolt-Glaser, J.K., et al., *Omega-3 supplementation lowers inflammation and anxiety in medical students: a randomized controlled trial*. Brain Behav Immun, 2011. **25**(8): p. 1725-34.
54. Groeger, A.L., et al., *Cyclooxygenase-2 generates anti-inflammatory mediators from omega-3 fatty acids*. Nat Chem Biol, 2010. **6**(6): p. 433-41.
55. Shiraki, T., et al., *Alpha,beta-unsaturated ketone is a core moiety of natural ligands for covalent binding to peroxisome proliferator-activated receptor gamma*. J Biol Chem, 2005. **280**(14): p. 14145-53.
56. Jamil, M.U., et al., *17-Oxo-docosahexaenoic acid induces Nrf2-mediated expression of heme oxygenase-1 in mouse skin in vivo and in cultured murine epidermal cells*. Arch Biochem Biophys, 2020. **679**: p. 108156.
57. Lu, M.C., et al., *The Keap1-Nrf2-ARE Pathway As a Potential Preventive and Therapeutic Target: An Update*. Med Res Rev, 2016. **36**(5): p. 924-63.
58. Yamamoto, M., T.W. Kensler, and H. Motohashi, *The KEAP1-NRF2 System: a Thiol-Based Sensor-Effector Apparatus for Maintaining Redox Homeostasis*. Physiol Rev, 2018. **98**(3): p. 1169-1203.
59. Bono, S., M. Feligioni, and M. Corbo, *Impaired antioxidant KEAP1-NRF2 system in amyotrophic lateral sclerosis: NRF2 activation as a potential therapeutic strategy*. Mol Neurodegener, 2021. **16**(1): p. 71.
60. Ma, Q., *Role of nrf2 in oxidative stress and toxicity*. Annu Rev Pharmacol Toxicol, 2013. **53**: p. 401-26.
61. Zhang, H., K.J.A. Davies, and H.J. Forman, *Oxidative stress response and Nrf2 signaling in aging*. Free Radic Biol Med, 2015. **88**(Pt B): p. 314-336.

62. Kim, S.H., et al., *Protective Effects of Taurine Chloramine on Experimentally Induced Colitis: NFkappaB, STAT3, and Nrf2 as Potential Targets*. *Antioxidants* (Basel), 2021. **10**(3).
63. Kim, S.H., et al., *Topically Applied Taurine Chloramine Protects against UVB-Induced Oxidative Stress and Inflammation in Mouse Skin*. *Antioxidants* (Basel), 2021. **10**(6).
64. Dall'igna, D.M., et al., *Taurine Chloramine decreases cell viability and cytokine production in blood and spleen lymphocytes from septic rats*. *An Acad Bras Cienc*, 2020. **92**(4): p. e20191311.
65. Kim, W., et al., *Role of heme oxygenase-1 in potentiation of phagocytic activity of macrophages by taurine chloramine: Implications for the resolution of zymosan A-induced murine peritonitis*. *Cell Immunol*, 2018. **327**: p. 36-46.
66. Cipollina, C., et al., *17-oxo-DHA displays additive anti-inflammatory effects with fluticasone propionate and inhibits the NLRP3 inflammasome*. *Sci Rep*, 2016. **6**: p. 37625.
67. Kim, B.S., et al., *Taurine chloramine inhibits NO and TNF-alpha production in zymosan plus interferon-gamma activated RAW 264.7 cells*. *J Drugs Dermatol*, 2011. **10**(6): p. 659-65.
68. Marcinkiewicz, J. and E. Kontny, *Taurine and inflammatory diseases*. *Amino Acids*, 2014. **46**(1): p. 7-20.
69. Nguyen, K.H., et al., *Examination of Taurine Chloramine and Taurine on LPS-Induced Acute Pulmonary Inflammation in Mice*. *Adv Exp Med Biol*, 2022. **1370**: p. 23-29.
70. Khanh Hoang, N., et al., *N-Chlorotaurine Reduces the Lung and Systemic Inflammation in LPS-Induced Pneumonia in High Fat Diet-Induced Obese Mice*. *Metabolites*, 2022. **12**(4).
71. Wang, Y., et al., *Taurine chloramine inhibits osteoclastogenesis and splenic lymphocyte proliferation in mice with collagen-induced arthritis*. *Eur J Pharmacol*, 2011. **668**(1-2): p. 325-30.
72. Cipollina, C., et al., *Dual anti-oxidant and anti-inflammatory actions of the electrophilic cyclooxygenase-2-derived 17-oxo-DHA in*

- lipopolysaccharide- and cigarette smoke-induced inflammation.*
Biochim Biophys Acta, 2014. **1840**(7): p. 2299-309.
73. Gagestein, B., et al., *Comparative Photoaffinity Profiling of Omega-3 Signaling Lipid Probes Reveals Prostaglandin Reductase 1 as a Metabolic Hub in Human Macrophages.* J Am Chem Soc, 2022. **144**(41): p. 18938-18947.
74. Siena, L., et al., *Electrophilic derivatives of omega-3 fatty acids counteract lung cancer cell growth.* Cancer Chemother Pharmacol, 2018. **81**(4): p. 705-716.

STATEMENT OF PURPOSE

Although many research papers have reported the protective effect of TauCl, the detailed signaling mechanism, including the expression of pro-inflammatory enzymes in colitis and dermatitis, still needs to be solved. While studying the cytoprotective effects of metabolites against acute inflammation, I focused on lipid metabolites, one of that is omega-3 fatty acids. It was confirmed that a small amount of 17-oxo-DHA was generated after DHA treatment. Other groups have conducted *in vitro* studies using 17-oxo-DHA, but there is no report on animal experiments. Previous studies in our laboratory confirmed the antioxidant effect of 17-oxo-DHA in mouse epidermis and cultured murine epidermal cells. This prompted me to explore the possible protective effect of this antioxidative and anti-inflammatory bioactive fatty acid metabolite against UVB-induced dermatitis and photocarcinogenesis.

Consequently, this study aims to investigate whether the up-regulation of anti-inflammatory/antioxidant protein induced by the administration of TauCl and 17-oxo-DHA can contribute to protective effects against experimentally induced inflammation-associated disorders and to elucidate the underlying molecular mechanisms.

Chapter II

Protective Effects of Taurine Chloramine on Experimentally Induced Colitis: NFκB, STAT3, and Nrf2 as Potential Targets

1. Abstract

Taurine chloramine (TauCl) is an endogenous anti-inflammatory substance which is derived from taurine, a semi-essential sulfur-containing β -amino acid found in some foods including meat, fish, eggs and milk. In general, TauCl as well as its parent compound taurine downregulates production of tissue-damaging proinflammatory mediators, such as chemokines and cytokines in many different types of cells. In the present study, we investigated the protective effects of TauCl on experimentally induced colon inflammation. Oral administration of TauCl protected against mouse colitis caused by 2,4,6-trinitrobenzene sulfonic acid (TNBS). TauCl administration attenuated apoptosis in the colonic mucosa of TNBS-treated mice. This was accompanied by reduced expression of an oxidative stress marker, 4-hydroxy-2-nonenal and proinflammatory molecules including tumor necrosis factor- α , interleukin-6 and cyclooxygenase-2 in mouse colon. TauCl also inhibited activation of NF κ B and STAT3, two key transcription factors mediating proinflammatory signaling. Notably, the protective effect of TauCl on oxidative stress and inflammation in the colon of TNBS-treated mice was associated with elevated activation of Nrf2 and upregulation of its target genes encoding heme oxygenase-1, NAD(P)H:quinone oxidoreductase, glutamate cysteine ligase catalytic subunit, and glutathione *S*-transferase. Taken together, these results suggest that TauCl exerts the protective effect against colitis through upregulation of Nrf2-dependent cytoprotective gene

expression while blocking the proinflammatory signaling mediated by NFκB and STAT3.

Keywords

Taurine; Taurine chloramine; Colitis; Heme oxygenase-1; 2,4,6-

Trinitrobenzene sulfonic acid; NFκB; STAT3; Nrf2

2. Introduction

Inflammatory bowel disease belongs to a distinct group of disorders characterized by prolonged systemic inflammation in the digestive tract. Crohn's disease (CD), together with ulcerative colitis (UC), represents a prototypic form of inflammatory bowel disease (IBD). CD commonly affects the tail end of the small intestine (the ileum) and proximal colon while UC involves inflammation of the large intestine [1]. The pathogenesis of CD as well as UC involves complex interactions among environmental factors, dysregulated immune response, gut microbiota, and disease susceptibility genes [2,3].

Chronic transmural inflammation of the intestinal wall provokes aberrant activation of the immune system. The hyper-reactive immune response often accompanies massive intracellular production of reactive oxygen species (ROS) with a concomitant decrease in the antioxidant defense. The resulting imbalance between ROS production and the antioxidant capacity causes oxidative stress [3]. Oxidative stress leads to mucosal layer damage and bacterial invasion, which in turn further stimulate the immune response. This amplifies a pathogenic cascade and exacerbates colonic inflammation [2]. While much effort has been directed at clinical trials to help CD, the disease is still incurable.

2,4,6-Trinitrobenzene sulfonic acid (TNBS)-induced inflammation in mouse colon is one of the most commonly utilized animal models that

replicate human CD [4–6]. In this model, intrarectal administration of TNBS produces symptoms similar to that of CD. These include bloody diarrhea, rectal bleeding, body weight loss, large bowel wall thickening, more diffuse intestinal inflammation, occasional adhesions, fibrosis, vascularized ulceration, etc. [5,6]. This experimental model has provided valuable insights to the molecular basis of the disease development and progression and also the preclinical testing of various anti-inflammatory and/or anti-oxidative compounds in regards to their potential to prevent the development or delay the progress of CD [5].

Despite remarkable progress in our understanding of the pathophysiology of CD, a cost effective and efficacious therapy has yet to be developed. Considering oxidative stress and inflammatory damage as prime etiological factors for CD, search for safe and easily accessible substances with pronounced antioxidant and anti-inflammatory activities can be a pragmatic approach in the management of the disease. Taurine, an amino sulfonic acid, is one such candidate. It is abundant in muscle meat (e.g., chicken and beef), fish (salmon) and eggs. Taurine has a wide spectrum of biological functions, such as conjugation of bile acids, antioxidation, osmoregulation, membrane stabilization, and modulation of calcium signaling [7].

Taurine reaches particularly high concentrations in some immune cells of inflamed tissues exposed to elevated levels of oxidants (e.g., neutrophils undergoing oxidative burst). This suggests that taurine may have a vital role in

inflammation associated with oxidative stress. Indeed, at the site of inflammation, taurine reacts with and neutralize hypochlorous acid generated by the myeloperoxidase (MPO)-hydrogen peroxide (H_2O_2)-halide system of the neutrophils. This reaction results in the formation of less toxic, but biologically active taurine chloramine (TauCl) [8]. The antioxidative and anti-inflammatory properties of TauCl have been reported [9–11]. In this study, we investigated the effects of TauCl on TNBS-induced murine colitis and underlying molecular mechanisms.

3. Materials and Methods

Materials

TauCl as a crystalline sodium salt (MW 181.57) was prepared as described previously [12]. Primary antibodies for protein modified with 4-hydroxynonenal (4-HNE) was purchased from Japan Institute for the Control of Aging (JaICA), Nikken SEIL Co., Ltd. (Shizuoka, Japan). Primary antibodies for cyclooxygenase-2 (COX-2), Signal transducer and activator of transcription (STAT3), phospho-STAT3^{Y705}, cyclin D1, α -tubulin, Kelch-like ECH-associated protein 1 (Keap1) and lamin B1 were provided by Cell Signaling Technology (Danvers, MA, USA), and those for Nrf2 and heme oxygenase-1 (HO-1) were supplied from Abcam (Cambridge, MA, USA) and Enzo Life Sciences (Farmingdale, NY, USA), respectively. Nuclear factor- κ B (NF κ B) p65 and phospho-NF κ B p65 were obtained from Santa Cruz Biotechnology (Dallas, TX, USA). Antibodies for caspase-3 & cleaved caspase-3 were purchased from Cell Signaling Technology (Danvers, MA, USA).

Animals

Male C57BL/6 mice (5 to 6 weeks of age) were purchased from Orient Bio Inc. (Seongnam-si, South Korea). Mice were housed in plastic cages under controlled conditions of temperature (23 ± 2 °C), humidity ($50 \pm 10\%$) and light (12/12 h light/dark cycle). All animal experiments were complied with

the Guide for the Care and Use of Laboratory Animals and approved by the Institutional Animal Care and Use Committee (IACUC) at Seoul National University (IACUC number; SNU-170823-2-2).

TNBS-Induced Colitis in Mice

Mice were anaesthetized with ketamine and xylazine. Colitis was induced by intrarectal administration of 2.5% TNBS (Sigma-Aldrich; St. Louis, MO, USA) in 50% ethanol via a thin round-tip needle equipped with a 1 ml syringe, and the animals were then kept in a vertical position for 30 s. The total injection volume was 100 μ L. TauCl (20 mg/kg/day) was given by gavage for 10 days before induction of colitis and thereafter until the end of the study. The mice were euthanized 3 days after TNBS administration. The colons were removed, opened longitudinally and washed with phosphate-buffered saline (PBS). Immediately after washing, an inflamed segment was cut for histopathological examination, whereas another portion was flash frozen in liquid nitrogen and kept at -70 °C until use.

Macroscopic Assessment

After 3 days of TNBS administration, the body weight of mice was measured every day. Disease activity index (DAI) was determined as the sum of scores of weight loss, rectal bleeding and stool consistency. Collected colon tissues were cut longitudinally, and the colon length was measured.

Histology

The mice were euthanized 3 days after TNBS administration. The isolated colons were washed with PBS. Immediately after washing, an inflamed segment was cut for histopathological examination, whereas another portion was flash frozen in liquid nitrogen and kept at -70°C until use. Specimens of distal parts of the colon were fixed with 10% phosphate buffered formalin, and embedded in paraffin. Each section was stained with hematoxylin and eosin (H&E). The fixed sections were examined by light microscope (Nikon; Tokyo, Japan) for the presence of lesions.

Measurement of MPO Activity

The MPO activity in mouse colon tissues was measured by using the Myeloperoxidase Colorimetric Activity Assay Kit (Sigma-Aldrich; St. Louis, MO, USA) according to the manufacturer's instructions.

Immunohistochemical Analysis

Immunohistochemical analysis of 4-hydroxy-2-nonenal (4-HNE)-modified protein was performed according to the standard protocols. Briefly, the freshly dissected colon tissues were fixed with 10% formalin, and the tissue block was embedded in paraffin. The paraffin-embedded tissues sections (5 μm thick) were then deparaffinised in xylene and transferred through graded

ethanol for rehydration. Using microwave, the deparaffinized and rehydrated sections were heated twice for 6 min each in 10 mM citrate buffer (pH 6.0) for antigen retrieval. To extinguish endogenous peroxidase activity and diminish background staining, each section was treated with 3% hydrogen peroxide and 4% peptone casein blocking solution for 15 min. The slides were incubated with diluted primary antibody at room temperature for 40 min in Tris-HCl-buffered saline containing 0.05% Tween 20. After removing antibody solution and washing three times, the sections were incubated with horseradish peroxidase-conjugated mouse secondary antibody (Dako; Glostrup, Denmark). The tissues were treated with 3,3'-diaminobenzidine tetrahydrochloride substrate solution to reveal the color of stained antibody. Finally, counterstaining was carried out using Mayer's hematoxylin.

Terminal Deoxynucleotidyl Transferase dUTP Nick End Labeling (TUNEL)

Assay

Apoptotic DNA fragmentation was detected by the TUNEL assay with the ApopTag[®] Peroxidase In Situ Apoptosis Detection Kit (Chemicon; Temecula, CA, USA). The isolated colon tissues were rinsed with PBS, and fixed in 10% buffered formalin (Sigma-Aldrich; St. Louis, MO, USA) for the TUNEL assay. The apoptotic cells were visualized by light microscope (Nikon; Tokyo, Japan).

Immunofluorescence Staining

Colorectal specimens were fixed, paraffin-embedded and sectioned, and the sections were deparaffinized and rehydrated by serial washes with graded xylene and alcohol. For immunofluorescence staining, tissue sections were boiled in 10 mM sodium citrate (pH 6.0) for antigen retrieval, subjected to serial washing and permeabilized for 45 min at room temperature using 0.2% Triton X-100 in PBS and blocked with 3% bovine serum albumin (BSA) in PBS for 1 h at room temperature. The tissue sections were stained with primary antibodies for p65, p-p65, STAT3 and p-STAT3 (Cell Signaling Technology; Danvers, MA, USA) diluted at 1:250 in 3% BSA overnight at 4 °C. After washing three times each 5 min to remove primary antibodies, tissues were incubated with appropriate secondary antibodies. Nuclei were counterstained with DAPI (Invitrogen; Carlsbad, CA, USA).

Immunofluorescence images were collected on a fluorescence microscope (Nikon; Tokyo, Japan).

Tissue Lysis and Protein Extraction

Colon tissues were homogenized with the lysis buffer [20 mM Tris-HCl (pH 7.5), 150 mM NaCl, 1 mM Na₂EDTA, 1 mM EGTA, 1% Triton, 2.5 mM sodium pyrophosphate, 1 mM β-glycerophosphate, 1 mM Na₃VO₄, 1 μg/mL leupeptin] including ethylenediaminetetraacetic acid (EDTA)-free protease inhibitor cocktail tablet and 1 mM phenylmethyl sulfonylfluoride (PMSF)] in

ice bath. The whole lysates were vortexed every 10 min for 3 h on the ice. The supernatants were collected and kept at -70°C until use.

Preparation of Cytosolic and Nuclear Extracts

For preparation of cytosolic extraction, tissues were homogenized with buffer A [10 mM 4-(2-hydroxyethyl)-1-piperazineethanesulfonic acid (HEPES, pH 7.8), 1.5 mM MgCl_2 , 10 mM KCl, 0.5 mM dithiothreitol (DTT), 0.2 mM PMSF] followed by vortex every 10 min for 3 h in ice bath. The lysates were mixed with 10% Nonidet P-40 (NP-40) 30 min before centrifuge. After centrifugation at 13,000 g for 15 min, the supernatants (the cytosolic extracts) were collected. Precipitated pellets were washed with buffer A containing 10% NP-40 three times to remove a residual cytosolic fraction. Nuclear pellets were resuspended in buffer C [20 mM HEPES, pH 7.8, 420 mM NaCl, 1.5 mM MgCl_2 , 0.2 mM EDTA, 0.5 mM DTT, 0.2 mM PMSF and 20% Glycerol]. The nuclear lysates were vortexed every 10 min for 1 h, followed by centrifugation at 13,000 g for 15 min. The supernatants (nuclear extracts) were collected and stored at -70°C until use.

Western Blot Analysis

The total protein concentration was measured by using the PierceTM BCA Protein Assay Kit (Thermo Fisher Scientific; Rockford, IL, USA). Protein lysates (20 μg) were electrophoresed by SDS-polyacrylamide gel

electrophoresis (PAGE) and transferred to the polyvinylidene difluoride membrane (Gelman Laboratory; Ann Arbor, MI, USA). The blots were blocked with 5% non-fat dry milk in Tris-buffered saline containing 0.1% Tween 20 (TBST) for 1 h at room temperature. The membranes were incubated overnight at 4 °C with diluted primary antibodies. The blots were rinsed three times with TBST buffer for 10 min each. Washed blots were incubated with 1:5000 dilution of respective horseradish peroxidase-conjugated secondary antibodies (Invitrogen; Carlsbad, CA, USA) for 1 h and washed again three times with TBST buffer. The proteins were visualized with an enhanced chemiluminescence detection kit (Absignal) (Abclon; Seoul, South Korea) and LAS-4000 image reader (Fujifilm; Tokyo, Japan).

Reverse Transcription-Polymerase Chain Reaction Analysis (RT-PCR)

Total RNA was isolated from mouse colon tissues using TRIzol[®] reagent (Invitrogen; Carlsbad, CA, USA) according to the manufacturer's protocol. To synthesize the complementary DNA (cDNA), 1 µg of total RNA was reverse transcribed with murine leukemia virus reverse transcriptase (Promega; Madison, WI, USA) for 50 min at 42 °C and again for 15 min at 72 °C. About 1 µL of cDNA was amplified with a Solg[™] 2X Taq PCR Smart mix (SolGent Co., Ltd.; Daejeon, South Korea) in sequential reactions. The primers used for each RT-PCR reactions are as follows: *tnf-α*, 5'-TGA ACT TCG GGG GTG ATC GGT C-3' and 5'-AGC CTT GTC CCT TGA AGA GAA-3'; *il-6*, 5'-AGT

TGC CTT CTT GGG ACT GA-3' and 5'-TCC ACG ATT TCC CAG AGA AC-3'; *cox-2*, 5'-CTG GTG CCT GGT CTG ATG ATG-3' and 5'-GGC AAT GCG GTT CTG ATA CTG-3'; *actin*, 5'-AGA GCA TAG CCC TCG TAG AT-3' and 5'-CCC AGA GCA AGA GAG GTA TC-3'; *ho-1*, 5'-TAC ACA TCC AAG CCG AGA AT-3' and 5'-GTT CCT CTG TCA GCA TCA CC-3'; *nqo1*, 5'-AGG ATG GGA GGT ACT CGA ATC-3' and 5'-AGG CGT CCT TCC TTA TAT GCT A-3'; *gclc*, 5'-GGC TAC TTC TGT ACT AGG AGA GC-3' and 5'-TGC CGG ATG TTT CTT GTT AGA G-3'; *gss*, 5'-CCC ATT CAC GCT TTT CCC CT-3' and 5'-GGG CAG TAT AGT CGT CCT TTT TG-3'; *nrf2*, 5'-CTT TAG TCA GCG ACA GAA GGA C-3' and 5'-AGG CAT CTT GTT TGG GAA TGT G-3' (forward and reverse, respectively). Amplification products were analyzed by 2% agarose gel electrophoresis, followed by staining with SYBR Green (Invitrogen; Carlsbad, CA, USA) and photographed using fluorescence in LAS-4000 (Fujifilm; Tokyo, Japan).

Statistical Analysis

All the values were expressed as the mean \pm standard deviation (SD) of at least three independent experiments. Statistical significance was determined by the Student's *t*-test and $p < 0.05$ was considered to be statistically significant. All the statistical analyses were applied using GraphPad Prism 8.0 (GraphPad Software; San Diego, CA, USA).

4. Results

TauCl Protects against TNBS-Induced Colitis in Mice

Administration of TNBS (**Fig. 2-1A**) via intra-rectal instillation caused severe body weight loss (**Fig. 2-1B**), rectal bleeding and stool inconsistency (**Fig. 2-1C**) and shortening of the colon (**Fig. 2-1D**). All these abnormalities were ameliorated by administration of TauCl. Histopathological analysis showed that TNBS administration completely disrupted the architecture of colonic mucosa as evidenced by colitis exhibiting epithelial degeneration, crypt loss and inflammatory cell infiltration (**Fig. 2-2A**). Administration of TauCl attenuated TNBS-induced mucosal damage of colon (**Fig. 2-2A**).

Myeloperoxidase (MPO) is lysosomal enzyme abundant in neutrophils that are recruited to the inflamed site. The levels of MPO, as biomarkers of oxidative damage and inflammation, are often escalated in the inflammatory disorders, including IBD [13,14]. There was a robust increase in the colonic MPO activity in TNBS-treated mice, and this was dampened by TauCl administration (**Fig. 2-2B**). 4-HNE is a reactive lipid peroxidation product that can modify protein. The TNBS-induced accumulation of 4-HNE-modified proteins in the colonic mucosa was attenuated by TauCl administration as assessed by immunohistochemical (**Fig. 2-2A**) and immunoblot (**Fig. 2-2C**) analyses. TauCl also protected against TNBS induced colonic cell death via apoptosis as assessed by immunohistochemical (**Fig. 2-2A**) and Western blot

(Fig. 2-2D) analyses in terms of TUNEL staining and cleavage of caspase-3, respectively.

TauCl Administration Attenuates the Expression of Proinflammatory Cytokines and Enzymes in the Colon of TNBS-Treated Mice

TNBS-induced colitis was accompanied by elevated colonic expression of genes encoding representative proinflammatory cytokines (TNF α and IL-6) and enzymes (COX-2), which was suppressed by TauCl administration (Fig. 2-3). Transcriptional regulation of these proinflammatory genes is mainly mediated by nuclear factor kappa B (NF κ B). Under normal physiologic conditions, NF κ B forms an inactive complex in the cytoplasm with the inhibitory protein I κ B α . When cells are challenged with the inflammatory stimuli, I κ B α undergoes phosphorylation which facilitates its proteasomal degradation via ubiquitination. We noticed the significant reduction in the levels of I κ B α in the TNBS-treated mouse colon and this was restored by TauCl administration (Fig. 2-4A). The degradation of I κ B α allows release of NF κ B for translocation into nucleus. p65 is a functionally active subunit of NF κ B, and its phosphorylation is known to facilitate the nuclear translocation of NF κ B and recruitment of coactivators, such as p300/CBP. As illustrated in Figure 4B, there was pronounced localization of phosphorylated p65 (p-p65) as well as p65 in the colon of TNBS treated mice, and this was abrogated by TauCl administration.

TNBS-Induced Colonic STAT3 Phosphorylation Was Inhibited by TauCl Administration

Besides NF κ B, STAT3 is another key player in inflammation and inflammation-associated carcinogenesis. One of the essential events in STAT3 activation is phosphorylation on tyrosine 705, which facilitates its nuclear translocation and transcriptional activity. TauCl administration significantly inhibited TNBS-induced phosphorylation of STAT3 and expression of its major target protein cyclin D1 (**Fig. 2-5**).

TauCl Administration Upregulates Antioxidant and Antiinflammatory Gene Expression

The cellular redox balance is maintained by a battery of antioxidant enzymes that counteract ROS. Many of these antioxidant enzymes also have anti-inflammatory functions. Administration of TauCl markedly enhanced the colonic expression of HO-1 (**Fig. 2-6A**) and its mRNA transcript (**Fig. 2-6B**). Expression of genes encoding some other representative antioxidant/anti-inflammatory enzymes as well as Nrf2 was also upregulated in the colon of mice administered TauCl (**Fig. 2-6C**). Nrf2 is a master switch in the transcriptional regulation of many antioxidant and anti-inflammatory genes. In unstressed conditions, Nrf2 is sequestered in the cytoplasm by Keap1 that degrades Nrf2 through ubiquitination. TauCl administration resulted in marked reduction in the cytoplasmic levels of Keap1 (**Fig. 2-7A**) with concomitant increase in the nuclear accumulation of Nrf2 (**Fig. 2-7B, C**).

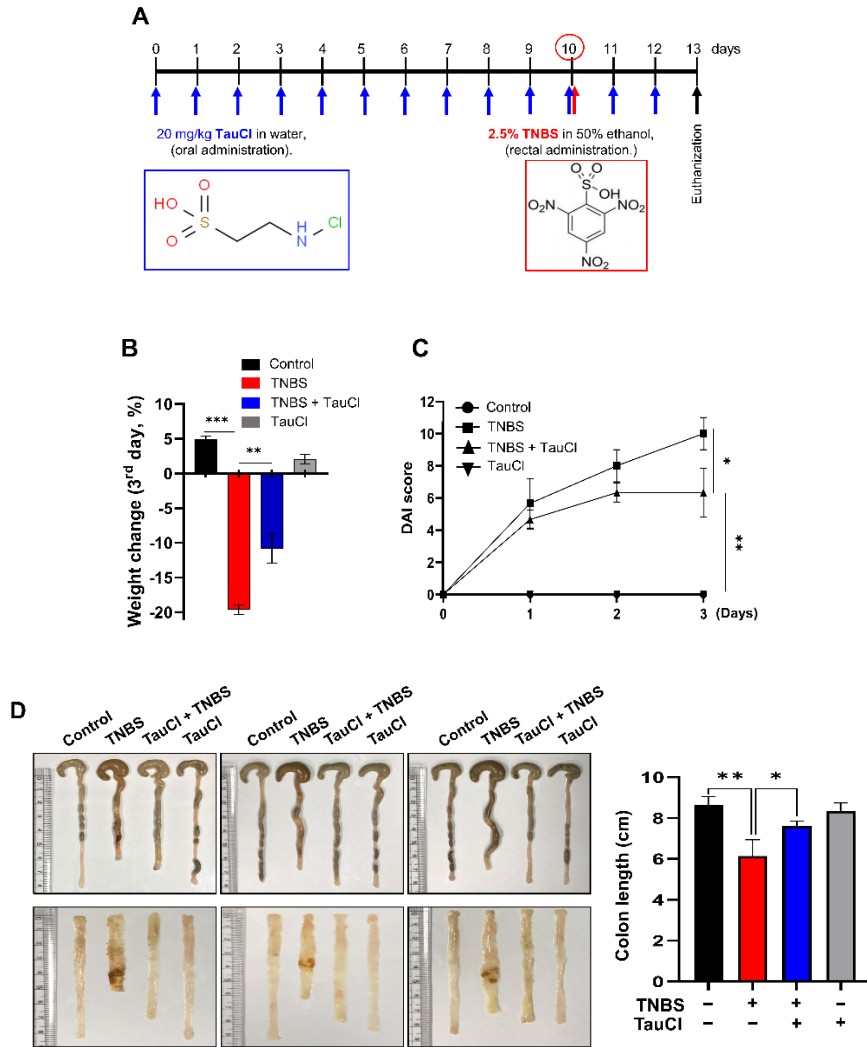


Figure 2-1. Effects of TauCl on inflammatory damage in the colon of TNBS-treated mice.

(A) TauCl (20 mg/kg) was given on daily basis by gavage for 10 days before and for 3 days after intrarectal administration of 2.5% TNBS in EtOH. The comparison of body weight change (B), DAI (C), and colon length (D). Data are expressed as means \pm SD ($n = 3$ for each group). *, **, *** Significantly different between groups compared (* $p < 0.05$; ** $p < 0.01$; *** $p < 0.001$).

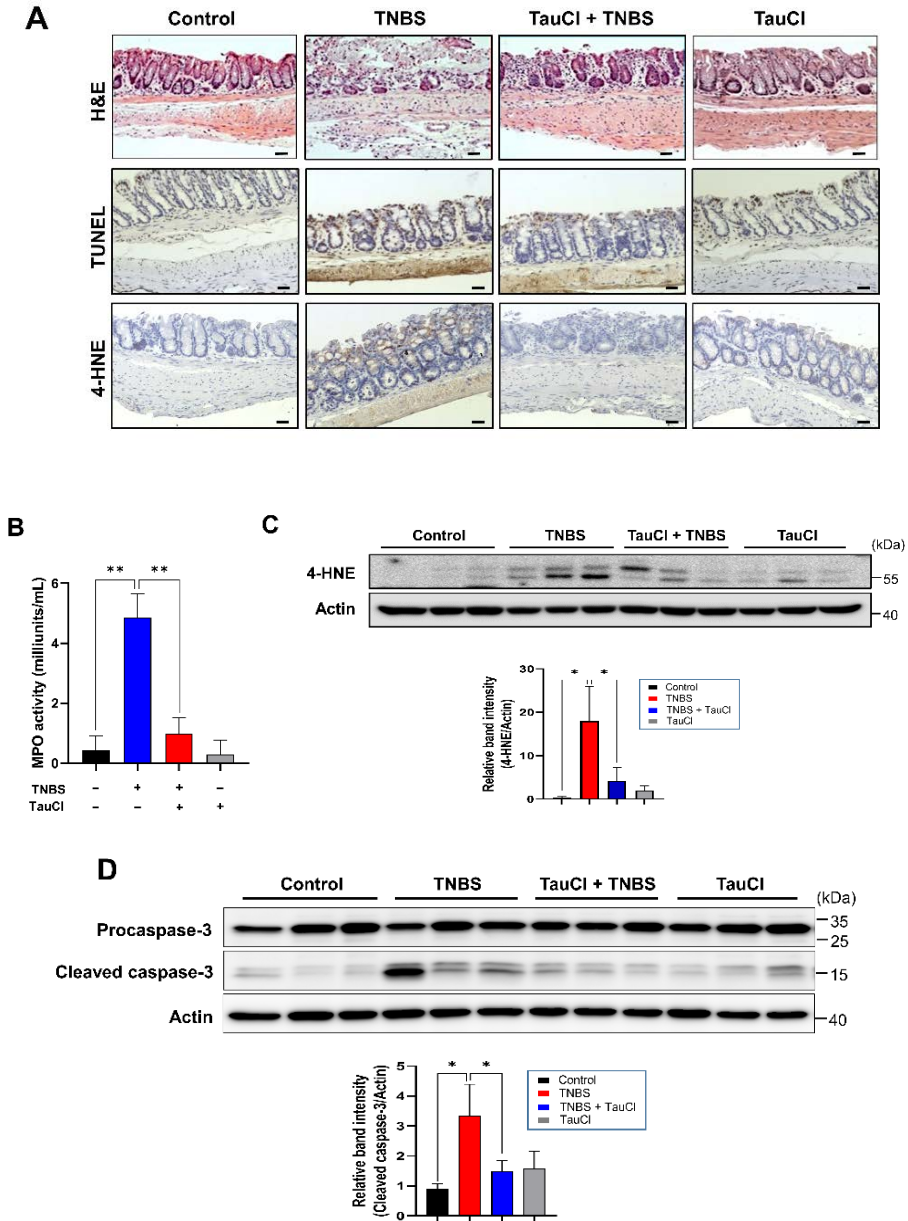


Figure 2-2. Attenuation of TNBS-induced colonic cell death, MPO activity, and oxidative damage by administration of TauCl.

(A) Microscopic examination of H&E stained colonic mucosa from control mice and those treated with TNBS alone for 3 days, TNBS plus TauCl and TauCl alone. Immunohistochemical detection of TUNEL-positive cells and 4-

HNE-modified proteins (brown spots) in mouse colon. Magnifications; $\times 100$.

(B) MPO activity in colonic mucosa. The enzyme assay was conducted as described in Materials and Methods. ** Significantly different between groups compared (** $p < 0.01$). **(C)** Western blot analysis of 4-HNE-modified protein expression in the colon strips of mice. Actin was used as an equal loading control. * $p < 0.05$. **(D)** Cleavage of caspase-3 was assessed by Western blot analysis. * $p < 0.05$.

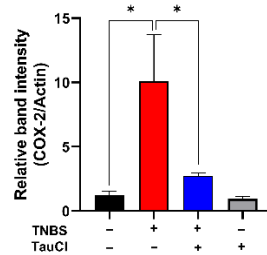
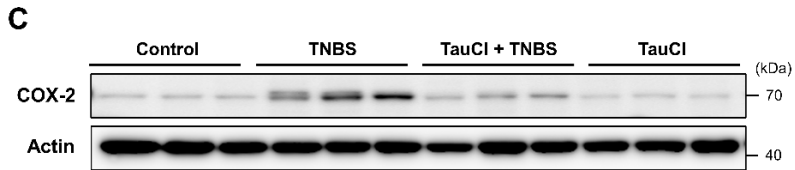
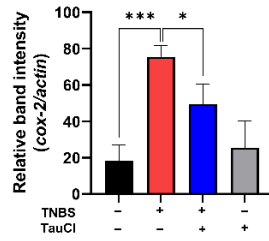
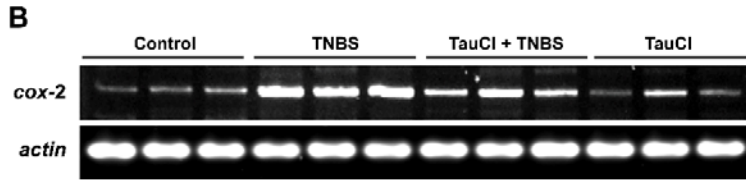
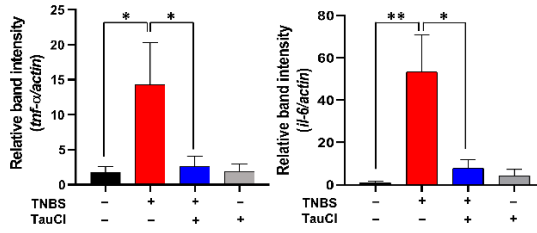
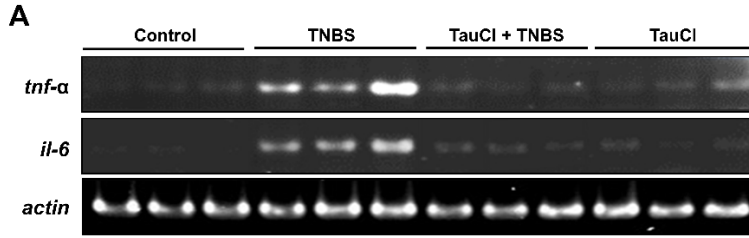


Figure 2-3. Effects of TauCl administration on expression of proinflammatory cytokines and COX-2 in mouse colonic mucosa.

(A) RT-PCR analysis of mRNA expression of proinflammatory cytokines (*tnf- α* , *il-6*) and *cox-2*. (B,C) Colonic expression of *cox-2* and COX-2 expression was assessed by RT-PCR and Western blot analysis, respectively. Data are expressed as means \pm SD (n = 3 for each group). *, **, *** Significantly different between groups compared (* $p < 0.05$; ** $p < 0.01$; *** $p < 0.001$).

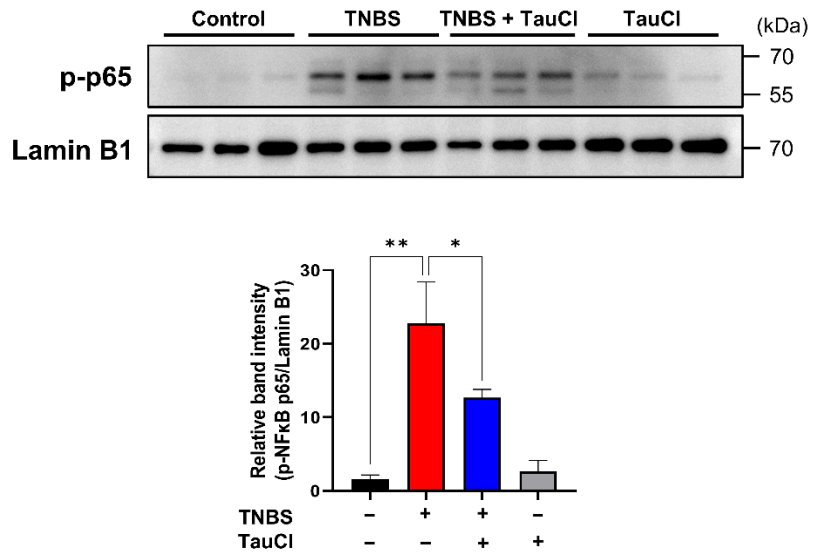
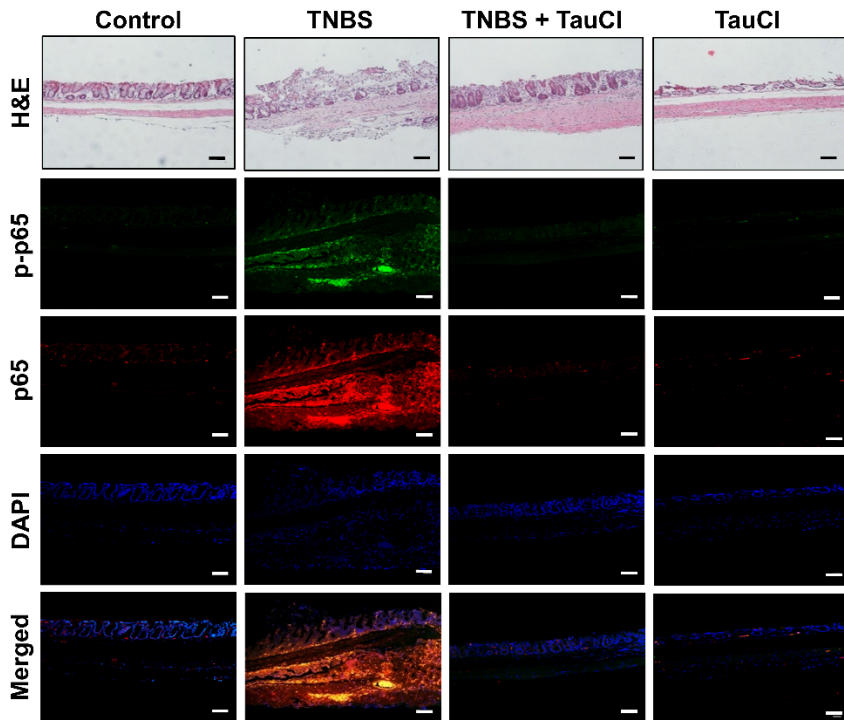
A**B**

Figure 2-4. Inhibitory effects of TauCl on TNBS-induced p65 phosphorylation and nuclear localization of NFκB.

(A) Expression of the phosphorylated NFκB p65 subunit was determined by Western blot analysis using nuclear extracts. (B) Accumulation of the phosphorylated as well as the total form of p65 was measured by immunofluorescence staining. The same tissue sections were stained with H&E. Scale bar, 200 μm. Results are presented as means ± SD. * $p < 0.05$; ** $p < 0.01$.

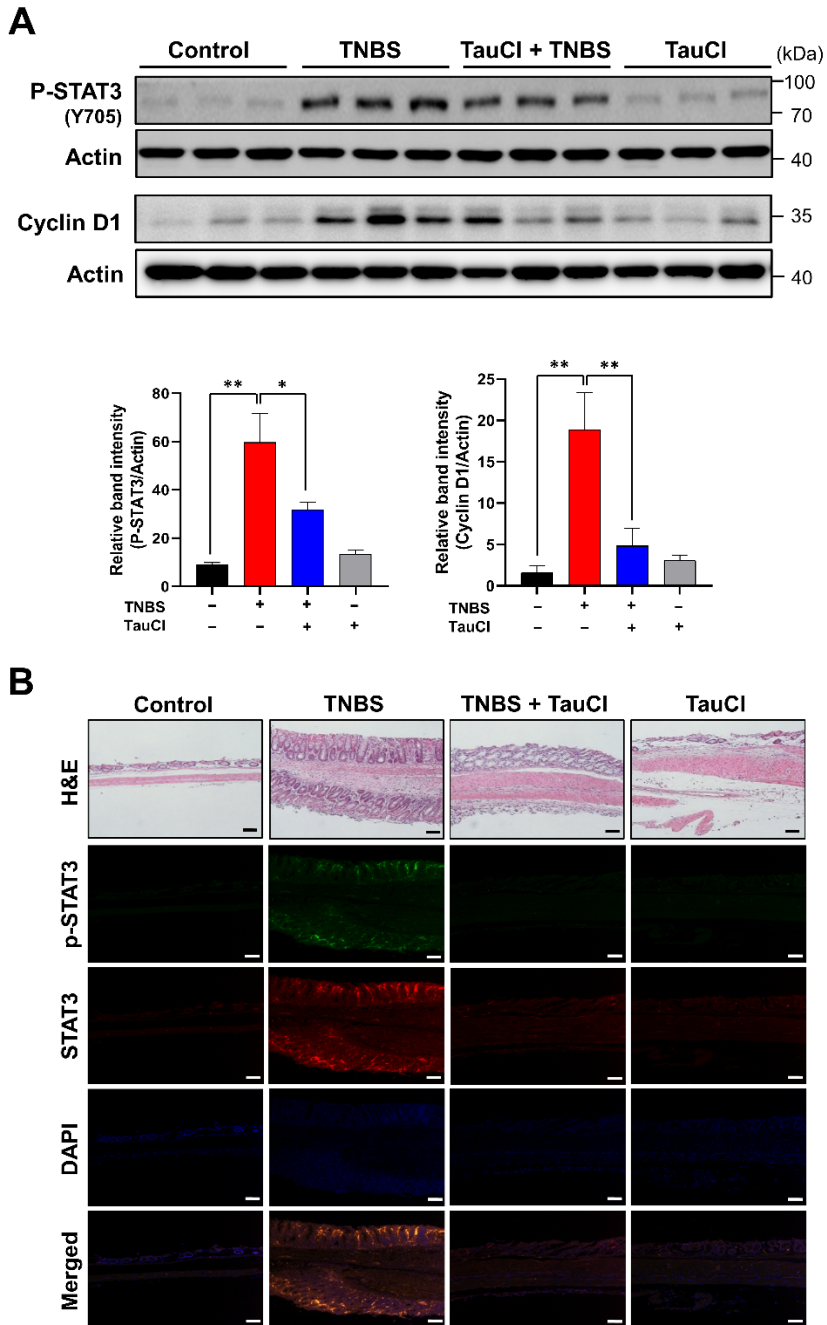
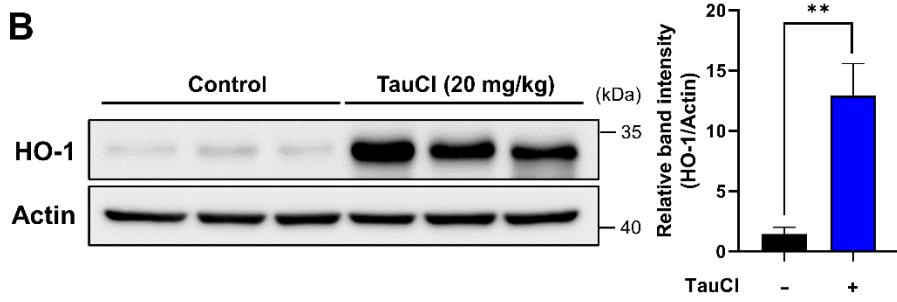
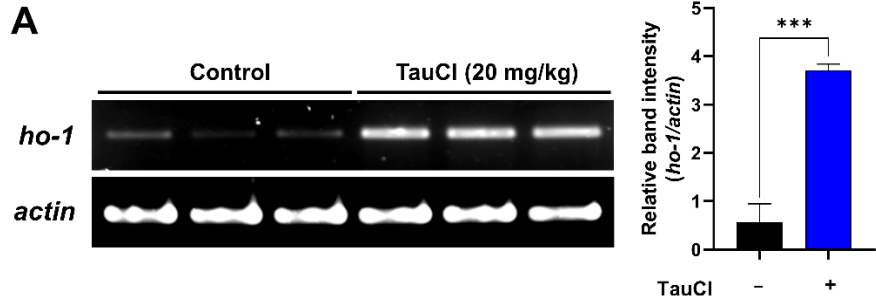


Figure 2-5. Inhibitory effects of TauCl on phosphorylation of STAT3 and its target protein expression in the colonic tissue of TNBS-treated mice.

(A) Expression of P-STAT3 and cyclin D1 was measured by Western blot

analysis. Actin was used as an equal loading control. * ** Significantly different between groups compared (* $p < 0.05$; ** $p < 0.01$). **(B)** Phosphorylated as well as total STAT3 was detected by immunofluorescence staining. The same tissue sections were stained with H&E. Scale bar, 200 μm .



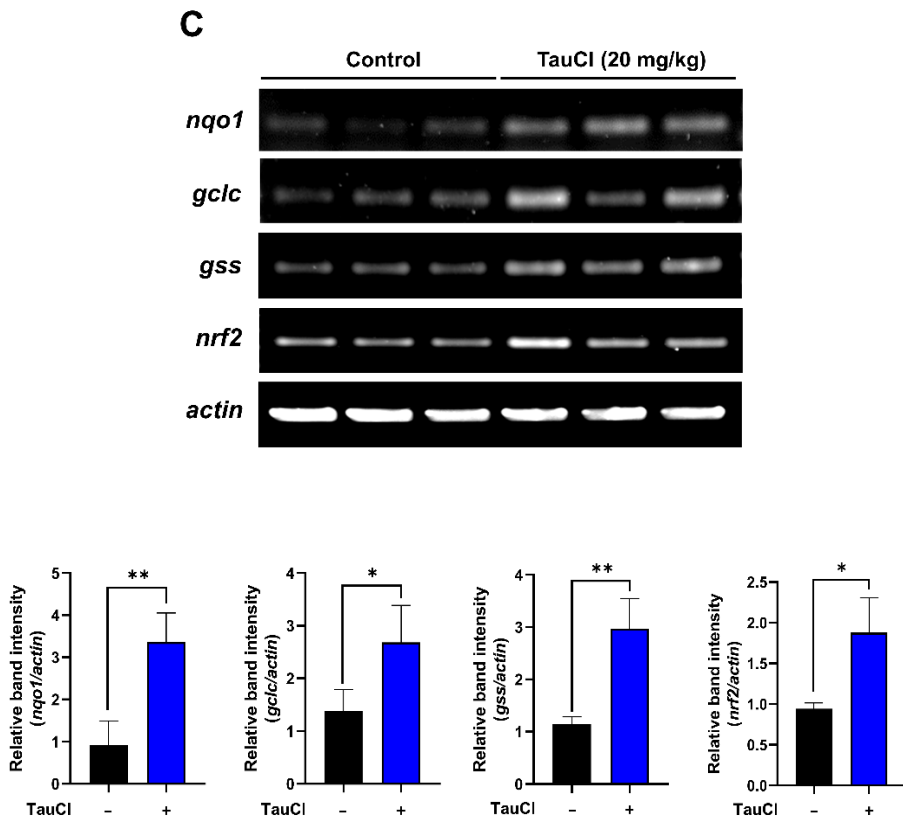


Figure 2-6. Upregulation of antioxidant signaling molecules induced by TauCl administration in mouse colon. The expression of HO-1 (A) and its mRNA transcript (B) was determined by Western blot analysis and RT-PCR, respectively. (C) Expression of other antioxidant genes and Nrf2 was measured by RT-PCR. *, **, *** Significantly different between groups compared (* $p < 0.05$; ** $p < 0.01$; *** $p < 0.001$).

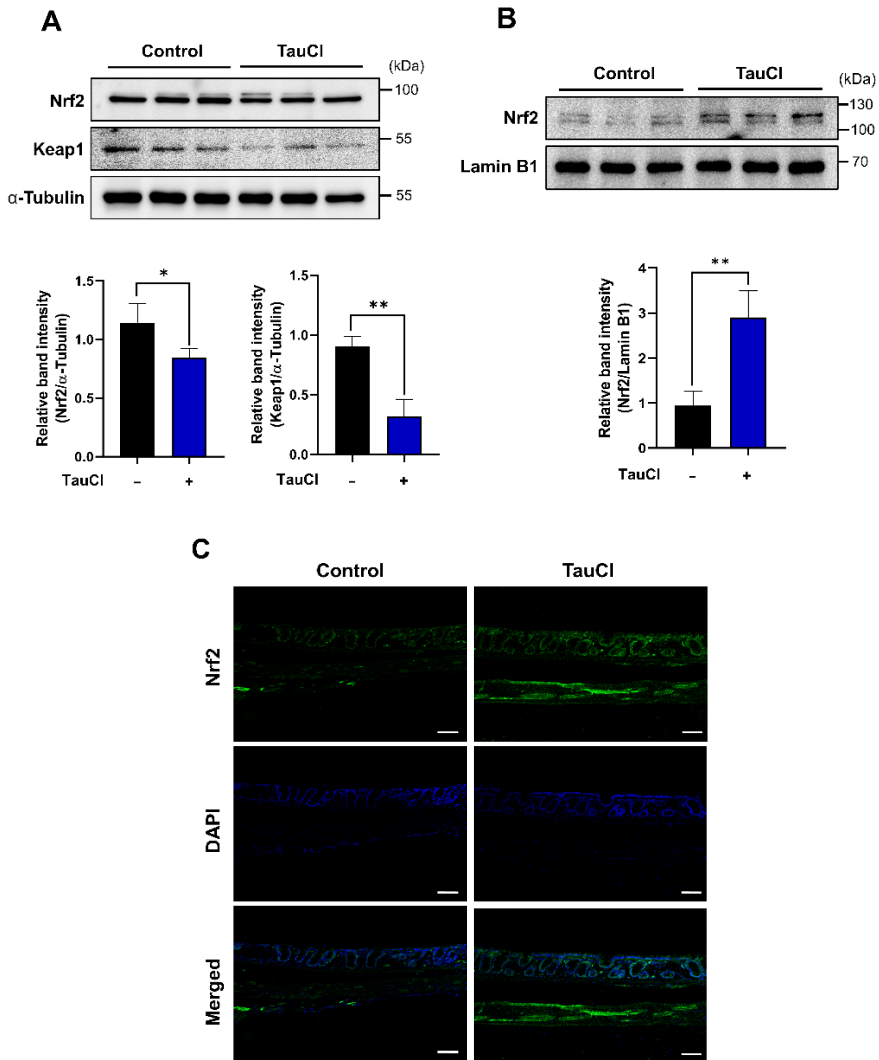


Figure 2-7. Induction of Keap1 degradation and nuclear translocation of Nrf2 by TauCl in mouse colon. Cytoplasmic levels of Nrf2 and Keap1 (A) and nuclear accumulation of Nrf2 (B) were measured by Western blot analysis. Nuclear localization of Nrf2 was verified by immunofluorescence staining (C). * ** Significantly different between groups compared (* $p < 0.05$; ** $p < 0.01$). Scale bar, 200 μ m.

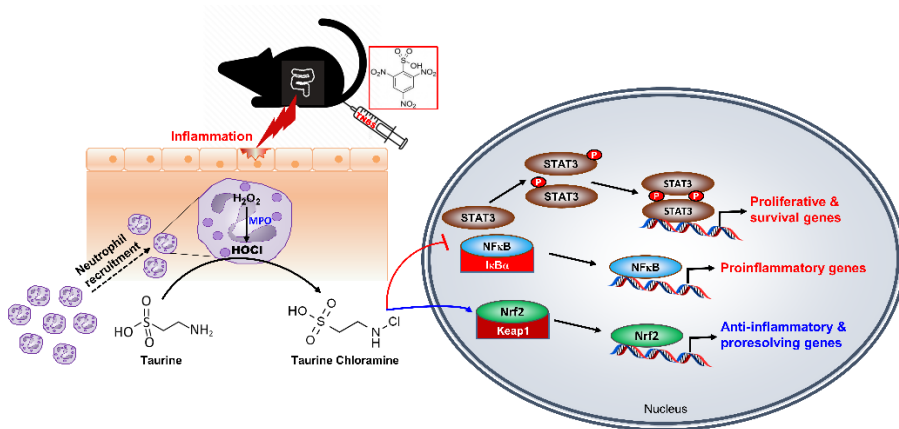


Figure 2-8. Molecular mechanisms by which TauCl protects against experimentally induced colitis. Abbreviations: MPO, myeloperoxidase; HOCl, hypochlorous acid.

5. Discussion

Taurine (2-aminoethylsulphonic acid), derived from the methionine and cysteine metabolism, plays an important role in various essential biological processes. Taurine is presented in neutrophilic granulocytes, lymphocytes and monocytes. Taurine is one of the most abundant free amino acids in our body with diverse health benefits [7]. The beneficial effects of taurine have been generally attributable to its antioxidant and anti-inflammatory effects [8,15,16]. The tissue-protective potential of taurine has been assessed in various animal models of oxidative and/or inflammatory injuries. In an early study, oral administration of taurine by gavage following TNBS treatment ameliorated colitis and related symptoms in rats [17]. In another study, rats given taurine (1.5% w/v) in drinking water for 15 days before and 15 days after administration of TNBS solution developed less severe colitis and oxidative colonic mucosal damage in rats. In addition, taurine reduced the expression of Bax and prevented the loss of Bcl-2 proteins in colon tissue of rats with TNBS-induced colitis [18]. Taurine supplementation significantly attenuated the weight decrease, diarrhea severity, colon shortening, and the increase in the colonic tissue MPO activity induced by dextran sulfate sodium (DSS) in mice, another animal model, mimicking clinical IBD. Taurine also significantly inhibited the increase in the expression of a pro-inflammatory chemokine, macrophage inflammatory protein 2 [19,20]. In a murine model of IBD-associated carcinogenesis, taurine administered in drinking water

significantly suppressed azoxymethane plus DSS-induced colon carcinogenesis [21].

Neutrophils are predominant immune cells that protect the human body against pathogenic microbes and other harmful agents through phagocytosis. In fighting exogenous pathogens, neutrophils utilize one powerful weapon in their arsenal: the generation of the strong oxidant, hypochlorous acid (HOCl) which is nature's germ killer [22]. HOCl is produced from H_2O_2 during the so-called oxidative burst by the MPO activity of the activated neutrophils in the presence of chloride ion. The escalation of MPO activity with concomitant generation of excessive HOCl, at the site of acute inflammation, can also be detrimental to host [22]. So it is necessary to detoxify or eliminate the residual excess HOCl as part of resolution of inflammation.

Taurine can act as a trap for HOCl forming the long-lived oxidant TauCl, which is more stable and less toxic than HOCl. Moreover, TauCl down-regulates the generation of pro-inflammatory mediators by phagocytic cells [15]. So taurine exerts an anti-inflammatory as well as antioxidant action by preventing cytolytic damage caused by HOCl generated by inflammatory cells, particularly neutrophils. At the beginning of inflammation occurs, neutrophils infiltrated into infected sites fight invaders and eventually die through apoptosis as a consequence of collateral host damage during oxidative burst. As the activated neutrophils undergo apoptosis, TauCl released into inflamed site stimulates the proresolving as well as anti-inflammatory action

of macrophages [23,24]. We have previously reported that TauCl upregulates HO-1 expression in macrophages and thereby facilitating the engulfment of apoptotic neutrophils as well as pathogenic agents derived from infectious microbes [25–27].

Though taurine has been extensively investigated with regards to its anti-inflammatory and antioxidative effects [8–10,28–30], there is paucity of data demonstrating the tissue-protective potential of TauCl *in vivo*. This may be partly due to the limitations on the availability of relatively large amounts of the compound. Based on the previous studies which evaluated the protective effects of taurine on experimentally induced colitis, we attempted to investigate the capability of its reactive metabolite, TauCl on TNBS-induced colonic inflammation in mice. Inflammatory cells, such as macrophages and neutrophils, secrete various cytokines and other signaling molecules that activate NF κ B and STAT3 in epithelial cells. In the present study, oral administration of TauCl inhibited the activation of these two proinflammatory transcription factors, NF κ B and their target proteins, COX-2 and cyclin D1, respectively in the colon of TNBS-treated mice. Besides anti-inflammatory activity, TauCl possesses antioxidant properties [8–10]. We have previously reported that TauCl can activate Nrf2 and thereby upregulate the expression of HO-1, which account for its potentiation of macrophage-mediated phagocytic removal of apoptotic neutrophils during the resolution of acute inflammation [24,25]. We report here that TauCl activates Nrf2 signaling by inducing its

nuclear translocation and upregulation of its target HO-1 in the colonic mucosa.

Taken these findings all together, TauCl protects against experimentally induced colitis by inhibiting proinflammatory signaling while augmenting anti-inflammatory and possibly proresolving mechanisms (Figure 8). To the best of our knowledge, this is the first report on the protective effects of TauCl on experimentally induced colitis in vivo. Though TauCl is formed endogenously, its production is transient during inflammation and limited to some immune cells, synthetic TauCl or its derivative in a more sustainable form may have a therapeutic potential in the management of IBD.

6. Reference

1. Available online: <https://www.cdc.gov/ibd/what-is-IBD.htm> (accessed on).
2. Luceri, C.; Bigagli, E.; Agostiniani, S.; Giudici, F.; Zambonin, D.; Scaringi, S.; Ficari, F.; Lodovici, M.; Malentacchi, C. Analysis of oxidative stress-related markers in crohn's disease patients at surgery and correlations with clinical findings. *Antioxidants* **2019**, *8*, 378.
3. Alemany-Cosme, E.; Sáez-González, E.; Moret, I.; Mateos, B.; Iborra, M.; Nos, P.; Sandoval, J.; Beltrán, B. Oxidative stress in the pathogenesis of Crohn's disease and the interconnection with Immuiological response, microbiota, external environmental factors, and epigenetics. *Antioxidants* **2021**, *10*, 64.
4. Elson, C.O.; Sartor, R.B.; Tennyson, G.S.; Riddell, R. Experimental models of inflammatory bowel disease. *Gastroenterology* **1995**, *109*, 1344–1367.
5. Antoniou, E.; Margonis, G.A.; Angelou, A.; Pikouli, A.; Argiri, P.; Karavokyros, I.; Papalois, A.; Pikoulis, E. The TNBS-induced colitis animal model: An overview. *Ann. Med. Surg.* **2016**, *11*, 9–15.
6. Neurath, M.; Fuss, I.; Strober, W. TNBS-colitis. *Intern. Rev. Immunol.*, **2000**, *19*, 51–62.
7. Huxtable, R.J. Physiological actions of taurine. *Physiol. Rev.* **1992**, *72*, 101–163.
8. Marcinkiewicz, J.; Kontny, E. Taurine and inflammatory diseases. *Amino Acids* **2014**, *46*, 7–20.
9. Kim, C.; Cha, Y.-N. Taurine chloramine produced from taurine under inflammation provides anti-inflammatory and cytoprotective effects. *Amino Acids* **2014**, *46*, 89–100.
10. Kang, I.S.; Kim, C. Taurine chloramine administered in vivo increases NRF2-regulated antioxidant enzyme expression in murine peritoneal macrophages. *Adv. Exp. Med. Biol.* **2013**, *775*, 259–267.

11. Jang, J.S.; Piao, S.; Cha, Y.N.; Kim, C. Taurine chloramine activates Nrf2, increases HO-1 expression and protects cells from death caused by hydrogen peroxide. *J. Clin. Biochem. Nutr.* **2009**, *45*, 37–43.
12. Gottardi, W.; Nagi, M. Chemical properties of N-chlorotaurine sodium, a key compound in the human defence system. *Arch. Pharm.* **2002**, *335*, 411–421.
13. Chami, B.; Martin, N.J.J.; Dennis, J.M.; Witting, P.K. Myeloperoxidase in the inflamed colon: A novel target for treating inflammatory bowel disease. *Arch. Biochem. Biophys.* **2018**, *645*, 61-71.
14. Hansberry, D.R., Shah, K., Agarwal, P., Agarwal, N. Fecal myeloperoxidase as a biomarker for inflammatory bowel disease. *Cureus* **2017**, *9*, e1004.
15. Lak, S.; Ostadrahimi, A.; Nagili, B.; Asghari-Jafarabadi, M.; Beigzali, S.; Salehi, F.; Djafarzadeh, R.. Anti-inflammatory effect of taurine in burned patients. *Adv. Pharm. Bull.* **2015**, *5*, 531–536.
16. Maleki, V.; Mahdavi, R.; Sharafabad, F.H.; Alizadeh, M. The effects of taurine supplementation on oxidative stress indices and inflammation biomarkers in patients with type 2 diabetes: A randomized, double-blind, placebo-controlled trial. *Diabetol. Metab. Syndr.* **2020**, *12*, 9.
17. Son, M.W.; Ko, J.I.; Doh, H.M.; Kim, W.B.; Park, T.S.; Shim, M.J.; Kim, B.K. Protective effect of taurine on TNBS-induced inflammatory bowel disease in rats. *Arch. Pharm. Res.* **1998**, *21*, 531–536.
18. Giriş, M.; Depboylu, B.; Dođru-Abbasođlu, S.; Erbil, Y.; Olgaç, V.; Alıř, H.; Aykaç-Toker, G.; Uysal, M. Effect of taurine on oxidative stress and apoptosis-related protein expression in trinitrobenzene sulphonic acid-induced colitis. *Clin. Exp. Immunol.* **2008**, *152*, 102–110.
19. Zhao, Z.; Satsu, H.; Fujisawa, M.; Hori, M.; Ishimoto, Y.; Totsuka, M.; Nambu, A.; Kakuta, S.; Ozaki, H.; Shimizu, M. Attenuation by dietary taurine of dextran sulfate sodium-induced colitis in mice and of THP-1-induced damage to intestinal Caco-2 cell monolayers. *Amino Acids* **2008**, *35*, 217–224.

20. Shimizu, M.; Zhao, Z.; Ishimoto, Y.; Satsu, H. Dietary taurine attenuates dextran sulfate sodium (DSS)-induced experimental colitis in mice. *Adv. Exp. Med. Biol.* **2009**, *643*, 265–271.
21. Wang, G.; Ma, N.; He, F.; Kawanishi, S.; Kobayashi, H.; Oikawa, S.; Murata, M. Taurine attenuates carcinogenicity in ulcerative colitis-colorectal cancer mouse model. *Oxid. Med. Cell Longev.* **2020**, *2020*, 7935917.
22. Ulfing, A.; Leichert, L.I. The effects of neutrophil-generated hypochlorous acid and other hypohalous acids on host and pathogens. *Cell. Mol. Life Sci.* **2021**, *78*, 385–414.
23. Barua, M.; Liu, Y.; Quinn, M.R. Taurine chloramine inhibits inducible nitric oxide synthase and TNF- α gene expression in activated alveolar macrophages: Decreased NF- κ B activation and I κ B kinase activity. *J. Immunol.* **2001**, *167*, 2275–2281.
24. Kanayama, A.; Inoue, J.; Sugita-Konishi, Y.; Shimizu, M.; Miyamoto, Y. Oxidation of I κ B α at methionine 45 is one cause of taurine chloramine-induced inhibition of NF- κ B activation. *J. Biol. Chem.* **2002**, *277*, 24049–24056.
25. Kim, W.; Kim, H.U.; Lee, H.N.; Kim, S.H.; Kim, C.; Cha, Y.N.; Joe, Y.; Chung, H.T.; Jang, J.; Kim, K. et al. Taurine chloramine stimulates efferocytosis through upregulation of Nrf2-mediated heme oxygenase-1 expression in murine macrophages: Possible involvement of carbon monoxide. *Antioxid. Redox Signal.* **2015**, *23*, 163–177.
26. Kim, S.H.; Zhong, X.; Kim, W.; Kim, K.; Suh, Y.G.; Kim, C.; Joe, Y.; Chung, H.T.; Cha, Y.N.; Surh, Y.J. Taurine chloramine potentiates phagocytic activity of peritoneal macrophages through up-regulation of dectin-1 mediated by heme oxygenase-1-derived carbon monoxide. *FASEB J.* **2018**, *32*, 2246–2257.
27. Kim, W.; Kim, S.H.; Jang, J.H.; Kim, C.; Kim, K.; Suh, Y.G.; Joe, Y.; Chung, H.T.; Cha, Y.N.; Surh, Y.J. Role of heme oxygenase-1 in potentiation of phagocytic activity of macrophages by taurine

- chloramine: Implications for the resolution of zymosan A-induced murine peritonitis. *Cell. Immunol.* **2018**, *327*, 36–46.
28. de Oliveira Ramos, C.; Campos, K. K. D.; de Paula Costa, G.; Cangussú, S. D.; Talvani, A.; Bezerra, F.S. Taurine treatment decreases inflammation and oxidative stress in lungs of adult mice exposed to cigarette smoke. *Regul. Toxicol. Pharmacol.* **2018**, *98*, 50-57.
29. Qaradakhi, T.; Gadanec, L. K.; McSweeney, K. R.; Abraham, J. R.; Apostolopoulos, V.; Zulli, A. Inflammatory effect of taurine on cardiovascular disease. *Nutrients* **2020**, *12*, 2847.
30. Schaffer, S. W.; Azuma, J.; Mozaffari, M. Role of antioxidant activity of taurine in diabetes. *Can. J. Physiol. Pharmacol.* **2009**, *87*, 91–99.

Chapter III

Topically Applied Taurine Chloramine Protects Against UVB-induced Oxidative Stress and Inflammation in Mouse Skin

1. Abstract

Excessive exposure to solar light, especially its UV component, is a principal cause of photoaging, dermatitis, and photocarcinogenesis. In searching for candidate substances that can effectively protect the skin from photodamage, the present study was conducted with taurine chloramine (TauCl), formed from taurine in phagocytes recruited to inflamed tissue. Irradiation with ultraviolet B (UVB) of 180 mJ/cm² intensity caused oxidative damage and apoptotic cell death in the murine epidermis. These events were blunted by topically applied TauCl, as evidenced by the lower level of 4-hydroxynonenal-modified protein, reduced proportions of TUNEL-positive epidermal cells, and suppression of caspase-3 cleavage. In addition, the expression of two prototypic inflammatory enzymes, cyclooxygenase-2 and inducible nitric oxide synthase, and transcription of some pro-inflammatory cytokines (*Tnf*, *Il6*, *Il1b*, *Il10*) were significantly lower in TauCl-treated mice than vehicle-treated control mice. The anti-inflammatory effect of TauCl was associated with inhibition of STAT3 activation and induction of antioxidant enzymes, such as heme oxygenase-1 and NAD(P)H:quinone oxidoreductase 1, through activation of nuclear factor erythroid 2-related factor 2.

Keywords

Taurine; Taurine chloramine; Skin inflammation; Heme oxygenase-1; STAT3;

Nrf2

2. Introduction

The skin is the largest organ constituting the outermost part of the human body, and it is vulnerable to external stressors [1–3]. Despite the important role of skin, intractable skin diseases are gradually increasing in modern society. Solar radiation is associated with the majority of skin disorders. Acute exposure to sunlight accounts for erythema/sunburn, tanning, and allergic contact dermatitis, whereas chronic exposure causes actinic keratosis, immunosuppression, premature aging of the skin, and melanoma [4,5]. Among the ultraviolet rays, ultraviolet A (UVA) and ultraviolet B (UVB) are the main causes of oxidative stress and inflammation on the skin [6]. UVA has weak energy intensity, but when exposed for a long period of time, it can provoke skin erythema, wrinkles, and pigmentation. UVB directly damages the skin, causing apoptosis, inflammation, and photoaging [7,8], and can also induce photocarcinogenesis [9,10]. Adequate exposure to sunlight helps to synthesize vitamin D, which facilitates calcium metabolism, improves immunity, supports cellular redox balance, and maintains homeostasis [8,11,12]. However, unbalanced and excessive production of reactive oxygen species (ROS), as a consequence of severe exposure to solar radiation, triggers various types of inflammatory responses.

Human bodies are equipped with a distinct set of substances that counteract oxidative stress and inflammatory tissue damage. Taurine, an amino sulfonic acid, is one such compound that has both antioxidant and anti-inflammatory

properties (reviewed in [13] and referenced therein). It also plays a vital role in various physiological processes [14]. Taurine is ubiquitously present in mammalian cells and tissues, and it is present at high concentrations in organs, such as the liver, heart, kidneys and brain, as well as in skeletal muscle and blood cells. Since the activity of cysteine sulfinate decarboxylase involved in the biosynthesis of taurine is low in humans, taurine is mainly supplied as part of a food or dietary supplement. It is abundant in fish and seafood and can also be obtained from meat and dairy products [15].

Human leukocytes contain 20–50 mM of taurine, and when inflammation occurs, its concentration in the inflamed site and surrounding tissues further increases [16]. Activated phagocytes, such as neutrophils, produce hydrogen peroxide (H_2O_2) in the process of defending against invading pathogens, which, in the presence of chloride, produces hypochlorous acid (HOCl) by myeloperoxidase (MPO) activity. HOCl then reacts with taurine to generate taurine chloramine (TauCl) that has strong anti-inflammatory as well as antioxidant properties [17]. The protective effects of TauCl on oxidative stress, metabolic syndrome, and inflammation have been reported [18,19]. In this study, we investigated the effect of topically applied TauCl on UVB-induced inflammation as well as oxidative stress in mouse skin.

3. Material and Methods

Materials

The crystalline sodium salt form of TauCl (MW 181.57) was prepared as described previously [20]. The primary antibody for detecting protein modified with 4-hydroxynonenal (4-HNE) was purchased from the Japan Institute for the Control of Aging (JaICA), Nikken SEIL Co., Ltd. (Shizuoka, Japan). Primary antibodies for Signal transducer and activator of transcription (STAT3), P-STAT3^{Y705}, cyclin D1, and lamin B1 were provided by Cell Signaling Technology (Danvers, MA, USA). Antibodies for detecting cyclooxygenase-2 (COX-2) and Nrf2 were purchased from Abcam (Cambridge, MA, USA). Antibodies for heme oxygenase-1 (HO-1) and inducible nitric oxide synthase (iNOS) were supplied by Enzo Life Sciences (Farmingdale, NY, USA) and BD Biosciences (San Jose, CA, USA), respectively. Antibodies for caspase-3 and its cleaved form were purchased from Cell Signaling Technology (Danvers, MA, USA).

Animals

Female SKH1-*Hr*^{hr} mice (5 to 6 weeks of age) were purchased from Orient Bio Inc. (Seongnam-si, Korea). Mice were randomly divided into four groups ($n = 3$ per group). Female SKH1 hairless mice have been shown to be more sensitive to inflammatory response, as determined by skin fold thickness and myeloperoxidase activity, as compared with males [21]. Mice were housed in

plastic cages under controlled conditions of temperature (23 ± 2 °C), humidity ($50 \pm 10\%$), and light (12/12 h light/dark cycle). All animal experiments complied with the Guide for the Care and Use of Laboratory Animals and were approved by the Institutional Animal Care and Use Committee (IACUC) at Seoul National University (IACUC number; SNU-160720-11-2).

UVB Irradiation and Treatment

For UVB irradiation, tubes (5 x 8 Watts) that emit wavelengths mainly in the UVB region, with a peak at 312 nm were used. The intensity of UVB irradiation to mouse skin was 180 mJ/cm^2 as measured by a Biolink BLX-312 (Vilber Lourmat; **Marne-la-Vallée, Paris, France**). The hairless mice were topically administered TauCl (10 μmol) dissolved in 200 μL of water: propylene glycol: ethanol solution (2:1:2, v/v) or vehicle to the dorsal skin 30 min prior to UVB irradiation. The dorsal epidermis samples of the euthanized mice were collected 6 h later. To obtain dorsal epidermis, skin was grasped with forceps, and an incision was made with scissors from the tail, past the flank, to the neck. The tissues were stored at -70 °C until use.

Histology

Parts of collected skin were fixed with 10% phosphate-buffered formalin and embedded in paraffin. Each section was stained with hematoxylin and eosin

(H&E). The H&E stained sections were examined under a light microscope (Nikon; Tokyo, Japan) to detect the presence of lesions.

Immunohistochemical Analysis

The dissected skin tissues were prepared for immunohistochemical analysis with antibodies directed against 4-HNE (JaICA; Shizuoka, Japan), COX-2 (Cell Signaling Technology; Danvers, MA, USA), and P-STAT3 (Cell Signaling Technology; Danvers, MA, USA). Five-micrometer sections of 10% formalin-fixed, paraffin-embedded tissues were deparaffinized and rehydrated in a series of xylene and ethanol. The deparaffinized sections were heated in a microwave and boiled twice for 6 min in a 10 mM citrate buffer (pH 6.0) for antigen retrieval. To diminish nonspecific staining, each section was treated with 3% hydrogen peroxide and 4% peptone casein blocking solution for 15 min. The slides were incubated with a diluted primary antibody at room temperature for 40 min in Tris-HCl-buffered saline containing 0.05% Tween 20, then incubated with a horseradish peroxidase-conjugated secondary antibody (Dako, Glostrup, Denmark). The tissues were treated with 3,3'-diaminobenzidine tetrahydrochloride to detect the peroxidase binding sites. Finally, counterstaining was performed using Mayer's hematoxylin.

Terminal Deoxynucleotidyl Transferase dUTP Nick End Labeling (TUNEL)

Assay

Apoptotic DNA fragmentation was detected by the TUNEL assay with the ApopTag[®] Peroxidase *In Situ* Apoptosis Detection Kit (Chemicon; Temecula, CA, USA). The isolated skin tissues were rinsed with phosphate-buffered saline (PBS) and fixed in 10% buffered formalin (Sigma-Aldrich; Saint Louis, MO, USA) for the TUNEL assay. The apoptotic cells were visualized under a light microscope (Nikon; Tokyo, Japan).

Immunofluorescence Staining

The skin specimens were fixed, paraffin-embedded, and sectioned, and the sections were deparaffinized and rehydrated by serial washes with graded xylene and alcohol. For immunofluorescence staining, tissue sections were boiled in 10 mM of sodium citrate (pH 6.0) for antigen retrieval, subjected to serial washing, and permeabilized for 45 min at room temperature using 0.2% Triton X-100 in PBS and blocked with 3% bovine serum albumin (BSA) in PBS for 1 h at room temperature. The tissue sections were stained with primary antibodies for P-STAT3 and Nrf2 (Cell Signaling Technology; Danvers, MA, USA) and diluted at 1:250 in 3% BSA overnight at 4 °C. After washing three times with PBS each 5 min to remove primary antibodies, tissues were incubated with appropriate secondary antibodies. Nuclei were counterstained with DAPI (Invitrogen; Carlsbad, CA, USA). Immunofluorescence images were collected on a fluorescence microscope (Nikon; Tokyo, Japan).

Tissue Lysis and Protein Extraction

The UVB-irradiated dorsal skin of mice was collected as described above, and fat was removed on ice to attain the epidermis. Collected epidermis was homogenized with the lysis buffer (20 mM Tris-HCl (pH 7.5), 150 mM NaCl, 1 mM Na₂EDTA, 1 mM EGTA, 1% Triton, 2.5 mM sodium pyrophosphate, 1 mM β -glycerophosphate, 1 mM Na₃VO₄, 1 μ g/mL leupeptin, 1 mM phenylmethyl sulfonylfluoride (PMSF), and an EDTA-free cocktail tablet) in an ice bath. The lysates were vortexed every 10 min for 3 h on the ice, followed by centrifugation (13,000 \times g, 15 min at 4 °C). The supernatants were collected and stored at -70 °C until use.

Preparation of Cytosolic and Nuclear Extracts

The fat-free dorsal skin tissues were homogenized with 1 mL buffer A (10 mM 4-(2-hydroxyethyl)-1-piperazineethanesulfonic acid (HEPES, pH 7.8), 1.5 mM MgCl₂, 10 mM KCl, 0.5 mM dithiothreitol (DTT), 0.2 mM PMSF) followed by vortex-mixing every 10 min for 3 h in an ice bath. The lysates were mixed with 0.1% Nonidet P-40 (NP-40) 30 min before centrifugation. After centrifugation at 13,000 \times g for 15 min, the supernatants (the cytosolic extracts) were collected. The precipitated nuclear pellets were washed three times with buffer A containing 0.625% NP-40 to remove a residual cytosolic fraction. Nuclear pellets were then resuspended in 300 μ L of buffer C (20 mM

HEPES (pH 7.8), 420 mM NaCl, 1.5 mM MgCl₂, 0.2 mM EDTA, 0.5 mM DTT, 0.2 mM PMSF and 20% glycerol). The nuclear lysates were vortexed every 10 min for 1 h, followed by centrifugation at 13,000× g for 15 min. The supernatants (nuclear extracts) were collected and kept at −70 °C until use.

Western Blot Analysis

The protein concentration in lysates was measured by using the PierceTM BCA Protein Assay Kit (Thermo Fisher Scientific; Rockford, IL, USA). The protein lysates were loaded on 7–15% SDS-polyacrylamide gel, and electrophoresis was performed under reducing conditions. Protein was transferred to the polyvinylidene difluoride membrane (PALL Life Sciences; Washington, NY, USA). The membranes were blocked with 5% non-fat, dry milk in Tris-buffered saline containing 0.1% Tween 20 (TBST) for 1 h at room temperature. After overnight incubation at 4 °C with diluted primary antibodies, the membranes were washed three times with TBST buffer for 10 min each. Then, membranes were incubated with a 1:5000 dilution of horseradish peroxidase-conjugated secondary antibody (Invitrogen; Carlsbad, CA, USA) for 1 h at room temperature, and washed again three times with TBST buffer. The protein expression was visualized with an enhanced chemiluminescent (ECL) detection kit (Absignal) (Abclon; Seoul, Korea) and LAS-4000 image reader (Fujifilm; Tokyo, Japan).

Real-Time Quantitative PCR (qPCR)

Total RNA was isolated from mouse skin tissues using TRIzol[®] reagent (Invitrogen; Carlsbad, CA, USA), according to the manufacturer's protocol. To synthesize the complementary DNA (cDNA), 1 µg of total RNA was reverse-transcribed with Moloney murine leukemia virus reverse transcriptase (Promega; Madison, WI, USA) for 50 min at 42 °C and again for 15 min at 72 °C. qPCR analysis was carried out in a 7500 Fast Real-Time PCR Instrument System (Applied Biosystems; Foster City, CA, USA) using the RealHelix[™] qPCR Kit (Green) (NanoHelix Co., Ltd.; Daejeon, Korea). The primers used for each qPCR reactions are as follows: *Il6*, 5'-TCT ATA CCA CTT CAC AAG TCG GA-3' and 5'-GAA TTG CCA TTG CAC AAC TCT TT-3'; *Ptgs2*, 5'-TTC CAA TCC ATG TCA AAA CCG T-3' and 5'-AGT CCG GGT ACA GTC ACA CTT-3'; *Nos2*, 5'-GTT CTC AGC CCA ACA ATA CAA GA-3' and 5'-GTG GAC GGG TCG ATG TCA C-3'; *Tnf*, 5'-CAG GCG GTG CCT ATG TCT C-3' and 5'-CGA TCA CCC CGA AGT TCA GTA G-3'; *Il1b*, 5'-TTC AGG CAG GCA GTA TCA CTC-3' and 5'-GAA GGT CCA CGG GAA AGA CAC-3'; *Il10*, 5'-GCT GGA CAA CAT ACT GCT AAC C-3' and 5'-ATT TCC GAT AAG GCT TGG CAA-3'; *Hmox1*, 5'-AGG TAC ACA TCC AAG CCG AGA-3' and 5'-CAT CAC CAG CTT AAA GCC TTC T-3'; *Nqo1*, 5'-AGG ATG GGA GGT ACT CGA ATC-3' and 5'-TGC TAG AGA TGA CTC GGA AGG-3'; *Gclc*, 5'- GGC TAC TTC TGT ACT AGG AGA GC-3' and 5'- TGC CGG ATG TTT CTT GTT AGA G-3'; *Gss*, 5'- CCC ATT CAC

GCT TTT CCC CT-3' and 5'-GGG CAG TAT AGT CGT CCT TTT TG-3';
Gapdh, 5'-AGG TCG GTG TGA ACG GAT TTG-3' and 5'-TGT AGA CCA
TGT AGT TGA GGT CA-3' (forward and reverse, respectively). The analysis
was performed in a 20 μ L final volume of reaction mixtures containing 10 μ L
of 2X Premix (Green) and 300 nM of each primer (forward and reverse). After
an enzyme activation at 95 °C for 15 min, 40 cycles for amplification were
performed at 95 °C for 20 s for denaturation and at 60 °C for 40 s for
annealing, extension, and fluorescence acquisition.

Statistical Analysis

All the values were expressed as the mean \pm standard deviation (SD) of at
least three independent experiments. Statistical significance was determined
by the Student's *t*-test, or one-way ANOVA, followed by Tukey's multiple
comparisons for post-hoc test, and $p < 0.05$ was considered to be statistically
significant. All the statistical analyses were applied using GraphPad Prism 8.0
(GraphPad Software; San Diego, CA, USA).

4. Results

UVB-Induced Oxidative Stress and Apoptosis Were Attenuated in TauCl-Treated Mice

Exposure to UVB irradiation leads to cutaneous inflammation and oxidative stress [6–8]. The images of H&E stained epidermal skin sections demonstrated attenuation of the skin hyperplasia and infiltration of inflammatory cells in TauCl-treated mice (**Fig. 3-1A**). ROS-mediated oxidative stress causes lipid peroxidation and apoptotic DNA fragmentation [22,23]. The accumulation of 4-HNE, the end-product of lipid peroxidation, was abrogated by topical application of TauCl (**Fig. 3-1A, B**). TauCl treatment also reduced the production of TUNEL-positive apoptotic cells (**Fig. 3-1A**) and the cleavage of caspase-3, a hallmark of apoptotic cell death, in whole lysates (**Fig. 3-1C**).

UVB-Induced Acute Skin Inflammation Was Ameliorated in TauCl-Treated mice skin

Aberrant overexpression of COX-2 and iNOS has been reported in murine models of dermatitis and photocarcinogenesis induced by UVB irradiation [24,25]. Immunohistochemical analysis was performed for detecting the expression level of COX-2 in mouse skin. As shown in **Fig. 3-2A**, topical application of TauCl ameliorated UVB-induced expression of COX-2, and this was verified by Western blot analysis (**Fig. 3-2B**). The UVB-induced

expression of iNOS, another prototypic pro-inflammatory enzyme, was also attenuated by topically applied TauCl (**Fig. 3-2B**). The analyses were performed with total protein lysates. Similarly, expression of genes encoding inflammation-associated cytokines (*Tnf*, *Il6*, *Il1b* and *Il10*), as well as *Ptgs2* and *Nos2* encoding COX-2 and iNOS, respectively, was diminished by TauCl treatment (**Fig. 3-3**).

UVB-Induced Phosphorylation of STAT3 Was Blunted by Topical

Application of TauCl

STAT3 is a key transcription factor that regulates immunity and inflammation by promoting pro-inflammatory factors [26,27]. The phosphorylation of the tyrosine 705 residue of STAT3 facilitates its translocation into the nucleus, where it regulates the transcription of the target genes. The topical application of TauCl reduced the expression of phosphorylated STAT3 (P-STAT3) in mouse skin, as measured by immunohistochemical analysis (**Fig. 3-4A**) and immunofluorescence staining (**Fig. 3-4B**), which was confirmed by Western blot analysis (**Fig. 3-5A**). TauCl also inhibited the nuclear translocation of P-STAT3 in UVB-irradiated mouse skin (**Fig. 3-5B**). The expression of cyclin D1, a major target of P-STAT3, was also decreased in the same tendency (**Fig. 3-5C**).

Topical Application of TauCl Upregulates Cytoprotective Gene Expression through Nrf2 Activation

Homeostatic imbalance is implicated in the pathogenesis of various disorders, such as autoimmune disease, inflammation, and tumorigenesis [28]. The master transcription factor Nrf2 plays a prominent role in the transcriptional regulation of stress-responsive genes, many of which encode antioxidant and anti-inflammatory proteins, including HO-1. The elevated expression of Nrf2 in the TauCl-treated mouse skin tissue was revealed by immunofluorescence staining (**Fig. 3-6A**), and the localization of Nrf2 in the nucleus was confirmed by Western blot analysis (**Fig. 3-6B**). There was a pronounced increase in the expression of HO-1 (**Fig. 3-6C**) and its mRNA transcript, as well as transcription of other Nrf2 target antioxidant genes (**Fig. 3-6D**).

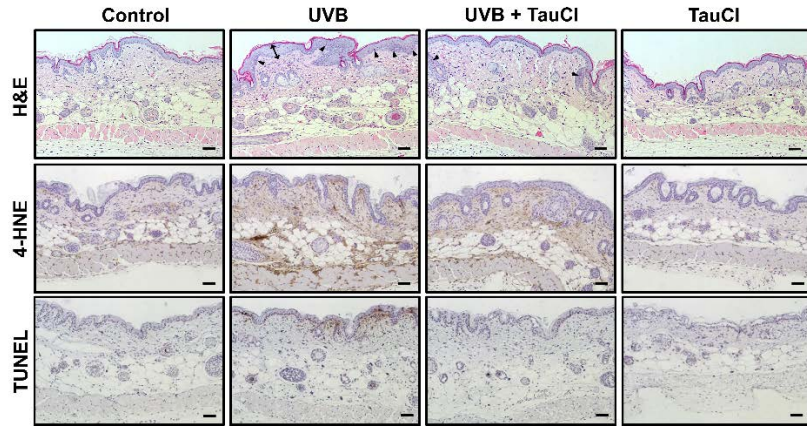
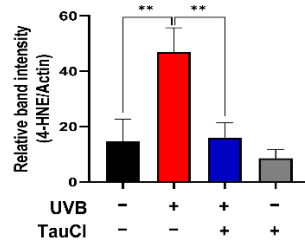
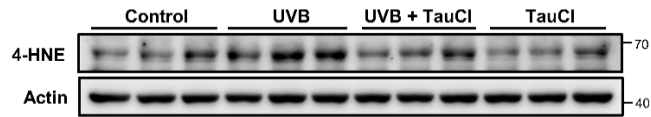
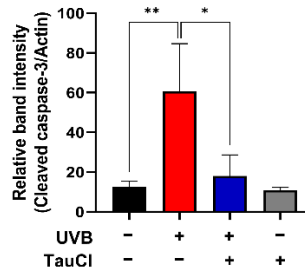
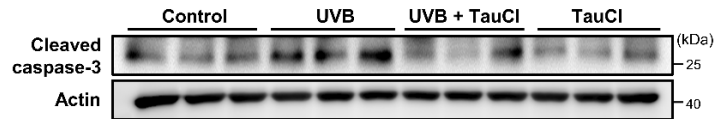
A**B****C**

Figure 3-1. UVB-induced oxidative stress and apoptotic cell death were ameliorated in TauCl-treated mouse skin. (A) Skin thickness (double-headed arrow) and leukocyte infiltration (arrow head) were detected by H&E staining. Immunohistochemical analysis of 4-HNE-modified proteins (brown spots) and TUNEL-positive apoptotic cells in mouse epidermis. Magnification $\times 100$. (B) The expression levels of 4-HNE-modified protein in UVB-irradiated mouse skin tissue with and without TauCl application were determined by Western blot analysis. Actin was used as an equal loading control. (C) Apoptosis was detected by measuring cleavage of caspase-3 by Western blot analysis. Data are analyzed by one-way ANOVA and expressed as means \pm SD ($n = 3$ per group). *, ** Significantly different between groups compared (* $p < 0.05$; ** $p < 0.01$).

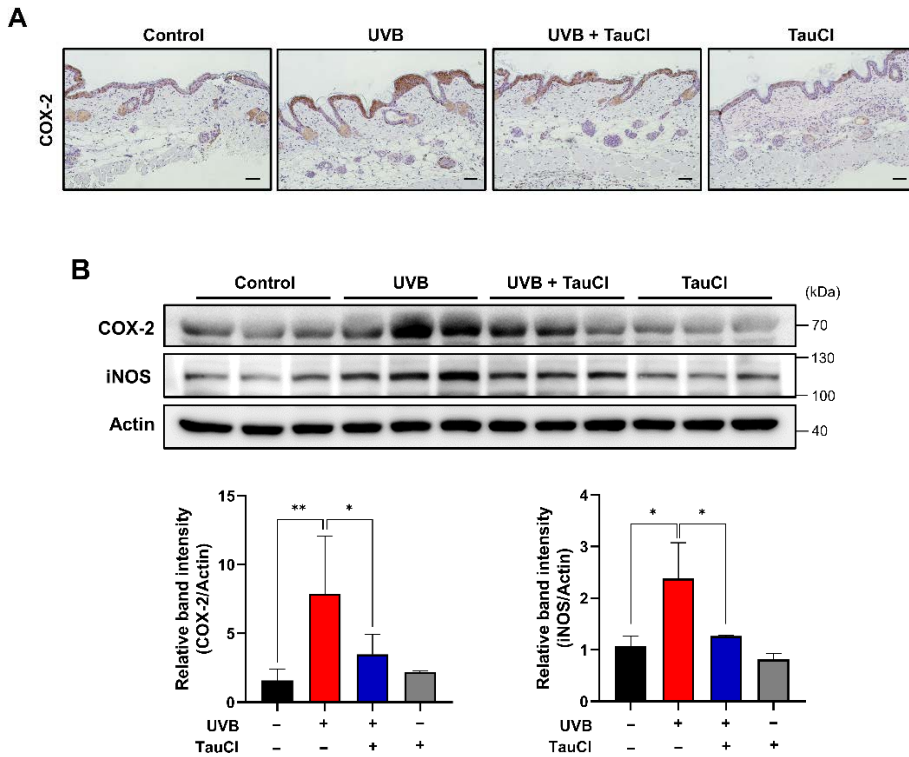


Figure 3-2. The expression of UVB-induced inflammatory enzymes was attenuated by topical application of TauCl. (A) Immunohistochemical analysis was performed for detecting COX-2 as described in Materials and Methods. (B) The expression levels of pro-inflammatory enzymes COX-2 and iNOS were measured by Western blot analysis of whole protein lysates. Actin was used as an equal loading control. Results are analyzed by one-way ANOVA and expressed as means \pm SD ($n = 3$ per group. * ** Significantly different between groups compared (* $p < 0.05$; ** $p < 0.01$).

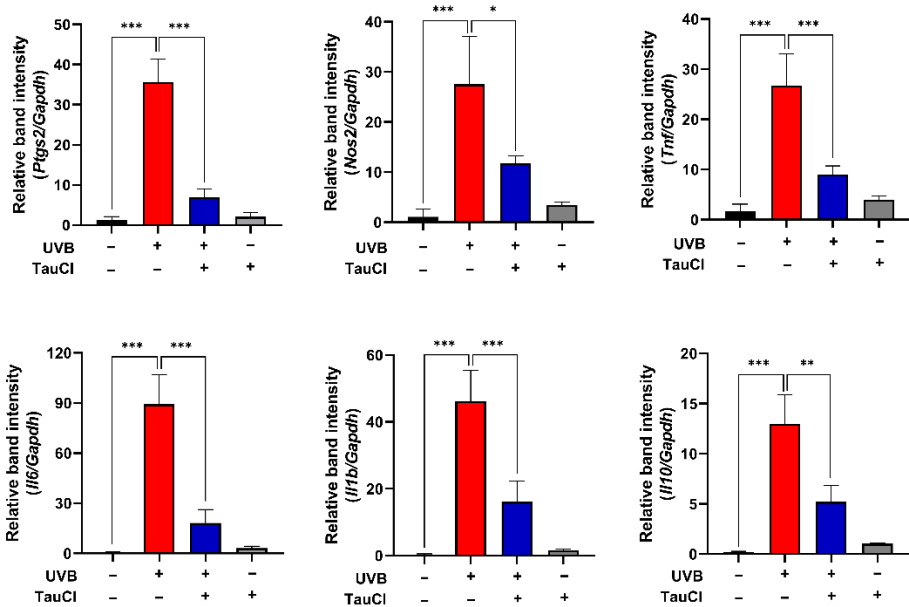


Figure 3-3. TauCl application inhibited UVB-induced expression of pro-inflammatory cytokines and enzymes in mouse skin. qPCR analysis of mRNA transcripts for pro-inflammatory cytokines (*Tnf*, *Il6*, *Il1b*, *Il10*) and enzymes (*Ptg2*, *Nos2*). The treatment conditions and other experimental details are as described in Materials and Methods. Results are analyzed by one-way ANOVA and expressed as means \pm SD ($n = 3$ per group). *, **, *** Significantly different between groups compared (* $p < 0.05$; ** $p < 0.01$; *** $p < 0.001$).

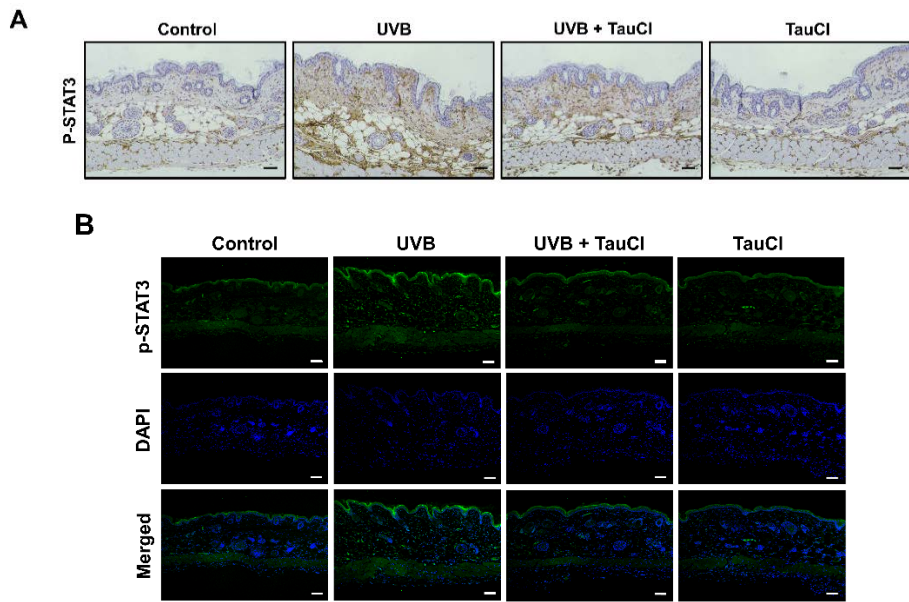
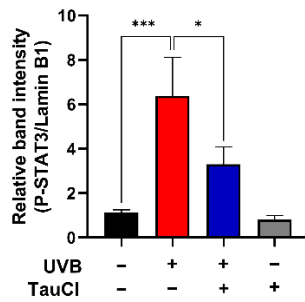
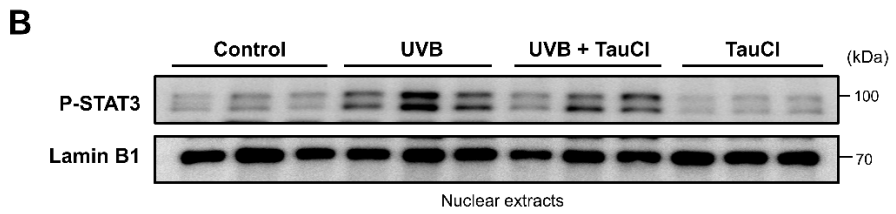
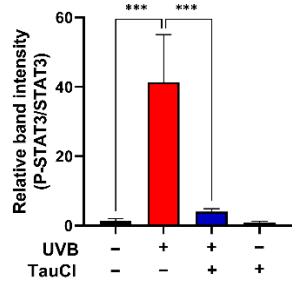
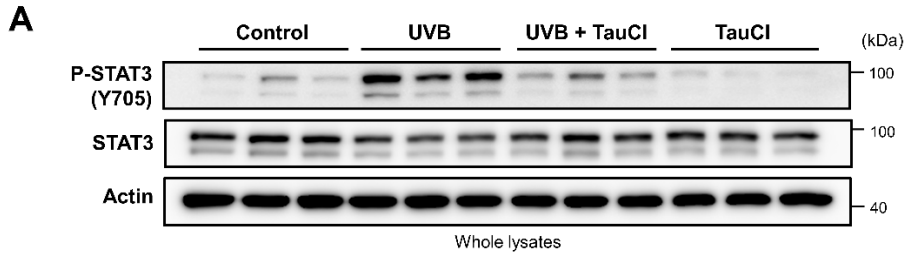


Figure 3-4. Topically applied TauCl attenuated UVB-induced phosphorylation of STAT3 in mouse skin. (A,B) Expression of P-STAT3 was measured by immunohistochemical analysis (A) and immunofluorescence staining (B). Scale bar, 200 μ m.



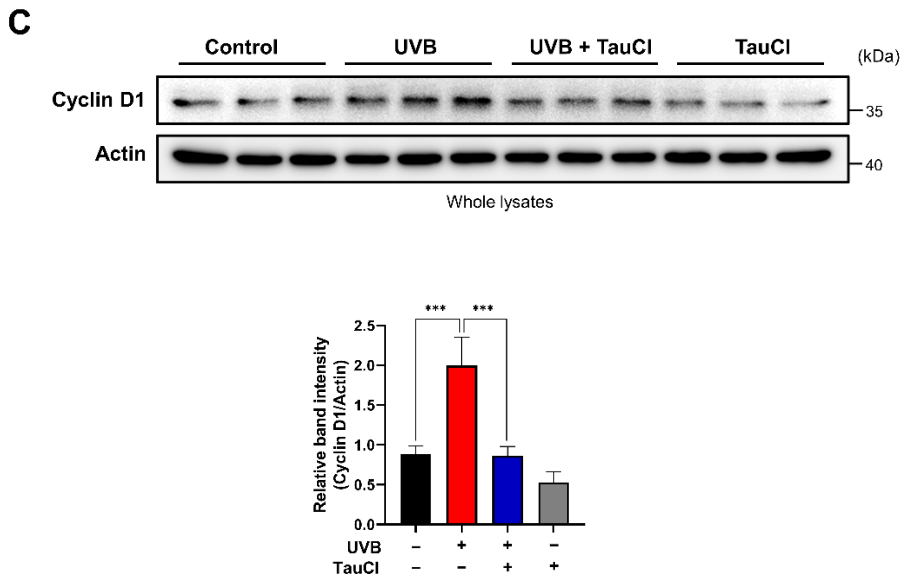


Figure 3-5. UVB-induced phosphorylation of STAT3 was diminished in TauCI-treated mouse skin. (A,B) The expression (A) and nuclear accumulation (B) of the phosphorylated STAT3 was measured by Western blot analysis. (C) The expression of Cyclin D1, a principal target protein of P-STAT3, was measured by Western blot analysis. Actin was used as an equal loading control. Data are expressed as means \pm SD ($n = 3$ per group), analyzed by one-way ANOVA. *,*** Significantly different between groups compared (* $p < 0.05$; *** $p < 0.001$).

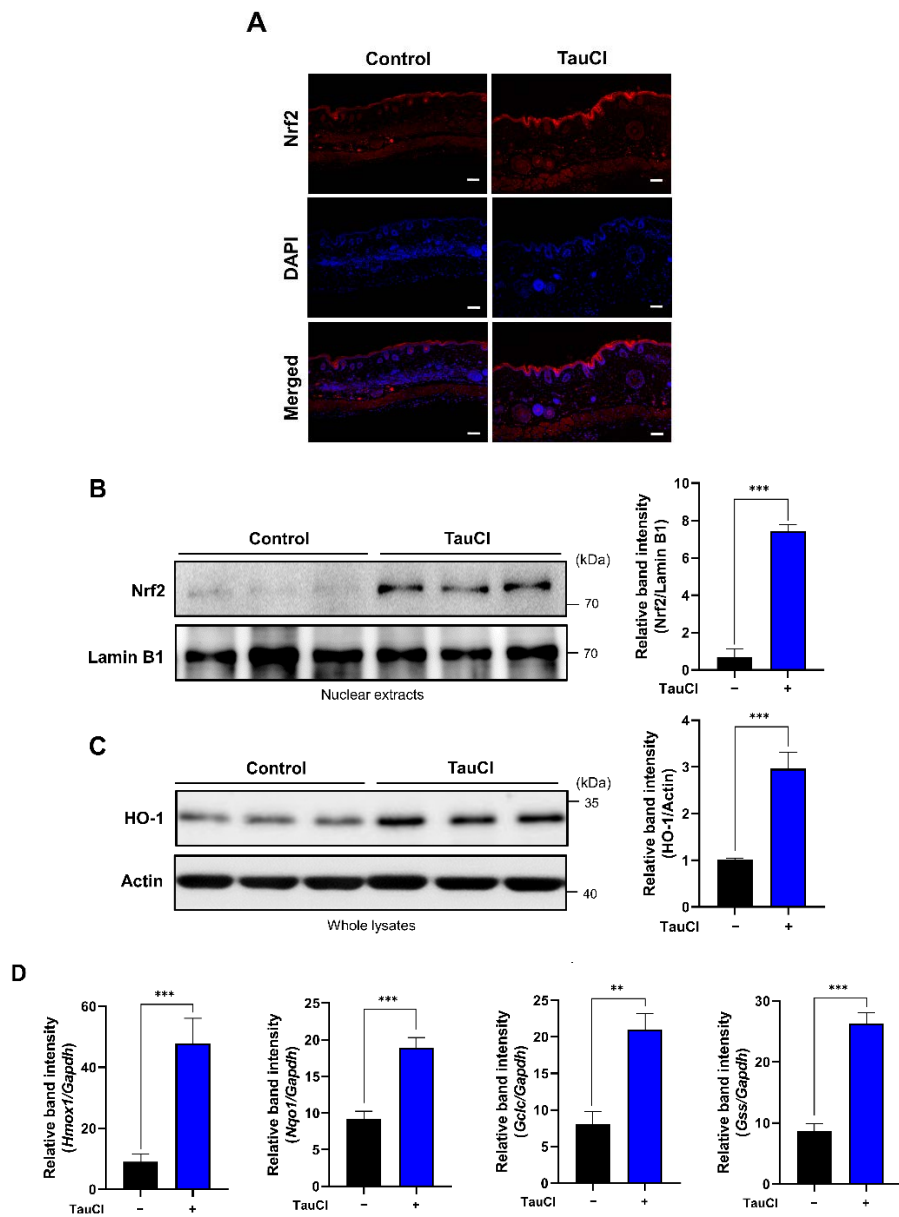


Figure 3-6. The Nrf2-mediated expression of antioxidant enzymes was elevated in TauCl-treated mice. (A,B) Nuclear localization of Nrf2 was assessed by immunofluorescence staining (A) and Western blot analysis (B). (C) The expression of HO-1 was determined by Western blot analysis. (D) Nrf2-mediated antioxidant gene expression was measured by qPCR. Results

are expressed as means \pm SD ($n = 3$ for each group), analyzed by Student's t -test. **,*** Significantly different between groups compared (** $p < 0.01$; *** $p < 0.001$). Scale bar, 200 μm .

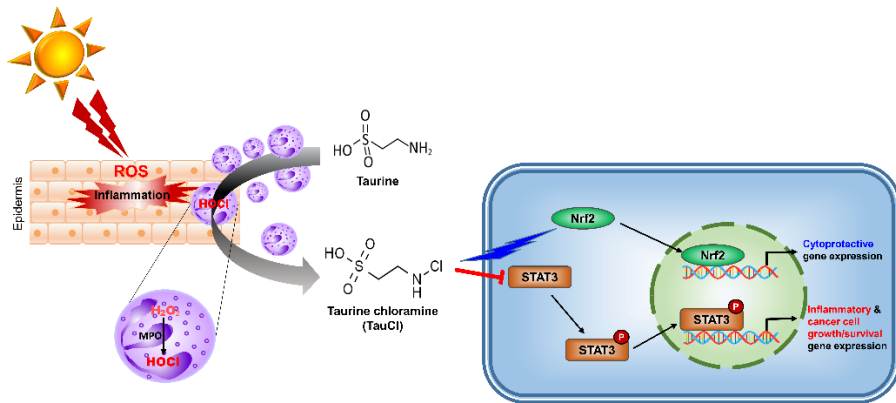


Figure 3-7. A proposed molecular mechanism underlying the protective effects of TauCl against UVB-induced dermatitis. Exposure to UVB causes inflammatory injury to the skin. Activated neutrophils recruited to the inflamed site generate ROS, such as hydrogen peroxide, with concomitant release of myeloperoxidase (MPO). MPO catalyzes the reaction of hydrogen peroxide and chloride ion to produce hypochlorous acid (HOCl). HOCl is a strong oxidant and is neutralized by reacting with taurine, which produces TauCl. TauCl exerts antioxidant and anti-inflammatory effects by activating Nrf2 and blocking STAT3 signaling, leading to protection against UVB-induced skin damage.

5. Discussion

Taurine, also called 2-aminoethylsulfonic acid, is one of the amino sulfonic acids involved in various physiologic and pharmacologic processes [14,29,30]. It is found in organs through which a large amount of blood flow passes including the brain and heart, and it is also in high concentrations in some immune cells, especially neutrophils and monocytes [14]. From a microscopic point of view, taurine regulates the balance of electrolytes and minerals in cells, but from a more expanded macro point of view, it supports the immune system through antioxidant and anti-inflammatory functions. The health beneficial effects of taurine have been extensively investigated and well documented, and dietary supplements containing taurine are popular [30,31].

Though taurine provides diverse health benefits, there is a paucity of data in regard to its photoprotective effects. In one study, accumulation of taurine protected keratinocytes from UVB-induced apoptosis by regulating the osmosis through taurine transporter (TAUT) in human skin [32]. In cases of psoriasis patients, it was confirmed that the concentration of neutrophil taurine was lower as compared with normal subjects, suggesting the role for taurine in the body's defense against skin inflammation [33]. Taurine reduced the generation of malondialdehyde, a marker for oxidative stress, and enhanced the collagen synthesis and the tensile strength, thereby accelerating wound healing [34].

Unlike chemically induced skin inflammation, the UVB-induced murine dermatitis model is useful in identifying the photoprotective substances and investigating their underlying molecular mechanisms [5,35,36]. Local skin inflammation caused by UVB irradiation is often associated with activation of NF- κ B and STAT3 responsible for transcriptional regulation of diverse proinflammatory cytokines and enzymes, including COX-2 and iNOS [37–39]. ROS is inevitably produced by oxidative phosphorylation in mitochondria as well as metabolism of xenobiotics and some endogenous substances, particularly those undergoing redox cycling. Under physiological conditions, the generation of ROS is balanced by the cellular antioxidant defense system. However, the redox balance is disrupted by external factors, such as air pollution, ionizing radiation, microbial infection, chemicals, etc., which lead to DNA damage or cell death [40–42]. In the short term, ROS-mediated oxidative stress evokes oxidative damage to biomolecules, including membrane lipids. In the long term, it causes photoaging and photocarcinogenesis.

While it is unclear how taurine exerts a protective effect against oxidative damage to various tissues in the human body including the skin, its efficacy has been evaluated largely in animal studies. Under excessive oxidative stress or inflammatory conditions, the human body responds by stimulating immune cells and modulating expression/production of pro- and anti-inflammatory mediators [43]. ROS are formed in the process of inflammation-mediated

tissue damage. Among these, hydrogen peroxide (H₂O₂) is converted to highly toxic HOCl through reaction with chloride ion, which is catalyzed by MPO [44,45]. Taurine reacts with HOCl to form TauCl, which is less toxic and has a strong antioxidant effect. TauCl not only ameliorates oxidative stress, but also suppresses the production of inflammatory mediators and stimulates the proliferation of activated immune cells [16,18,46,47].

Based on the research on antioxidant and anti-inflammatory actions exerted by taurine [13,14,48], we attempted to investigate the protective effect of TauCl on UVB-induced skin inflammation and underlying mechanisms. ROS production as a consequence of sustained UVB irradiation can cause oxidative stress and cell death [10]. In the present study, topical application of TauCl inhibited the expression of 4-HNE, the product of lipid peroxidation; cleavage of caspase-3, a marker for apoptosis; and activation of the pro-inflammatory transcription factor STAT3 and expression of its target protein, cyclin D1. It also suppressed the expression of COX-2, iNOS, and selected pro-inflammatory cytokines.

TauCl was found to regulate Nrf2-mediated antioxidant gene expression [18,49]. Our previous studies have demonstrated that TauCl potentiates the phagocytic and efferocytic capability of macrophages through Nrf2-mediated HO-1 upregulation [50,51]. In this study, the topical application of TauCl induced the accumulation of Nrf2 in the nucleus, thereby increasing the Nrf2-mediated anti-oxidant gene expression. The role of TauCl in phagocytic

removal of apoptotic neutrophils, as well as dying epidermal cells in the context of resolution of UVB-irradiated mouse skin, merits further investigation.

In conclusion, TauCl reduces the expression of proinflammatory factors by fortifying antioxidant systems and inhibiting oxidative cell death in mouse skin. Thus, it protects against UVB-induced skin inflammation by promoting the expression of Nrf2-mediated antioxidant/anti-inflammatory enzymes, while suppressing pro-inflammatory gene expression (**Fig. 3-7**). The amount of TauCl that is produced in response to inflammation is not sufficient enough to resolve inflammation effectively. In this context, direct application of exogenous TauCl onto skin can potentiate the cytoprotection against UVB-induced inflammation as well as oxidative tissue injury. The results of our present work suggest the possibility of TauCl as a lead compound in the development of effective therapeutics targeting dermatitis.

6. References

1. Quaresma, J.A.S. Organization of the skin immune system and compartmentalized immune responses in infectious diseases. *Clin. Microbiol. Rev.* **2019**, *32*, doi:10.1128/CMR.00034-18.
2. Handfield, C.; Kwock, J.; MacLeod, A.S. Innate antiviral immunity in the skin. *Trends Immunol.* **2018**, *39*, 328–340, doi:10.1016/j.it.2018.02.003.
3. Egawa, G.; Kabashima, K. Barrier dysfunction in the skin allergy. *Allergol. Int.* **2018**, *67*, 3–11, doi:10.1016/j.alit.2017.10.002.
4. D’Orazio, J.; Jarrett, S.; Amaro-Ortiz, A.; Scott, T. UV radiation and the skin. *Int. J. Mol. Sci.* **2013**, *14*, 12222–12248, doi:10.3390/ijms140612222.
5. Ryser, S.; Schuppli, M.; Gauthier, B.; Hernandez, D.R.; Roye, O.; Hohl, D.; German, B.; Holzwarth, J.A.; Moodycliffe, A.M. UVB-induced skin inflammation and cutaneous tissue injury is dependent on the MHC class I-like protein, CD1d. *J. Invest. Dermatol.* **2014**, *134*, 192–202, doi:10.1038/jid.2013.300.
6. Andrew, R.; Blaustein, C.S. Ultraviolet radiation. In *Encyclopedia of Biodiversity*, 2nd ed.; Simon, A.L., Ed.; Elsevier: Amsterdam, The Netherlands, 2013; pp. 296–303.
7. Gilchrest, B.A. Photoaging. *J. Invest. Dermatol.* **2013**, *133*, E2–E6, doi:10.1038/skinbio.2013.176.

8. Kammeyer, A.; Luiten, R.M. Oxidation events and skin aging. *Ageing Res. Rev.* **2015**, *21*, 16–29, doi:10.1016/j.arr.2015.01.001.
9. Afaq, F.; Adhami, V.M.; Mukhtar, H. Photochemoprevention of ultraviolet B signaling and photocarcinogenesis. *Mutat. Res.* **2005**, *571*, 153–173, doi:10.1016/j.mrfmmm.2004.07.019.
10. Halliday, G.M. Inflammation, gene mutation and photoimmunosuppression in response to UVR-induced oxidative damage contributes to photocarcinogenesis. *Mutat. Res.* **2005**, *571*, 107–120, doi:10.1016/j.mrfmmm.2004.09.013.
11. Berridge, M.J. Vitamin D, reactive oxygen species and calcium signalling in ageing and disease. *Philos. Trans. R. Soc. Lond. B Biol. Sci.* **2016**, *371*, 20150434, doi:10.1016/j.nmd.2017.06.356.
12. Stengel, F. Homeostasis in topical photoprotection: Getting the spectral balance right. *Am. J. Clin. Dermatol.* **2018**, *19*, 40–44, doi:10.1007/s40257-018-0369-2.
13. Arthur, P.; Terrill, J.; Grounds, M. Taurine: An anti-inflammatory and antioxidant with strong potential benefits for Duchenne muscular dystrophy. *Neuromusc. Disord.* **2017**, *27*, S191–S192, doi:10.1016/j.nmd.2017.06.356.
14. Huxtable, R.J. Physiological actions of taurine. *Physiol. Rev.* **1992**, *72*, 101–163, doi:10.1152/physrev.1992.72.1.101.

15. Geggel, H.S.; Ament, M.E.; Heckenlively, J.R.; Martin, D.A.; Kopple, J.D. Nutritional requirement for taurine in patients receiving long-term parenteral nutrition. *N. Engl. J. Med.* **1985**, *312*, 142–146, doi:10.1056/NEJM198501173120302.
16. Schuller-Levis, G.B.; Park, E. Taurine and its chloramine: Modulators of immunity. *Neurochem. Res.* **2004**, *29*, 117–126, doi:10.1023/b:nere.0000010440.37629.17.
17. Marcinkiewicz, J.; Kontny, E. Taurine and inflammatory diseases. *Amino Acids* **2014**, *46*, 7–20, doi:10.1007/s00726-012-1361-4.
18. Kim, C.; Cha, Y.N. Taurine chloramine produced from taurine under inflammation provides anti-inflammatory and cytoprotective effects. *Amino Acids* **2014**, *46*, 89–100, doi:10.1007/s00726-013-1545-6.
19. Kim, C.; Kang, I.S. Taurine chloramine, a taurine metabolite from activated neutrophils, inhibits osteoclastogenesis by suppressing NFATc1 expression. *Adv. Exp. Med. Biol.* **2015**, *803*, 99–107, doi:10.1007/978-3-319-15126-7_9.
20. Gottardi, W.; Nagl, M. Chemical properties of *N*-chlorotaurine sodium, a key compound in the human defence system. *Arch. Pharm.* **2002**, *335*, 411–421, doi:10.1002/1521-4184(200212)335:9<411::AID-ARDP411>3.0.CO;2-D.
21. Thomas-Ahner, J.M.; Wulff, B.C.; Tober, K.L.; Kusewitt, D.F.; Riggenschach, J.A.; Oberyszyn, T.M. Gender differences in UVB-

induced skin carcinogenesis, inflammation, and DNA damage.

Cancer Res. **2007**, *67*, 3468–3474, doi:10.1158/0008-5472.CAN-06-3798.

22. Lundgren, C.A.K.; Sjostrand, D.; Biner, O.; Bennett, M.; Rudling, A.; Johansson, A.L.; Brzezinski, P.; Carlsson, J.; von Ballmoos, C.; Hogbom, M. Scavenging of superoxide by a membrane-bound superoxide oxidase. *Nat. Chem. Biol.* **2018**, *14*, 788–793, doi:10.1038/s41589-018-0072-x.
23. Higuchi, Y. Chromosomal DNA fragmentation in apoptosis and necrosis induced by oxidative stress. *Biochem. Pharmacol.* **2003**, *66*, 1527–1535, doi:10.1016/s0006-2952(03)00508-2.
24. Gu, M.; Singh, R.P.; Dhanalakshmi, S.; Agarwal, C.; Agarwal, R. Silibinin inhibits inflammatory and angiogenic attributes in photocarcinogenesis in SKH-1 hairless mice. *Cancer Res.* **2007**, *67*, 3483–3491, doi:10.1158/0008-5472.CAN-06-3955.
25. Abbas, S.; Alam, S.; Pal, A.; Kumar, M.; Singh, D.; Ansari, K.M. UVB exposure enhanced benzanthrone-induced inflammatory responses in SKH-1 mouse skin by activating the expression of COX-2 and iNOS through MAP kinases/NF-kappaB/AP-1 signalling pathways. *Food Chem. Toxicol.* **2016**, *96*, 183–190, doi:10.1016/j.fct.2016.07.034.

26. Yu, H.; Pardoll, D.; Jove, R. STATs in cancer inflammation and immunity: A leading role for STAT3. *Nat. Rev. Cancer* **2009**, *9*, 798–809, doi:10.1038/nrc2734.
27. Fan, Y.; Mao, R.; Yang, J. NF-kappaB and STAT3 signaling pathways collaboratively link inflammation to cancer. *Protein Cell* **2013**, *4*, 176–185, doi:10.1007/s13238-013-2084-3.
28. Kotas, M.E.; Medzhitov, R. Homeostasis, inflammation, and disease susceptibility. *Cell* **2015**, *160*, 816–827, doi:10.1016/j.cell.2015.02.010.
29. Jakaria, M.; Azam, S.; Haque, M.E.; Jo, S.H.; Uddin, M.S.; Kim, I.S.; Choi, D.K. Taurine and its analogs in neurological disorders: Focus on therapeutic potential and molecular mechanisms. *Redox Biol.* **2019**, *24*, 101223, doi:10.1016/j.redox.2019.101223.
30. Froger, N.; Moutsimilli, L.; Cadetti, L.; Jammoul, F.; Wang, Q.P.; Fan, Y.; Gaucher, D.; Rosolen, S.G.; Neveux, N.; Cynober, L.; et al. Taurine: The comeback of a nutraceutical in the prevention of retinal degenerations. *Prog. Retin. Eye Res.* **2014**, *41*, 44–63, doi:10.1016/j.preteyeres.2014.03.001.
31. Guta, R.C. Is taurine a pharmacconutrient? *J. Pharmacol. Ther. Res.* **2018**, *2*, 18–20, doi:10.35841/pharmacology.2.2.18-20.
32. Janeke, G.; Siefken, W.; Carstensen, S.; Springmann, G.; Bleck, O.; Steinhart, H.; Hoyer, P.; Wittern, K.P.; Wenck, H.; Stab, F.; et al.

Role of taurine accumulation in keratinocyte hydration. *J. Invest.*

Dermatol. **2003**, *121*, 354–361, doi:10.1046/j.1523-

1747.2003.12366.x.

33. Stapleton, P.P.; Molloy, A.M.; Rogers, S.; Bloomfield, F.J.
Neutrophil taurine in psoriasis. *Ir. J. Med. Sci.* **1996**, *165*, 173–176,
doi:10.1007/BF02940245.
34. Degim, Z.; Celebi, N.; Sayan, H.; Babul, A.; Erdogan, D.; Take, G.
An investigation on skin wound healing in mice with a taurine-
chitosan gel formulation. *Amino Acids* **2002**, *22*, 187–198,
doi:10.1007/s007260200007.
35. Hruza, L.L.; Pentland, A.P. Mechanisms of UV-induced
inflammation. *J. Invest. Dermatol.* **1993**, *100*, 35S–41S,
doi:10.1111/1523-1747.ep12355240.
36. De Gruijl, F.R.; Forbes, P.D. UV-induced skin cancer in a hairless
mouse model. *Bioessays* **1995**, *17*, 651–660,
doi:10.1002/bies.950170711.
37. Yum, H.W.; Kim, S.H.; Kang, J.X.; Surh, Y.J. Amelioration of UVB-
induced oxidative stress and inflammation in fat-1 transgenic mouse
skin. *Biochem. Biophys. Res. Commun.* **2018**, *502*, 1–8,
doi:10.1016/j.bbrc.2018.05.093.
38. Kim, D.J.; Angel, J.M.; Sano, S.; DiGiovanni, J. Constitutive
activation and targeted disruption of signal transducer and activator

- of transcription 3 (Stat3) in mouse epidermis reveal its critical role in UVB-induced skin carcinogenesis. *Oncogene* **2009**, 28, 950–960, doi:10.1038/onc.2008.453.
39. Fisher, G.J.; Datta, S.C.; Talwar, H.S.; Wang, Z.Q.; Varani, J.; Kang, S.; Voorhees, J.J. Molecular basis of sun-induced premature skin ageing and retinoid antagonism. *Nature* **1996**, 379, 335–339, doi:10.1038/379335a0.
40. D’Autreaux, B.; Toledano, M.B. ROS as signalling molecules: Mechanisms that generate specificity in ROS homeostasis. *Nat. Rev. Mol. Cell Biol* **2007**, 8, 813–824, doi:10.1038/nrm2256.
41. Apel, K.; Hirt, H. Reactive oxygen species: Metabolism, oxidative stress, and signal transduction. *Annu. Rev. Plant. Biol.* **2004**, 55, 373–399, doi:10.1146/annurev.arplant.55.031903.141701.
42. Ursini, F.; Maiorino, M.; Forman, H.J. Redox homeostasis: The Golden Mean of healthy living. *Redox Biol.* **2016**, 8, 205–215, doi:10.1016/j.redox.2016.01.010.
43. Mittal, M.; Siddiqui, M.R.; Tran, K.; Reddy, S.P.; Malik, A.B. Reactive oxygen species in inflammation and tissue injury. *Antioxid. Redox Signal.* **2014**, 20, 1126–1167, doi:10.1089/ars.2012.5149.
44. Chen, S.; Chen, H.; Du, Q.; Shen, J. Targeting myeloperoxidase (MPO) mediated oxidative stress and inflammation for reducing

- brain ischemia injury: Potential application of natural compounds. *Front. Physiol.* **2020**, *11*, 433, doi:10.3389/fphys.2020.00433.
45. Maiocchi, S.L.; Ku, J.; Thai, T.; Chan, E.; Rees, M.D.; Thomas, S.R. Myeloperoxidase: A versatile mediator of endothelial dysfunction and therapeutic target during cardiovascular disease. *Pharmacol. Ther.* **2021**, *221*, 107711, doi:10.1016/j.pharmthera.2020.107711.
46. Kim, B.S.; Cho, I.S.; Park, S.Y.; Schuller-Levis, G.; Levis, W.; Park, E. Taurine chloramine inhibits NO and TNF- α production in zymosan plus interferon- γ activated RAW 264.7 cells. *J. Drugs Dermatol.* **2011**, *10*, 659–665.
47. Walczewska, M.; Marcinkiewicz, J. Taurine chloramine and its potential therapeutical application. *Przegl. Lek.* **2011**, *68*, 334–338.
48. Qaradakhi, T.; Gadanec, L.K.; McSweeney, K.R.; Abraham, J.R.; Apostolopoulos, V.; Zulli, A. The anti-inflammatory effect of taurine on cardiovascular disease. *Nutrients* **2020**, *12*, 2847, doi:10.3390/nu12092847.
49. Kang, I.S.; Kim, C. Taurine chloramine administered in vivo increases NRF2-regulated antioxidant enzyme expression in murine peritoneal macrophages. *Adv. Exp. Med. Biol.* **2013**, *775*, 259–267, doi:10.1007/978-1-4614-6130-2_22.
50. Kim, W.; Kim, H.U.; Lee, H.N.; Kim, S.H.; Kim, C.; Cha, Y.N.; Joe, Y.; Chung, H.T.; Jang, J.; Kim, K.; et al. Taurine chloramine

stimulates efferocytosis through upregulation of Nrf2-mediated heme oxygenase-1 expression in murine macrophages: pPossible involvement of carbon monoxide. *Antioxid. Redox Signal.* **2015**, *23*, 163–177, doi:10.1089/ars.2013.5825.

51. Kim, W.; Kim, S.H.; Jang, J.H.; Kim, C.; Kim, K.; Suh, Y.G.; Joe, Y.; Chung, H.T.; Cha, Y.N.; Surh, Y.J. Role of heme oxygenase-1 in potentiation of phagocytic activity of macrophages by taurine chloramine: Implications for the resolution of zymosan A-induced murine peritonitis. *Cell. Immunol.* **2018**, *327*, 36–46, doi:10.1016/j.cellimm.2018.02.003.

Chapter IV

**Protective effects of an electrophilic metabolite of
docosahexaenoic acid on UVB-induced oxidative cell
death, dermatitis, and carcinogenesis**

1. Abstract

Docosahexaenoic acid (DHA), a representative omega-3 (ω -3) polyunsaturated fatty acids, undergoes metabolism to produce biologically active electrophilic species. 17-Oxo-DHA is one such metabolite generated from DHA by cyclooxygenase-2 and dehydrogenase in activated macrophages. The present study was aimed to investigate the effects of 17-oxo-DHA on ultraviolet B (UVB)-induced oxidative stress, inflammation, and carcinogenesis in mouse skin. UVB-induced epidermal cell death was ameliorated by topically applied 17-oxo-DHA. Topical application of 17-oxo-DHA onto hairless mouse skin inhibited UVB-induced phosphorylation of STAT3 on tyrosine 705. The 17-oxo-DHA treatment also reduced the levels of oxidative stress markers, 4-hydroxynonenal-modified protein, malondialdehyde, and 8-oxo-2'-deoxyguanosine. The protective effects of 17-oxo-DHA against oxidative damage in UVB-irradiated mouse skin were associated with activation of Nrf2. 17-Oxo-DHA enhanced the engulfment of apoptotic JB6 cells by macrophages, which was related to the increased expression of the scavenger receptor CD36. The 17-oxo-DHA-mediated potentiation of efferocytic activity of macrophages was attenuated by the pharmacologic inhibition or knockout of Nrf2. The pretreatment with 17-oxo-DHA reduced the UVB-induced skin carcinogenesis and tumor angiogenesis. It was also confirmed that 17-oxo-DHA treatment significantly inhibited the phosphorylation of the Tyr705 residue of STAT3 and decreased the expression

of its target proteins in cutaneous papilloma. In conclusion, 17-oxo-DHA protects against UVB-induced oxidative cell death, dermatitis, and carcinogenesis. These effects were achieved through activation of Nrf2 and subsequent upregulation of the expression of antioxidant and anti-inflammatory proteins.

Keywords

17-Oxo-DHA; UVB-induced inflammation; Dermatitis; Photocarcinogenesis; Efferocytosis; Resolution of inflammation; STAT3; Nrf2

2. Introduction

Skin interacts with the environment and is the first barrier against noxious stimuli such as chemical toxicants, infectious pathogens, and solar radiation. The skin constantly adapts to external changes and maintains internal balance by regulating hormones, cytokines, and microbiota [1-3]. When such homeostasis is imbalanced due to excessive noxious stimuli and/or insufficient self-protection, this can cause skin rash, skin aging, immune system disorder, and cancer [4, 5].

Continuous exposure to solar light, especially ultraviolet B (UVB), results in physical and biological changes in the skin barrier which can induce dermatitis and photocarcinogenesis [6, 7]. In this process, the stimulated epithelial cells transmit the signals to tissue-resident cells. As a result, phagocytes including macrophages and neutrophils directly recognize and destroy the pathogens, while dendritic cells mediate adaptive immune signaling by modulating T cell differentiation [8]. Neutrophils have long been considered short-lived frontliner cells of innate immunity, with a primary function against acute inflammation. Since neutrophils have a short lifespan, the subsequent reactions are mainly regulated by macrophages [9].

Acute inflammation is a self-limiting process for tissue repairing and the restoration of homeostasis [10]. If acute inflammation is not adequately resolved, the inflammatory response can persist and trigger the pathogenesis of several chronic disorders such as asthma, arthritis, atherosclerosis, and

even cancer [11]. Apoptosis is the most prominent process of programmed cell death observed in the resolution phase of tissue. Since the accumulation of dead or dying cells triggers or exacerbates a persistent inflammatory response, the elimination of apoptotic cells is essential for the proper termination of acute inflammation [12].

Efferocytosis is a process by which dead/dying cells are removed by the phagocytic activity of macrophages [13, 14]. Various scavenger receptors, including CD36, present on the surface of macrophages recognize those cells that are supposed to be phagocytosed. Efferocytosis is hence critical in preventing secondary necrosis and intensification of inflammation, contributing to the resolution of inflammation.

Nrf2 is an essential transcription factor that plays a pivotal role in chemoresistance and biological defense by upregulating the expression of many antioxidative and anti-inflammatory enzymes, such as heme oxygenase-1 (HO-1) and NAD(P)H:quinone oxidoreductase 1 (NQO1), and other cytoprotective proteins [15]. Under oxidative stress and inflammatory conditions, the Nrf2 translocates to the nucleus and binds to the antioxidant response element (ARE), resulting in the expression of cytoprotective proteins [16]. Signal transducer and activator of transcription 3 (STAT3), a representative proinflammatory transcription factor, promotes cell growth by upregulating target proteins including c-Myc and Cyclin D1 [17]. Activated STAT3 augments inflammatory signaling and disrupts the balance of

homeostasis, thereby contributing to chronic inflammation and carcinogenesis [18].

The acute inflammatory response can be divided into initiation and resolution phases. A group of specialized pro-resolving mediators (SPMs) has emerged as endogenous substances involved in the resolution of acute inflammation. SPMs are enzymatically synthesized from ω -3 polyunsaturated fatty acids, including docosahexaenoic acid (DHA) [19, 20]. They are capable of limiting polymorphonuclear neutrophil infiltration and enhancing macrophage clearance of apoptotic cells [21]. In a previous study, we demonstrated that topically applied DHA alleviated UVB-induced inflammation and carcinogenesis in mouse skin [22]. DHA undergoes alternative metabolism to produce a series of biologically reactive electrophilic fatty acids [23]. 17-Oxo-DHA is one such electrophilic metabolite generated by cyclooxygenase-2 and dehydrogenase activity activities of macrophages recruited in the inflamed sites. Though 17-oxo-DHA was reported to inhibit the inflammatory signaling [24-26], its anti-inflammatory and chemoprotective/chemopreventive effects *in vivo* have not been reported yet. In the present study, we explored the effects of 17-oxo-DHA on UVB-induced oxidative cell death, dermatitis and carcinogenesis in mouse skin.

3. Materials and Methods

Chemicals and reagents

17-Oxo-DHA (4Z,7Z,10Z,13Z,15E,19Z-17-oxo-docosahexaenoic acid) was purchased from Cayman Chemical Co. (Ann Arbor, MI, USA). Dulbecco's modified Eagle's medium (DMEM), Minimum Essential Media (MEM), fetal bovine serum (FBS), sodium pyruvate, and gentamicin were supplied by Gibco (Grand Island, NY, USA). Trypsin and ethylenediaminetetraacetic acid (EDTA) were purchased from Welgene (Gyeongsan-si, Gyeongsangbuk-do, South Korea). The primary antibodies for detecting 4-hydroxynonenal (4-HNE) and malondialdehyde (MDA) were provided by the Japan Institute for the Control of Aging (JaICA), Nikken SEIL Co., Ltd. (Shizuoka, Japan). Anti-8-hydroxy-2'-deoxyguanosine (8-oxo-dG) antibody was purchased from TREVIGEN® (Gaithersburg, MD, USA). Antibodies for STAT3, P-STAT3^{Y705}, and c-Myc were supplied by Cell Signaling Technology (Danvers, MA, USA). The antibodies for NQO1, β -actin and CD36 were obtained from Santa Cruz Biotechnology (Dallas, TX, USA). Anti-Nrf2 and Anti-HO-1 were the products of Abcam (Cambridge, MA, USA) and Enzo Life Sciences (Farmingdale, NY, USA), respectively. pHrodo Red and 4',6-diamidino-2-phenylindole (DAPI) were obtained from Thermo Fisher Scientific (Waltham, MA, USA). The antibody against F4/80, recombinant mouse M-CSF, and red blood cell lysis buffer were supplied by Biolegend (San Diego, CA, USA). ML385 (N-[4-[2,3-Dihydro-1-(2-methylbenzoyl)-1H-indol-5-yl]-

5-methyl-2-thiazolyl]-1,3-benzodioxole-5-acetamide) was the product of Sigma-Aldrich Co. (St. Louis, MO, USA).

UVB-induced dermatitis

Female SKH1-*Hr^{hr}* mice (5 to 6 weeks of age) were obtained from Orient Bio Inc. (Seongnam-si, Gyeonggi-do, South Korea). Mice were randomly divided into four groups ($n = 3$ per group) and housed in plastic cages under the controlled conditions of temperature (23 ± 2 °C), humidity ($50 \pm 10\%$), and light (12/12 h light/dark cycle). All experiments on animals complied with the Guide for the Institutional Animal Care and Use Committee (IACUC) at Seoul National University (Approval number; SNU-190812-2). For the UVB irradiation, 5 x 8 Watts tubes were used, which emit wavelengths mainly in the 312 nm UVB region. Mice were irradiated with UVB (180 mJ/cm² and 500 mJ/cm²) using the Biolink BLX-312 UV crosslinker (Vilber Lourmat; **Marne-la-Vallée, Paris, France**). 17-Oxo-DHA (20 nmol) was dissolved in 200 µL of acetone and topically treated onto the dorsal skin of mice. The degree of UVB-induced inflammation was identified by the clinical skin score system based on the symptoms consisting of erythema, scarring, edema, and erosion. Each of these symptoms was rated on a scale of 0 to 3. The thickness of the dorsal skin was measured by a caliper.

UVB-induced skin carcinogenesis

Female SKH1-*Hr^{hr}* mice (5 to 6 weeks of age) were randomly divided into three groups ($n = 7$ per group). The mice were irradiated with UVB (180 mJ/cm²) using the Biolink BLX-312 UV crosslinker (Wilber Lourmat; **Marne-la-Vallée, Paris, France**) three times a week for 26 weeks. 17-Oxo-DHA (20 nmol) dissolved in 200 μ L of acetone was topically applied onto the dorsal skin of mice 30 min prior to each UVB exposure. Mice were euthanized and their skin tissues were collected for adequate analysis.

Histological analysis

The parts of skin biopsies were fixed with 10% phosphate-buffered formalin and embedded in paraffin. The skin sections were stained with hematoxylin and eosin (H&E). The H&E stained tissue sections were visualized under a light microscope (Nikon; Tokyo, Japan) to verify the presence of inflammatory lesions.

Immunohistochemical analysis

The dissected mouse skin tissues were prepared for immunohistochemical analysis with primary antibodies against 4-HNE, MDA (JaICA; Shizuoka, Japan), and 8-oxo-dG (TREVIGEN[®]; Gaithersburg, MD, USA). Four-micrometer sections of 10% formalin-fixed, paraffin-embedded tissues were deparaffinized and rehydrated in a series of xylene and ethanol buffer. The sections were heated in a microwave and boiled twice for 6 min in a 10 mM

citrate buffer (pH 6.0) for antigen retrieval. To reduce nonspecific staining, each section was treated with 3% hydrogen peroxide and 4% peptone casein blocking solution for 15 min. The slides were incubated with a diluted primary antibody at room temperature for 40 min in Tris-HCl-buffered saline containing 0.05% Tween 20, followed by incubation with a horseradish peroxidase-conjugated secondary antibody (Dako; Glostrup, Denmark). The tissues were treated with 3,3'-diaminobenzidine tetrahydrochloride to detect the peroxidase binding sites. Finally, counterstaining was performed with Mayer's hematoxylin.

Immunofluorescence staining

The mouse skin specimens were fixed, paraffin-embedded, and sectioned, and the sections were deparaffinized and rehydrated by serial washes with graded xylene and alcohol. For immunofluorescence staining, tissue sections were boiled in 10 mM of sodium citrate (pH, 6.0) for antigen retrieval, subjected to serial washing with phosphate-buffered saline (PBS), and permeabilized for 45 min at room temperature using 0.2% Triton X-100 in PBS and blocked with 3% bovine serum albumin (BSA) in PBS for 1 h at room temperature. The skin tissue sections were stained with primary antibodies for P-STAT3, Nrf2 (Cell Signaling Technology; Danvers, MA, USA), and F4/80 (Biolegend; San Diego, CA, USA) diluted at 1:250 in 3% BSA overnight at 4 °C. After washing three times with PBS each 5 min, tissues were incubated

with appropriate secondary antibodies. Nuclei were counterstained with DAPI (Invitrogen; Carlsbad, CA, USA). Immunofluorescence images were visualized under a fluorescence microscope (Nikon; Tokyo, Japan).

Terminal Deoxynucleotidyl Transferase dUTP Nick End Labeling (TUNEL) assay

The apoptotic DNA fragmentation was measured by the TUNEL assay with the ApopTag[®] Peroxidase *In Situ* Apoptosis Detection Kit (Chemicon; Temecula, CA, USA). The isolated mouse skin tissues were rinsed with PBS and fixed in 10% buffered formalin (Sigma-Aldrich; Saint Louis, MO, USA) for the TUNEL assay. The apoptotic cells were detected under a light microscope (Nikon; Tokyo, Japan).

Lysis of tissue and protein extraction

The UVB-treated mouse dorsal skin was collected, and fat was removed on ice to attain the epidermal layer. Collected epidermis was homogenized with the lysis buffer (20 mM Tris-HCl (pH 7.5), 150 mM NaCl, 1 mM Na₂EDTA, 1 mM EGTA, 1% Triton, 2.5 mM sodium pyrophosphate, 1 mM β-glycerophosphate, 1 mM Na₃VO₄, 1 μg/mL leupeptin, 1 mM phenylmethyl sulfonylfluoride (PMSF), and an EDTA-free cocktail tablet) in an ice bath. The whole lysates were vortexed every 10 min for 3 h on the ice, followed by

centrifugation (13,000× g, 15 min at 4 °C). The supernatants were collected and stored at −70 °C until use.

Cytosolic and nuclear extraction

The fat-free dorsal skin tissues were homogenized with 1 mL buffer A [10 mM 4-(2-hydroxyethyl)-1-piperazineethanesulfonic acid (HEPES, pH 7.8), 1.5 mM MgCl₂, 10 mM KCl, 0.5 mM dithiothreitol (DTT), 0.2 mM PMSF] followed by vortex-mixing every 10 min for 3 h in an ice bath. The lysates were mixed with 0.1% Nonidet P-40 (NP-40) 30 min before centrifugation. After centrifugation at 13,000× g for 15 min, the supernatants (the cytosolic extracts) were obtained. The precipitated nuclear pellets were washed three times with buffer A containing 0.625% NP-40 to remove a residual cytosolic fraction. Nuclear pellets were then resuspended in 300 μL of buffer C [20 mM HEPES (pH 7.8), 420 mM NaCl, 1.5 mM MgCl₂, 0.2 mM EDTA, 0.5 mM DTT, 0.2 mM PMSF and 20% glycerol]. The nuclear lysates were vortexed every 10 min for 1 h, followed by centrifugation at 13,000× g for 15 min. The supernatants (nuclear extracts) were collected and kept at −70 °C until use.

Western blot analysis

The protein concentration of lysates was measured by the PierceTM BCA Protein Assay Kit (Thermo Fisher Scientific; Rockford, IL, USA). The lysates were loaded on 8-15% SDS-polyacrylamide gel for performing

electrophoresis under reducing conditions. Protein was transferred to the polyvinylidene difluoride membrane (PALL Life Sciences; Washington, NY, USA). The membranes were blocked with 5% non-fat dry milk in Tris-buffered saline containing 0.1% Tween 20 (TBST) for 1 h at room temperature. Each blot was incubated with its respective primary antibody diluted in TBST at 4 °C overnight. The membranes were rinsed three times for 10 min with TBST buffer. Then, washed blots were probed with 1:5000 dilution of horseradish peroxidase-conjugated secondary antibody (Invitrogen; Carlsbad, CA, USA) for 1 h at room temperature and washed three times again with TBST buffer. The immunoblots with protein-antibody complexes were visualized with an enhanced chemiluminescent (ECL) detection kit (Abclon; Seoul, South Korea) and LAS-4000 image reader (Fujifilm; Tokyo, Japan).

Quantitative real-time polymerase chain reaction (qPCR)

Total RNA was isolated from mouse skin tissues with Trizol[®] (Invitrogen; Carlsbad, CA, USA), and the reverse transcription reaction was conducted using the Moloney murine leukemia virus (M-MLV) reverse transcriptase (Promega; Madison, WI, USA) to synthesize the complementary DNA (cDNA). qPCR was carried out with a 7500 Real-Time PCR instrument (Applied Biosystems; Foster City, CA, USA) using the RealHelix[™] qPCR Kit (Green) (NanoHelix Co. Ltd.; Daejeon, South Korea). The primers used for

each qPCR reactions are as follows; *il-6*, 5'-TCT ATA CCA CTT CAC AAG TCG GA -3' and 5'- GAA TTG CCA TTG CAC AAC TCT TT-3'; *tnf- α* , 5'- CAG GCG GTG CCT ATG TCT C -3' and 5'- CGA TCA CCC CGA AGT TCA GTA G -3'; *actin*, 5'-GGC TGT ATT CCC CTC CAT CG -3' and 5'- CCA GTT GGT AAC AAT GCC ATG T -3' (forward and reverse, respectively). Target gene expression was normalized to actin. The relative gene expression was analyzed by the comparative cycle threshold (Ct) ($\Delta\Delta Ct$) method.

Cytokines analysis

The lysate of mouse skin tissues was analyzed using ELISA kits according to the manufacturer's instruction. Mouse IL-6 and TNF- α ELISA kits were obtained from RayBiotech (Norcross, GA, USA).

Isolation of bone marrow-derived macrophages (BMDMs)

The femur and tibia were harvested from mice. After cutting both ends of the bone, bone marrow was flushed out by cold PBS. The cells from bone marrow were filtered through a 100 μ m FALCON nylon cell strainer (Thermo Fisher Scientific; Waltham, MA, USA) and centrifuged at 500 \times g for 5 min at 4 $^{\circ}$ C. The cell pellet was resuspended and incubated with red blood cell lysis buffer for 1 min at room temperature. After discarding the lysis buffer, the isolated cells were plated in DMEM containing 20 ng/mL M-CSF and incubated at

37 °C in a humidified incubator containing 5% CO₂ for 4 days. Cells were then switched to media supplemented with 10 ng/mL M-CSF for 3 days.

Efferocytosis assay

The mouse epidermal JB6 Cl4 cells (American Type Culture Collection; Manassas, VA, USA) were incubated with 5% MEM media. JB6 Cl4 cells were irradiated with UVB (200 mJ/cm²) and incubated at 37 °C and 5% CO₂ for 24 h. Apoptotic cells induced by UVB radiation were collected and stained with pHrodo Red for 30 min at 37 °C. The dead epithelial cells were centrifuged at 300× g for 3 min and washed twice with PBS. To the 1×10⁶ BMDMs in a 60 mm plate, 3×10⁶ pHrodo-labelled apoptotic cells were added followed by co-incubation at 37 °C for 1 h. After the incubation, these plates were washed twice with PBS to remove residual apoptotic cells.

Estimation of hemoglobin

The tissue lysate was used to measure the amount of hemoglobin with Drabkin's reagent (Sigma-Aldrich; St. Louis, MO, USA). After the mixed well with the reagent, absorbance at 540 nm was detected to estimate the content of hemoglobin in mouse skin tissue.

Flow cytometry assay

Adherent cells were detached from the plates by treating 5 mM EDTA and spun down at 500 g for 5 min at 4 °C. Following the removal of unwanted debris-free isotype control antibody, incubation with CD16/32 antibody was performed to block the non-specific binding of other antibodies. After blocking, F4/80 antibody was added and incubated for 30 min at 4 °C. Prepared samples were detected by FACS Calibur™ flow cytometer (Becton, Dickinson and Company; Franklin Lakes, NJ, USA) and analyzed with FlowJo software.

Sample preparation for LC-MS/MS analysis

Recombinant STAT3 protein (Abcam; Cambridge, MA, USA) treated with 17-oxo-DHA was digested by the in-solution method. To this, 6 M urea in 50 mM ammonium bicarbonate (pH 8.0) was added to denature the proteins. The proteins were incubated for 1 h at 37 °C with 10 mM DTT and then alkylated with 30 mM iodoacetic acid (IAA). The MS-grade trypsin protease was added and incubated at 37 °C overnight (enzyme-to-protein ratio = 1: 10). The peptides were desalted using Pierce® C-18 spin columns and dried using Speed-Vac.

Direct infusion mass spectrometry (DIMS) analysis of 17-oxo-DHA

17-Oxo-DHA was reconstituted in 50% methanol and loaded in a Hamilton syringe. The sample was injected by a syringe pump with a flow rate of 5

$\mu\text{L}/\text{min}$ into the heated electrospray ionization (HESI) source and measured for 30 s on a Q-Exactive HF-X Hybrid Quadrupole orbitrap mass spectrometer (Thermo Fisher Scientific; San Jose, CA, USA). The source conditions for MS scan in the negative ESI mode were optimized: spray voltage, 3.8 kV; heated capillary temperature, 320 °C; nitrogen was used as damping gas. MS scans were acquired for the mass range of 340.2-342.2 m/z at a resolution of 60,000 in MS1 level and 15,000 for HCD experiments and normalized collision energies (NCE) was set at 27.

LC-MS/MS analysis

For LC-MS/MS analysis, Ultimate 3000 UHPLC system (Thermo Fisher Scientific; San Jose, CA, USA) was coupled to Q-Exactive HF-X Hybrid Quadrupole orbitrap mass spectrometer (Thermo Fisher Scientific) equipped with analytical columns (EASY-Spray™ LC Columns, C18, 75 $\mu\text{m} \times 50 \text{ cm}$, 2 μm , 100 Å; Thermo Fisher Scientific) and trap columns (C18, 75 $\mu\text{m} \times 2 \text{ cm}$, 3 μm , 100 Å, Thermo Fisher Scientific). The peptide samples were separated by the mobile phase comprising of 0.1 % formic acid in water (solvent A) and 0.1 % formic acid in 90 % acetonitrile (solvent B). The gradient condition was set as follows: (T min/% of solvent B) 0/2, 6/2, 10/10, 65/40, 90/60, 99/90, 104/90, 105/2, 120/2. The column temperature was set at 60 °C and the flow rate of the mobile phase was 300 nL/min.

The source conditions for MS scan in the positive ESI mode were optimized: spray voltage, 1.5 kV; heated capillary temperature, 250 °C; nitrogen was used as damping gas. The MS1 scan range was set of 350-2,000 m/z and the resolution was set at 60,000. The 12 most abundant ions were selected from MS1 scan and fragmented by data-dependent mode at a resolution of 15,000. MS2 scans were acquired with the dynamic exclusion for 30 s, an isolation window of 1.2 m/z and NCE of 27.

Statistical analysis

All the data were analyzed by mean \pm standard deviation (SD) of at least three independent experiments. The Student's *t*-test determined statistical significance. All the statistical analyses were applied using GraphPad Prism 8.0 (GraphPad Software; San Diego, CA, USA). The value of $p < 0.05$ was considered statistically significant.

4. Results

UVB-induced dermatitis and oxidative stress were attenuated in 17-oxo-DHA treated mice

In order to assess the anti-inflammatory effects of 17-oxo-DHA, the UVB-induced mouse dermatitis model was employed (**Supplementary Fig.1**). Four days after UVB irradiation, when the severity of the inflammation peaked, 17-oxo-DHA (20 nmol) was topically applied to mouse dorsal skin. On the fifth day of the experiment, mice were euthanized, and the lysates of skin tissue were prepared for subsequent analyses. The clinical skin score evaluated the degree of UVB-induced dermatitis based on symptoms of erythema, edema, scarring, and erosion. The topical application of 17-oxo-DHA accelerated resolution of inflammation (**Fig. 4-1A**). Mice treated with 17-oxo-DHA had a lower skin severity score and the reduced thickness of dorsal skin measured by a digital caliper (**Fig. 4-1B**), which was verified by H&E staining (**Fig. 4-1C**). The UVB irradiation can cause apoptosis (**Supplementary Fig. 2**), lipid peroxidation and DNA fragmentation. 4-HNE and MDA are ubiquitous markers of oxidative tissue damage, and the formation of 8-oxo-dG was used as a biomarker of DNA damage. Topically applied 17-oxo-DHA attenuated the expression of 4-HNE, MDA, and 8-oxo-dG in mouse epidermis (**Fig. 4-1D, E**).

17-Oxo-DHA enhanced the expression of cytoprotective proteins through Nrf2 activation in mouse skin

The redox-sensitive transcription factor Nrf2 is involved in cellular protection against oxidative and inflammatory stresses. To investigate whether the 17-oxo-DHA-induced potentiation of cytoprotective capacity contributes to the reduction of oxidative and inflammatory damage caused by UVB irradiation, we first measured the level of Nrf2 in the skin of 17-oxo-DHA-treated mice. The expression level of Nrf2 was elevated in the both cytoplasm and nucleus of 17-oxo-DHA treated mouse skin as measured by immunoblot (**Fig. 4-2A**) and immunofluorescence (**Fig. 4-2B**) analyses. The expression of Nrf2 was transiently upregulated upon treatment with 20 nmol 17-oxo-DHA, which was accompanied by upregulation of its major target proteins, HO-1 and NQO1 in a time-dependent manner (**Fig. 4-2C**).

UVB-induced phosphorylation of STAT3 was reduced by topical application of 17-oxo-DHA

Aberrant overactivation of STAT3 is implicated in dermatitis and photocarcinogenesis [27]. STAT3 is activated through phosphorylation of its Tyr705 residue which facilitates the dimerization. The dimerized STAT3 translocates to the nucleus and binds to the promotor regions of target genes. The topical application of 17-oxo-DHA diminished the Tyr705 phosphorylation of STAT3 in mouse epidermis, as confirmed by the

immunofluorescence staining (**Fig. 4-3A**) and Western blot analysis (**Fig. 4-3B**). Inhibition of nuclear translocation of phosphorylated STAT3 (STAT3) was also demonstrated by immunoblot analysis (**Fig 4-3C**).

The resolution of inflammation induced by UVB-irradiation was increased by 17-oxo-DHA

According to previous studies, UVB irradiation induced the generation of inflammatory cytokines in mouse skin [22]. The production of TNF- α and IL-6 (**Fig. 4-4A**), two prototypic proinflammatory cytokines, and expression of their gene transcripts (**Fig. 4-4B**) were diminished by topical application of 17-oxo-DHA. Under the same experimental conditions, there was no significant difference in the proportion of macrophages in mouse epidermis (**Fig. 4-4C**). CD36 is one of the scavenger receptors required for macrophages to detect damaged cells for adequate clearance (**Fig. 4-4D**). As shown in **Fig. 4-4E**, the expression of CD36 was significantly elevated in 17-oxo-DHA treated mouse skin.

17-Oxo-DHA potentiated the efferocytic activity of macrophages by augmenting the expression of CD36 in BMDMs

In the resolving phase of acute inflammation, a series of steps are involved. Phagocytic removal of damaged cells by macrophages, termed 'efferocytosis', is critical to prevent the persistence of inflammation. To clarify whether 17-

oxo-DHA could affect the capability of macrophages engulfing apoptotic cells, we utilized BMDMs isolated from the same strain of mice used in the *in vivo* experiments. For this purpose, JB6 murine epithelial cells were irradiated with UVB, and the resulting apoptotic JB6 cells were stained with pHrodo and co-incubated with BMDMs in the absence or presence of 5 μ M 17-oxo-DHA (**Fig. 4-5A**). BMDMs with positive staining for both F4/80 (macrophage marker) and pHrodo (apoptotic cell marker) were selectively sorted by flow cytometry. As shown in **Fig. 4-5B**, 17-oxo-DHA treatment enhanced the proportion of BMDMs engulfing apoptotic epidermal cells (F4/80⁺/pHrodo⁺). BMDMs treated with 17-oxo-DHA displayed elevated expression of CD36 (**Fig. 4-5C**) and Nrf2 (**Fig. 4-5D**). To confirm the association between CD36 and Nrf2, immunofluorescence staining was performed with skin tissues from Nrf2 knockout (KO) and wildtype (WT) mice. F4/80 showed no significant difference between the two groups, but the expression of CD36 was decreased in Nrf2 KO mice (**Fig. 4-5E**).

The inhibition of Nrf2 restrained the effecrocytic capability of mouse

BMDMs

ML385 is a chemical inhibitor of Nrf2, which is widely used to interrupt the transcription of this transcription factor. In line with this notion, the expression of Nrf2 was inhibited by pretreating BMDMs with ML385 (**Fig. 4-6A**). The proportion of BMDMs engulfing apoptotic epidermal cells was

diminished by treatment with ML385 (**Fig. 4-6B**). To verify the role of Nrf2 in efferocytosis, BMDMs from Nrf2 KO mice were also employed. The 17-oxo-DHA-induced potentiation of efferocytosis was abrogated in BMDMs isolated from Nrf2 KO mice (**Fig. 4-6C**). The increase in efferocytosis activity expedites the resolution of inflammation, and this often accompanies the reduced level of inflammatory cytokines. Thus, there was significant dampening of the inhibitory effect of 17-oxo-DHA on the production of proinflammatory cytokines, TNF- α (**Fig. 4-6D**) and IL-6 (**Fig. 4-6E**), in the skin of Nrf2 KO mice.

17-Oxo-DHA protected against UVB-induced mouse skin tumor development

After confirming that the topical application of 17-oxo-DHA to the dorsal skin of mice increased the Nrf2-mediated expression of cytoprotective proteins and accelerated the resolution of inflammation, we conducted a long-term experiment to assess its chemopreventive potential against photocarcinogenesis. The results showed that UVB-induced tumor development was diminished by 17-oxo-DHA pretreatment. The body weight loss of UVB-irradiated mice was also attenuated by 17-oxo-DHA treatment (**Fig. 4-7A**). Repeated topical application of 17-oxo-DHA before irradiation of UVB significantly reduced the number of papillomas per mouse (**Fig. 4-7B**) and the cumulative number of tumors in mouse skin (**Fig. 4-7C**). At the

termination of the experiment, the number of total tumor burden was significantly decreased by 42.37% in the 17-oxo-DHA-treated group compared to the vehicle treated control counterparts. Notably, the number of large-sized tumors was more markedly reduced compared to that of small-sized tumors (**Fig. 4-7D**). For the growth and maintenance of tumor, blood vessels expand around the tumor, which is called angiogenesis. The topical application of 17-oxo-DHA suppressed angiogenesis (**Fig. 4-7E**), and this was corroborated by the reduced amount of hemoglobin accumulated in the skin (**Fig. 4-7F**).

17-Oxo-DHA inhibited oxidative damage and activation of STAT3 in UVB-induced mouse skin carcinogenesis

Repeated exposure to UVB radiation can lead to aggregation of the epidermal layer as verified by H&E staining (**Fig. 4-8A**). The resulting thickening of the mouse epidermis was attenuated by topically applied 17-oxo-DHA. Likewise, oxidative tissue and DNA damage were ameliorated as evidenced by the reduced expression of 4-HNE, MDA, and 8-oxo-dG (**Fig. 4-8A**). Repeated UVB irradiation resulted in overactivation of STAT3 in mouse skin through phosphorylation of Tyr705. 17-Oxo-DHA treatment significantly dampened the phosphorylation of STAT3 on Try705 and the expression of c-Myc, a major STAT3 target oncoprotein, in the skin tumor tissues (**Fig. 4-8B**).

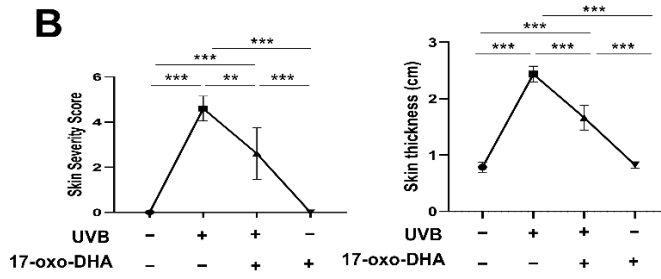
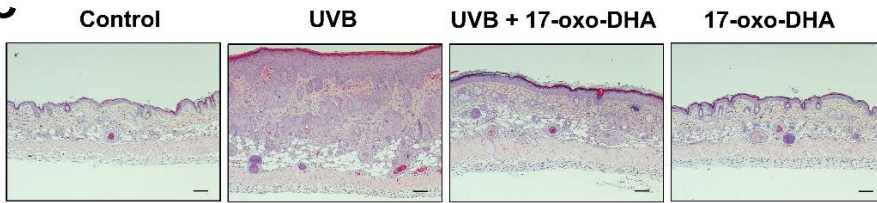
17-Oxo-DHA directly binds to cysteine 718 residue in STAT3 through the Michael addition reaction

The modification of proteins at critical cysteine thiols can affect the functions of many redox-sensitive proteins [28, 29]. We speculated that the electrophilic α,β -unsaturated carbonyl group of 17-oxo-DHA could modify the cysteine residue of STAT3 (**Fig. 4-9A**), which might impede the phosphorylation and transcriptional activity of STAT3. As shown in **Fig. 4-9B**, STAT3 has characteristic domains and several cysteine residues.

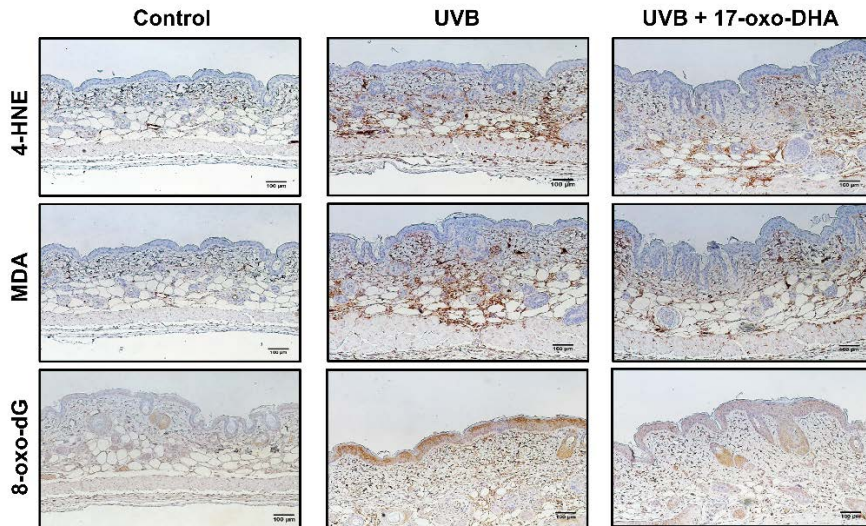
To identify the binding site(s) of 17-oxo-DHA to STAT3 protein, MS/MS analysis was performed with recombinant STAT3 protein treated with 17-oxo-DHA. First, the 17-oxo-DHA was analyzed by DIMS in the negative electrospray ionization (ESI) mode. Fragmentation MS scans were acquired by higher-energy collision dissociation (HCD) of the precursor ion corresponding to 17-oxo-DHA. The MS/MS spectrum shows the information on 17-oxo-DHA (m/z 342.21) fragmentation during HCD (**Supplementary Fig.3**). Secondly, peptide samples of STAT3 protein treated with 17-oxo-DHA were analyzed by LC-MS/MS. Based on the fragmentation information of 17-oxo-DHA (**Supplementary Fig.3**), we were able to confirm that 17-oxo-DHA bound tryptic peptide derived from STAT3 protein. The molecular ion matching to $[M+2H]^{2+}$ (m/z 1270.1322) of 710-FICVTPPTCSNTIDLPMSPR-729 was acquired, indicative of STAT3 modified by 17-oxo-DHA at the cysteine 718 residue (**Fig. 4-9C**).

A

UVB	-	+	+	-
17-oxo-DHA	-	-	+	+

B**C**

D



E

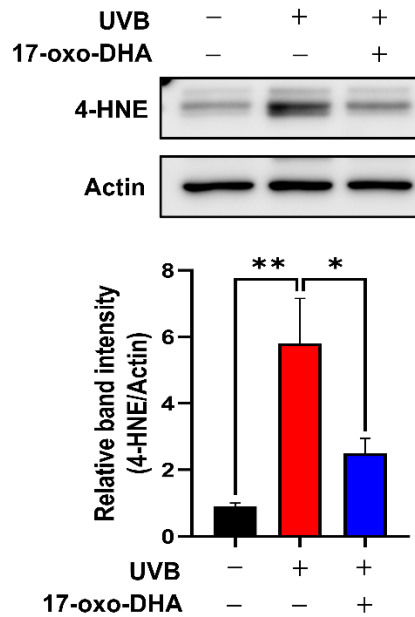
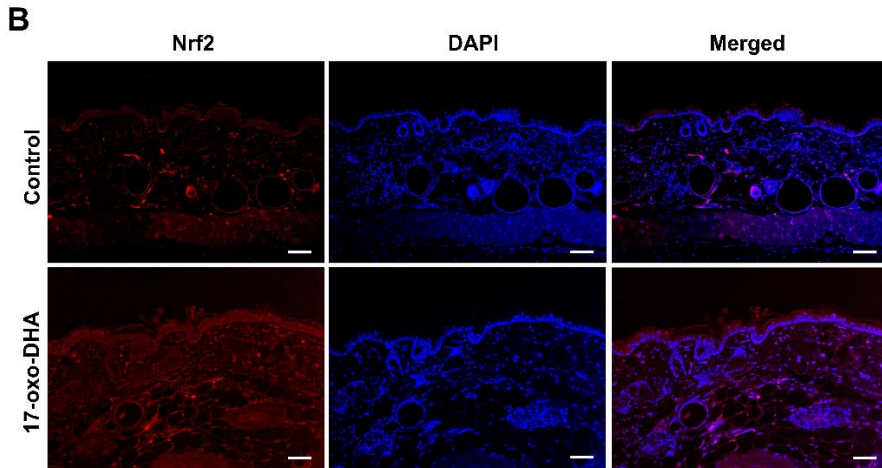
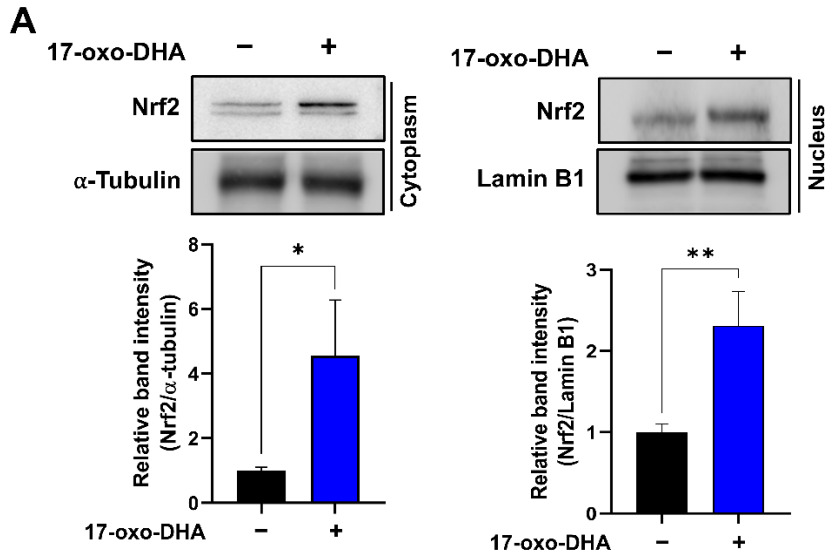


Figure 4-1. Protective effects of topically applied 17-oxo-DHA on UVB-induced inflammation and oxidative stress in mouse skin.

17-Oxo-DHA (20 nmol) was topically applied for four days onto the dorsal skin of hairless female SKH1-*Hr^{hr}* mice after single UVB irradiation (500 mJ/cm²). Twenty-four hours later, skin tissues were collected for histological and biochemical analyses. (A) The photographic images represent the wound of each group after the UVB irradiation. (B) Skin severity was scored based on the symptoms, and skin thickness was measured with a caliper. (C) Paraffin-embedded skin tissue blocks were stained with H&E. Magnification, 100×. Female hairless mice were topically applied with 17-oxo-DHA (20 nmol) 30 min before UVB irradiation (180 mJ/cm²). (D) The paraffin sections of epidermal tissue were immunostained for 4-HNE, MDA, and 8-oxo-dG. (E) The protein levels of 4-HNE in UVB-induced mouse skin with or without 17-oxo-DHA treatment were measured by Western blot analysis. Data are expressed as means ± SD (n=3 per group). * $p < 0.05$; ** $p < 0.01$; *** $p < 0.001$.



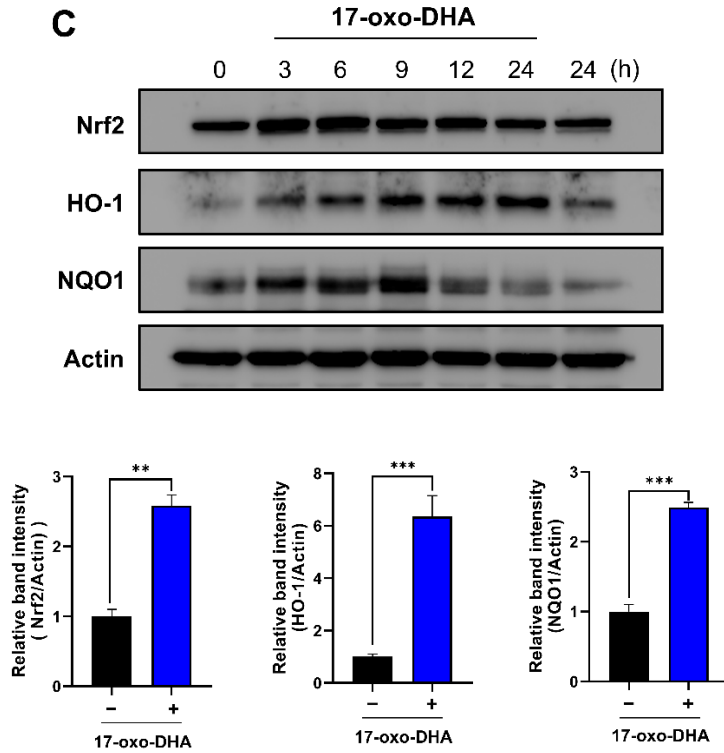


Figure 4-2. Enhanced nuclear translocation of Nrf2 and its target protein expression in 17-oxo-DHA treated mice.

(A, B) The accumulation of Nrf2 in cytoplasm and nucleus was verified by immunoblot analysis (A) and immunofluorescence staining (B). (C) Dorsal skins of mice were applied with 20 nmol 17-oxo-DHA for the indicated time. Protein lysates were isolated and subjected to Western blot analysis to measure the expression levels of Nrf2 and target proteins. Data are expressed as means \pm SD (n=3 per group). * $p < 0.05$; ** $p < 0.01$; *** $p < 0.001$.

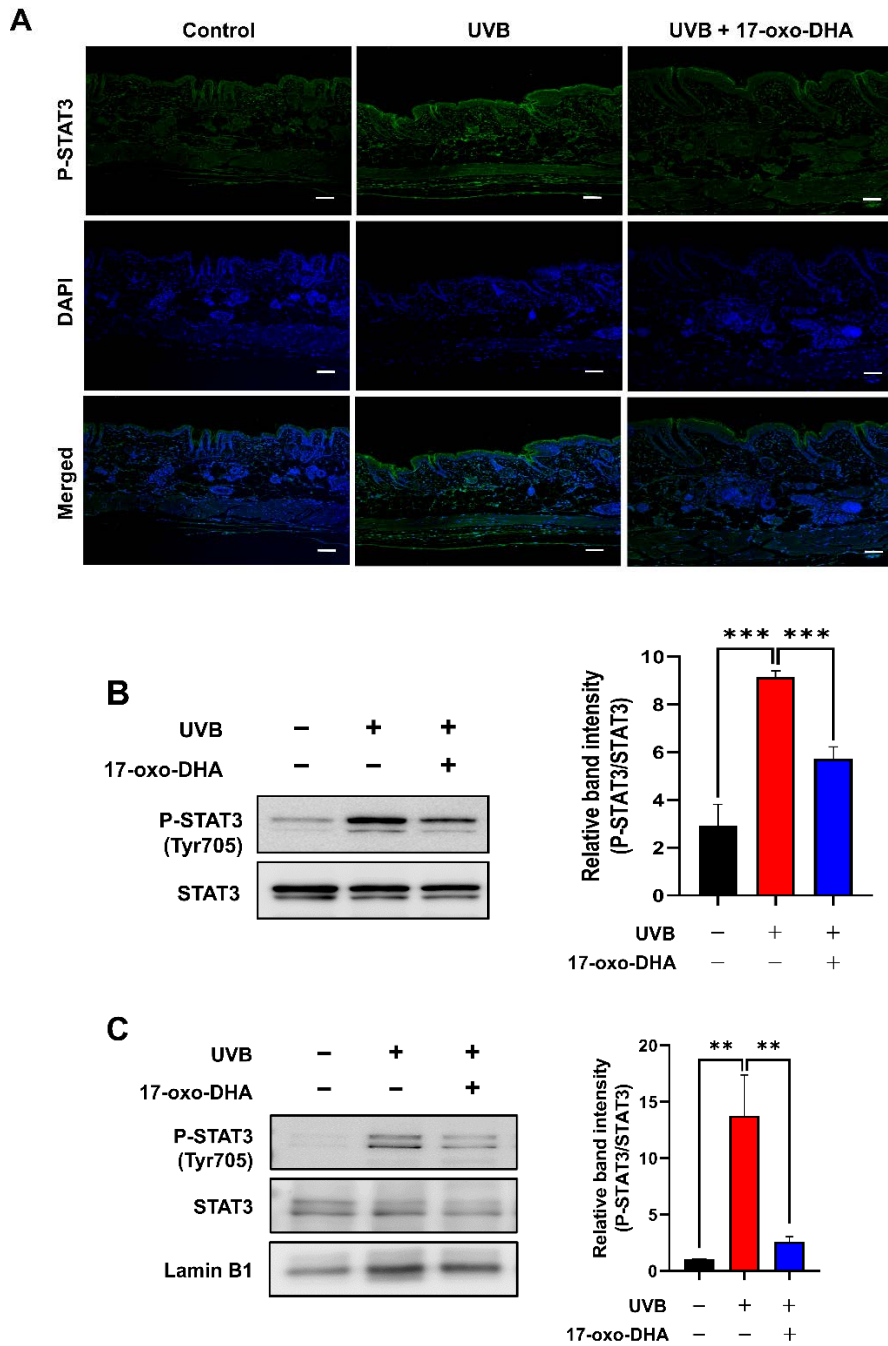
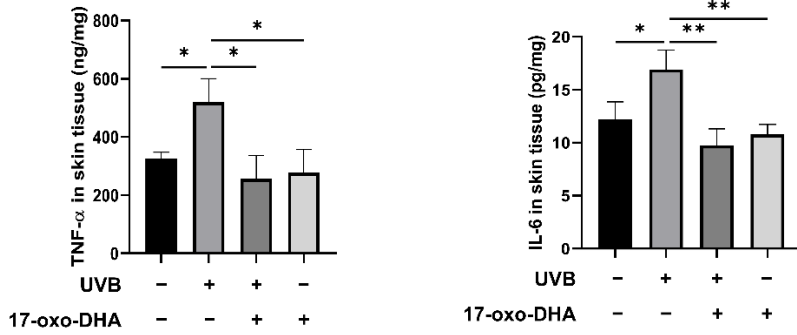


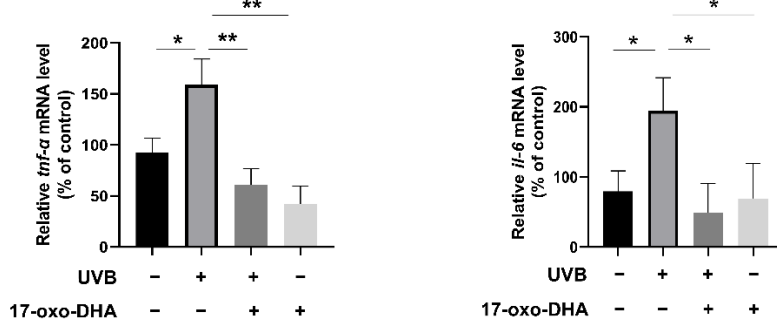
Figure 4-3. Attenuation of UVB-induced STAT3 phosphorylation in mouse skin treated with 17-oxo-DHA.

(A) The expression of P-STAT3 was measured by immunofluorescence staining. (B, C) Total protein lysate (B) and nuclear extract (C) were used for Western blot analysis to determine the levels of P-STAT3. Data are expressed as means \pm SD (n=3 per group). ** $p < 0.01$; *** $p < 0.001$.

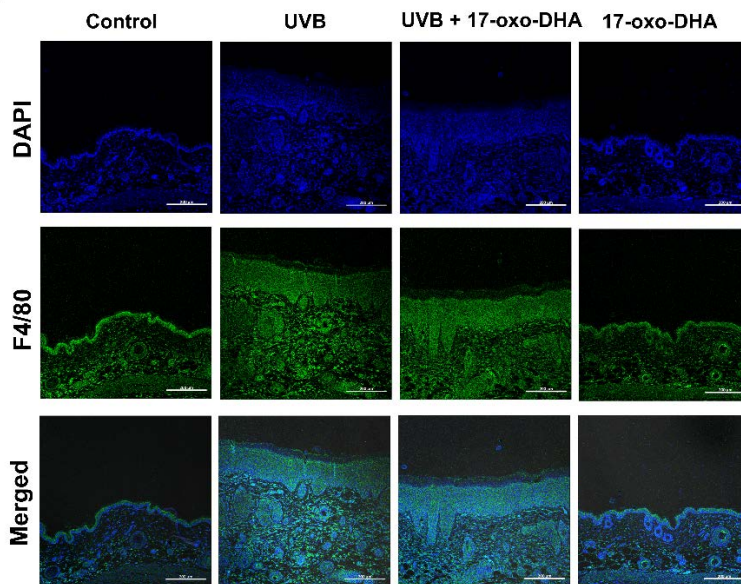
A



B



C



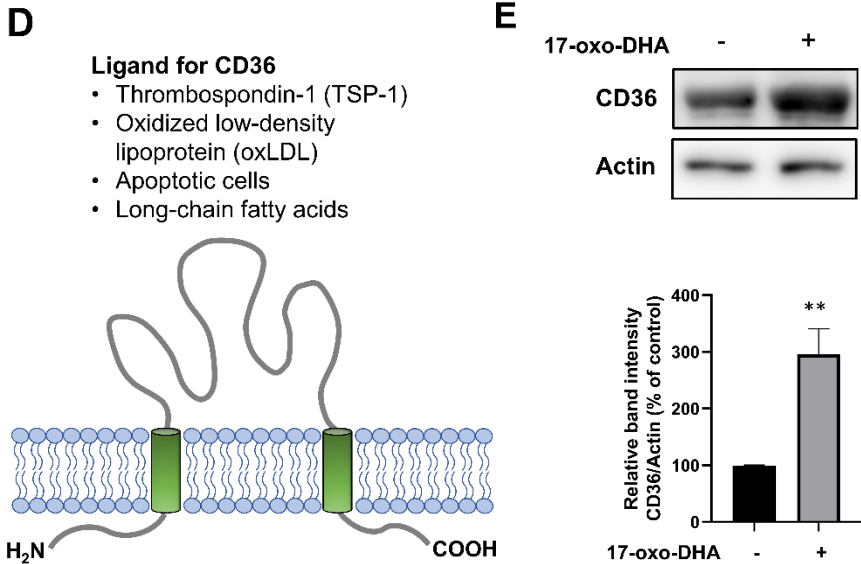
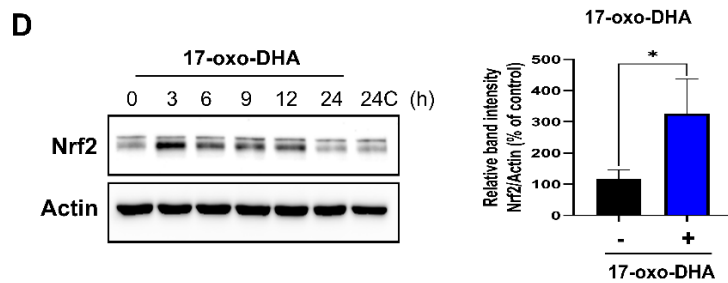
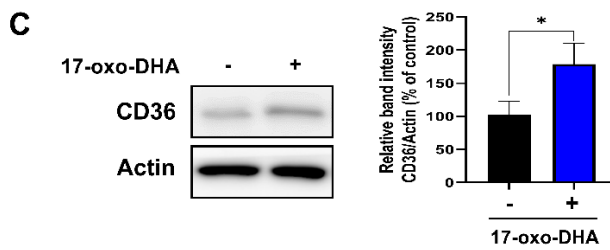
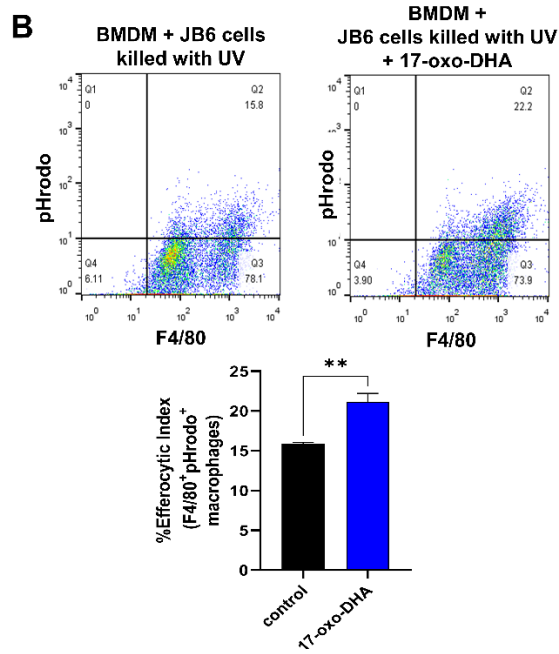
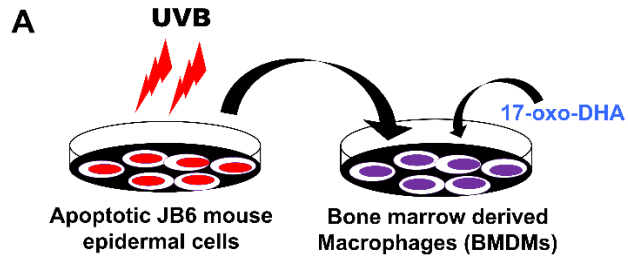


Figure 4-4. 17-Oxo-DHA-mediated acceleration of the resolution of UVB-induced inflammation in mouse skin.

(A) The amounts of TNF- α and IL-6 in mouse skin were determined by ELISA. (B) Tissue lysates were subjected to Real-Time Quantitative PCR to determine the mRNA levels of the same targets. (C) The macrophages were visualized by immunofluorescence staining. Magnification, 200 \times . Scale bars correspond to 200 μ m. (D) The biological functions of CD36, a representative scavenger receptor present in macrophages. (E) The expression level of CD36 was measured by immunoblot analysis. Data are expressed as means \pm SD (n=3 per group). * $p < 0.05$; ** $p < 0.01$.



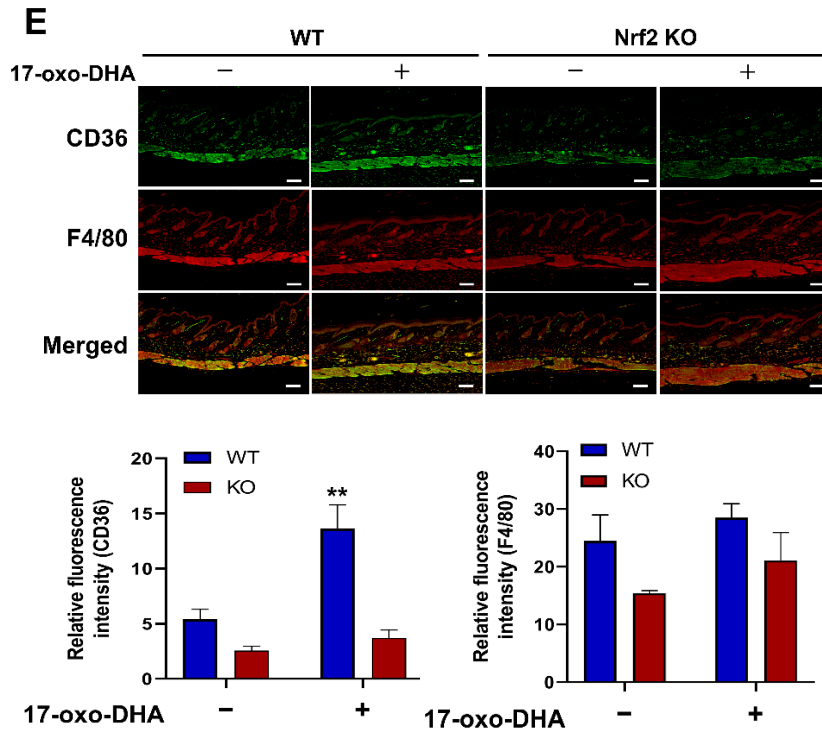
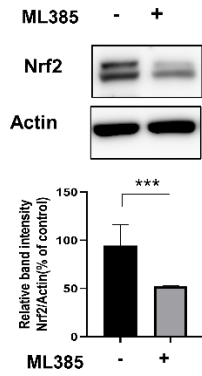
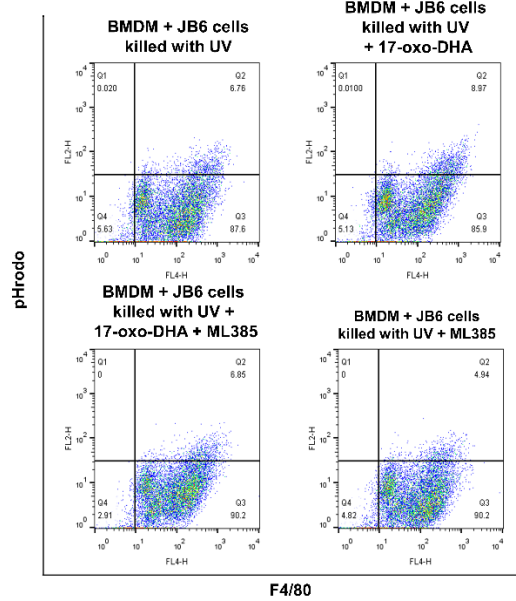
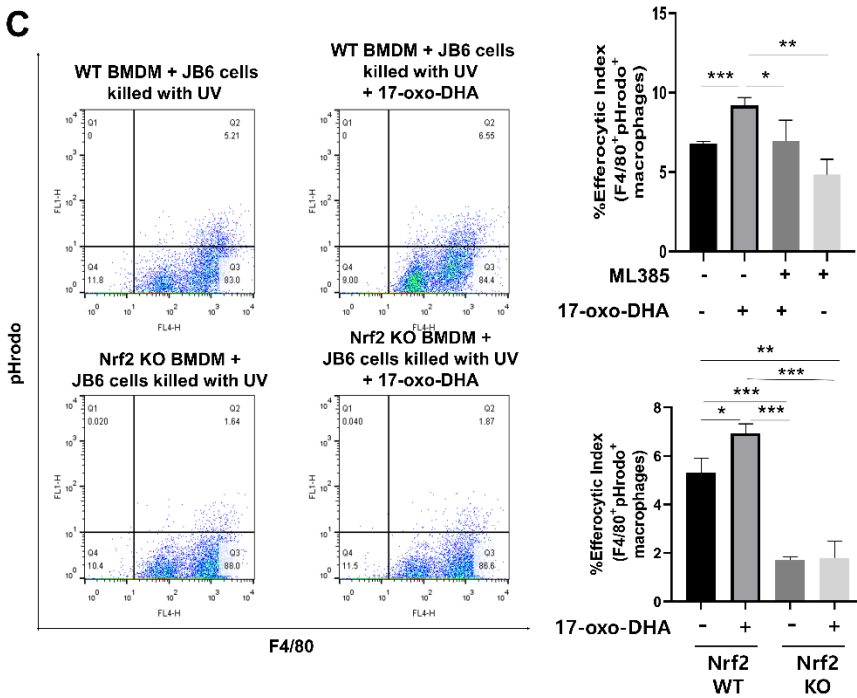


Figure 4-5. Nrf2-mediated enhancement of efferocytosis activity of macrophages by 17-oxo-DHA.

(A) BMDMs were treated with 17-oxo-DHA (5 μ M) for 12 h, and co-incubated with apoptotic JB6 mouse epidermal cell debris for 1 h. (B) The flow cytometric analysis to assess the efferocytosis capability of macrophages. BMDMs were treated with 17-oxo-DHA (5 μ M) for 24 h. The expression of CD36 (C) and Nrf2 (D) was measured by immunoblot analysis. (E) Fixed skin tissues were stained with anti-CD36 (green) or anti-F4/80 (red) antibody, and counterstained with DAPI (blue). Magnification, 200 \times . Scale bars correspond to 200 μ m. Data are expressed as means \pm SD (n=3 per group). * $p < 0.05$; ** $p < 0.01$.

A**B****C**

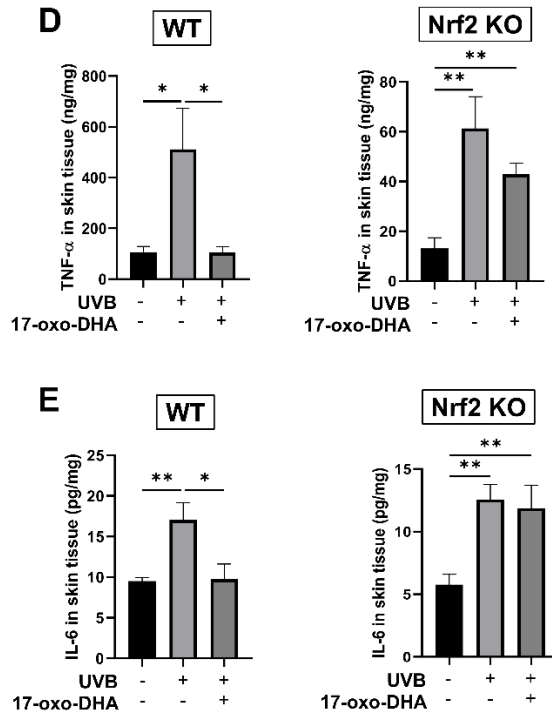


Figure 4-6. Effects of pharmacologic and genetic inhibition of Nrf2 on effecrocytic activity of macrophages.

BMDMs were co-cultured with apoptotic epidermal JB6 cells. Before the co-incubation with dead cells, macrophages were pre-treated with a pharmacological Nrf2 inhibitor, ML385 (20 μ M) for 90 min. 17-Oxo-DHA (5 μ M) was added, after the wash-out with PBS for removing ML385. Twelve-hours after the incubation, BMDMs were co-cultured with pHrodo-SE-labelled apoptotic epidermal JB6 cells for 1 h. (A) The pharmacological inhibition of Nrf2 by ML385 in BMDMs was confirmed by Western blot analysis. (B) The engulfment of dead cells by macrophages was measured by flow cytometry. (C) BMDMs isolated from Nrf2 WT and KO mice were

compared for their capability to engulf the apoptotic JB6 cells. (D, E) The mouse skin epidermis lysates were subjected to ELISA to measure the concentration of TNF- α (D) and IL-6 (E). Data are expressed as means \pm SD (n=3 per group). * $p < 0.05$; ** $p < 0.01$; *** $p < 0.001$.

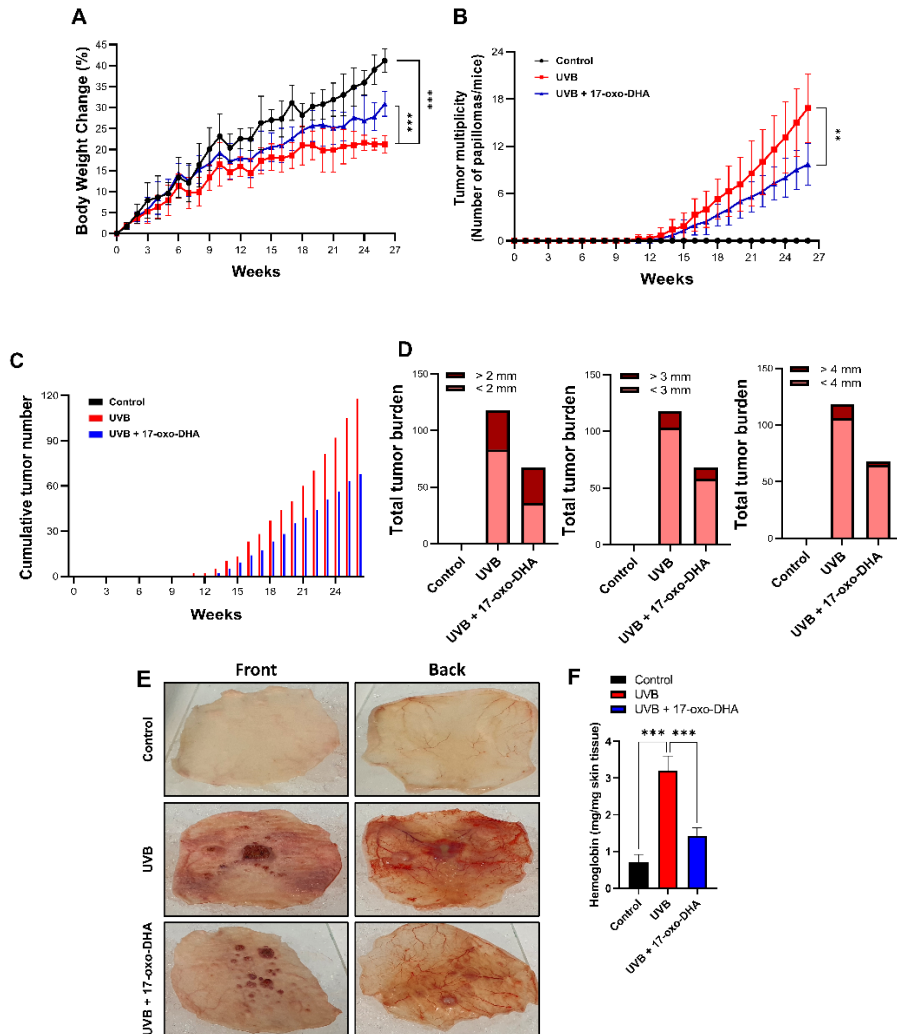


Figure 4-7. Protective effects of 17-oxo-DHA against UVB-induced tumor development in hairless mouse skin.

Female hairless mice were topically applied to dorsal skin with 17-oxo-DHA (20 nmol) 30 min prior to UVB irradiation (180 mJ/cm²) three times a week until termination of the experiment on the 26th week. (A) Body weight changes during UVB-induced carcinogenesis. (B) The average number of tumors per mouse in different groups. (C) Comparison of the cumulative

number of papillomas among tumor-bearing mice. (D) Tumors were counted according to the size, and the distribution of each size calculated at the termination of the experiment is shown. (E) Photographic images represent angiogenesis, the formation of new blood vessels, around the skin tumors. (F) Amount of hemoglobin in UVB-induced mouse skin tissues was measured by Drabkin's reagent as described in Materials and Methods. Data are expressed as means \pm SD (n=7 per group). ** $p < 0.01$; *** $p < 0.001$.

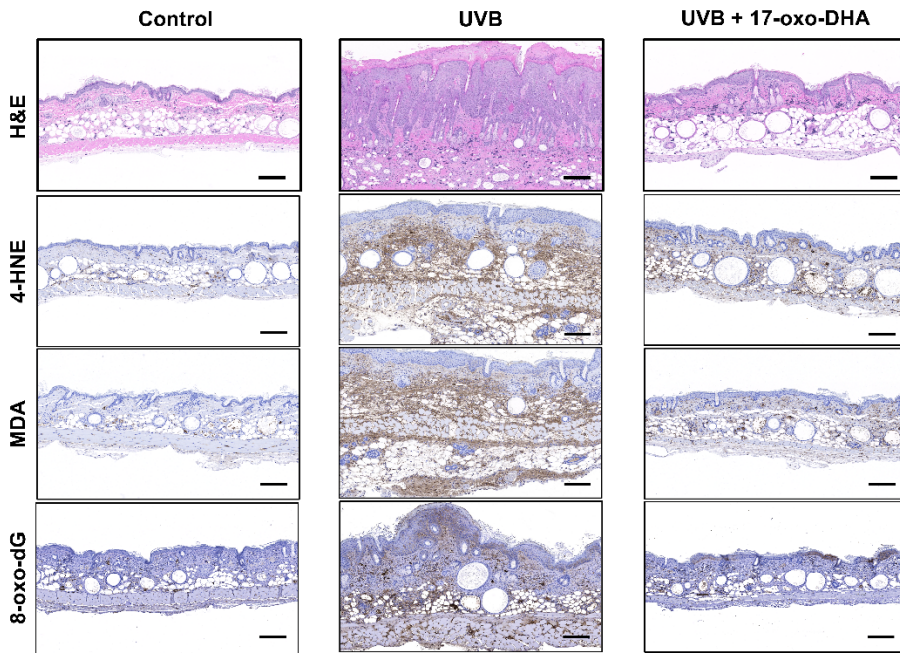
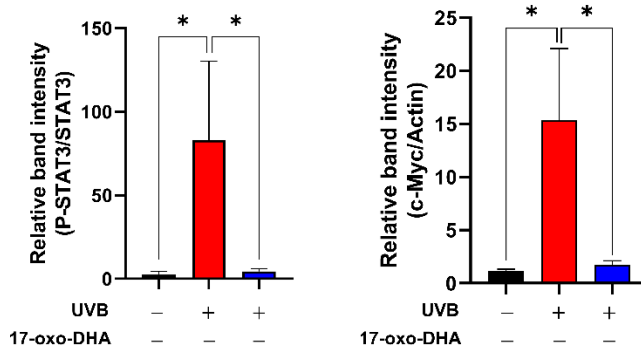
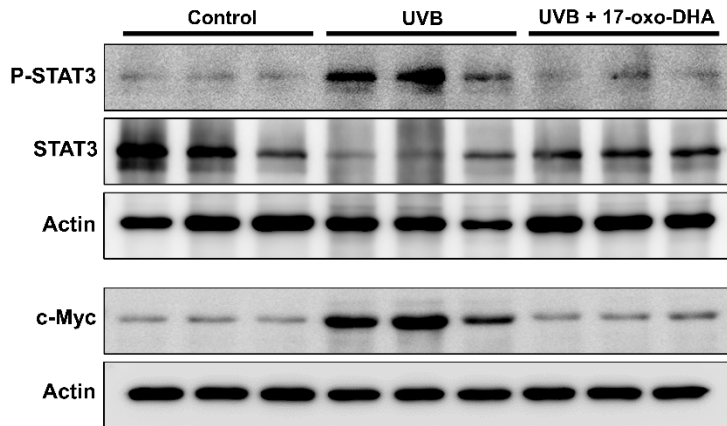
A**B**

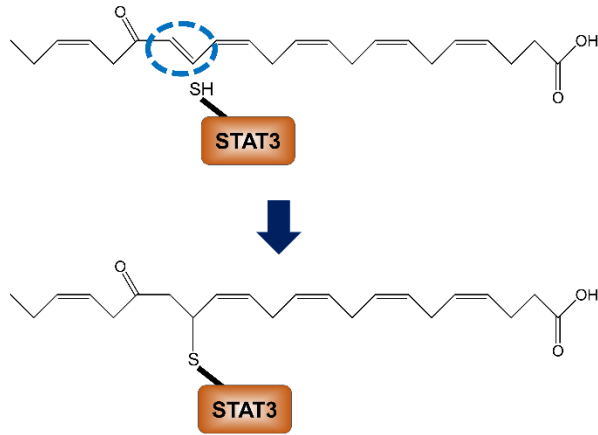
Figure 4-8. Attenuation of long-term UVB-induced oxidative skin damage in 17-oxo-DHA treated mice.

Tissues collected mice from the long-term tumor experiments were saved and subjected to histological, immunohistochemical and immune blot analyses.

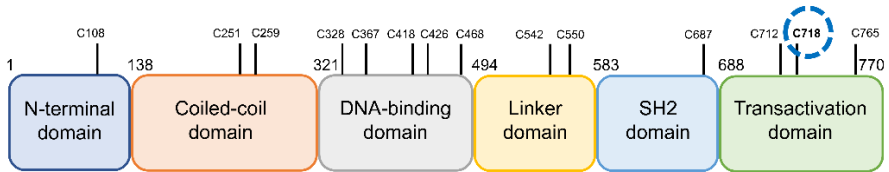
(A) Skin thickness and hyperplasia were confirmed by H&E staining.

Immunohistochemical analysis of 4-HNE, MDA, and 8-oxo-dG in mouse epidermis. (B) The phosphorylation of STAT3 and expression of its target protein, c-Myc was measured by immunoblot analysis. Data are expressed as means \pm SD (n=3 per group). * $p < 0.05$.

A

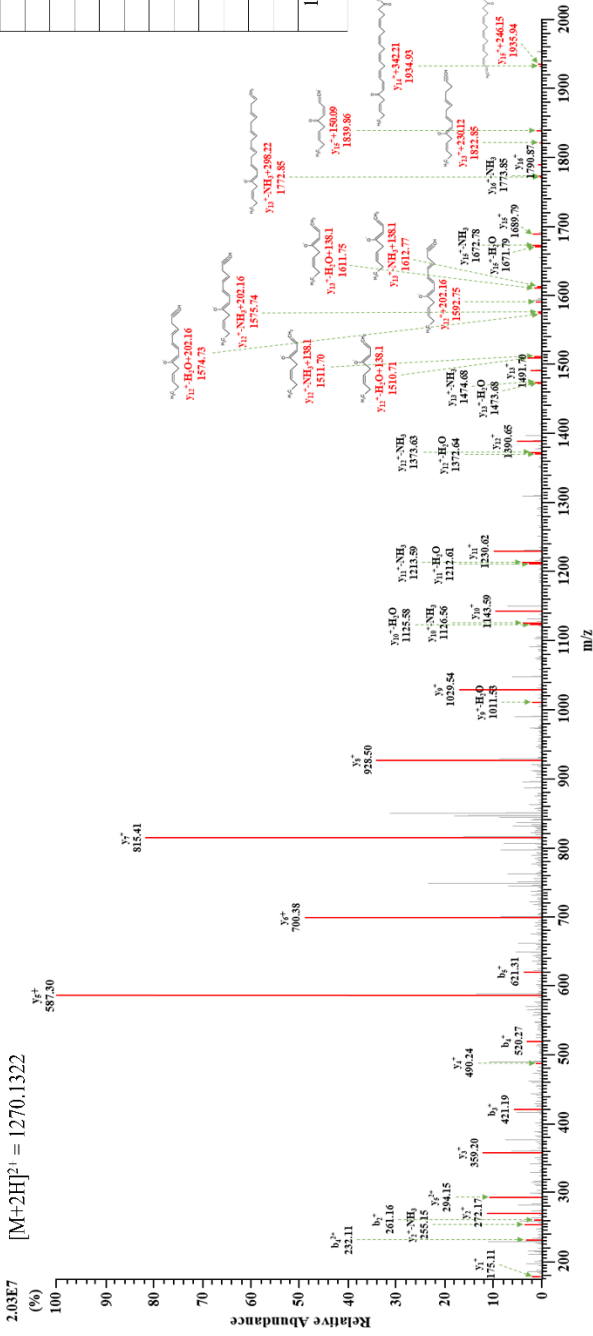


B



C **FICVTPPTCSNTIDLPLMSPR**
^{-y12}

[M+2H]²⁺ = 1270.1322



17-oxo-DHA fragment m/z	m/z
C ₇ H ₄ O ₂	60.01
C ₇ H ₂ O	112.08
C ₉ H ₄ O	138.1
C ₁₀ H ₁₄ O	150.09
C ₁₀ H ₁₆ O	152.11
C ₁₁ H ₁₆ O	164.12
C ₁₂ H ₁₈ O	178.13
C ₁₃ H ₁₈ O	190.13
C ₁₂ H ₁₈ O ₂	194.12
C ₁₄ H ₁₈ O	202.16
C ₁₃ H ₁₇ O ₂	206.12
C ₁₆ H ₂₂ O	230.12
C ₁₆ H ₂₂ O ₂	246.15
C ₂₁ H ₃₀ O	298.22
17-oxo-DHA (C ₂₃ H ₃₀ O ₃)	342.21

Figure 4-9. Mass spectrometric analysis of covalent modification of STAT3 by 17-oxo-DHA.

(A) The expected interaction between a thiol group of STAT3 and 17-oxo-DHA. (B) Schematic domain structure of STAT3, which contains six different unique functions. (C) Identified mass spectrum of STAT3 peptide (FICVTPTTCSNTIDLPMSPR) covalently modified by 17-oxo-DHA. Annotated LC-MS/MS spectrum illustrating the binding of 17-oxo-DHA to STAT3 protein at cysteine 718 residues. The precursor ion for a peptide with 17-oxo-DHA binding is $[M+2H]^{2+}$ (m/z 1270.1322). The list of elucidated 17-oxo-DHA fragmentation is inserted into the spectrum as a table. The molecular symbol labeled with y ion on the spectrum represents the fragment ion of 17-oxo-DHA bound to Cys718.

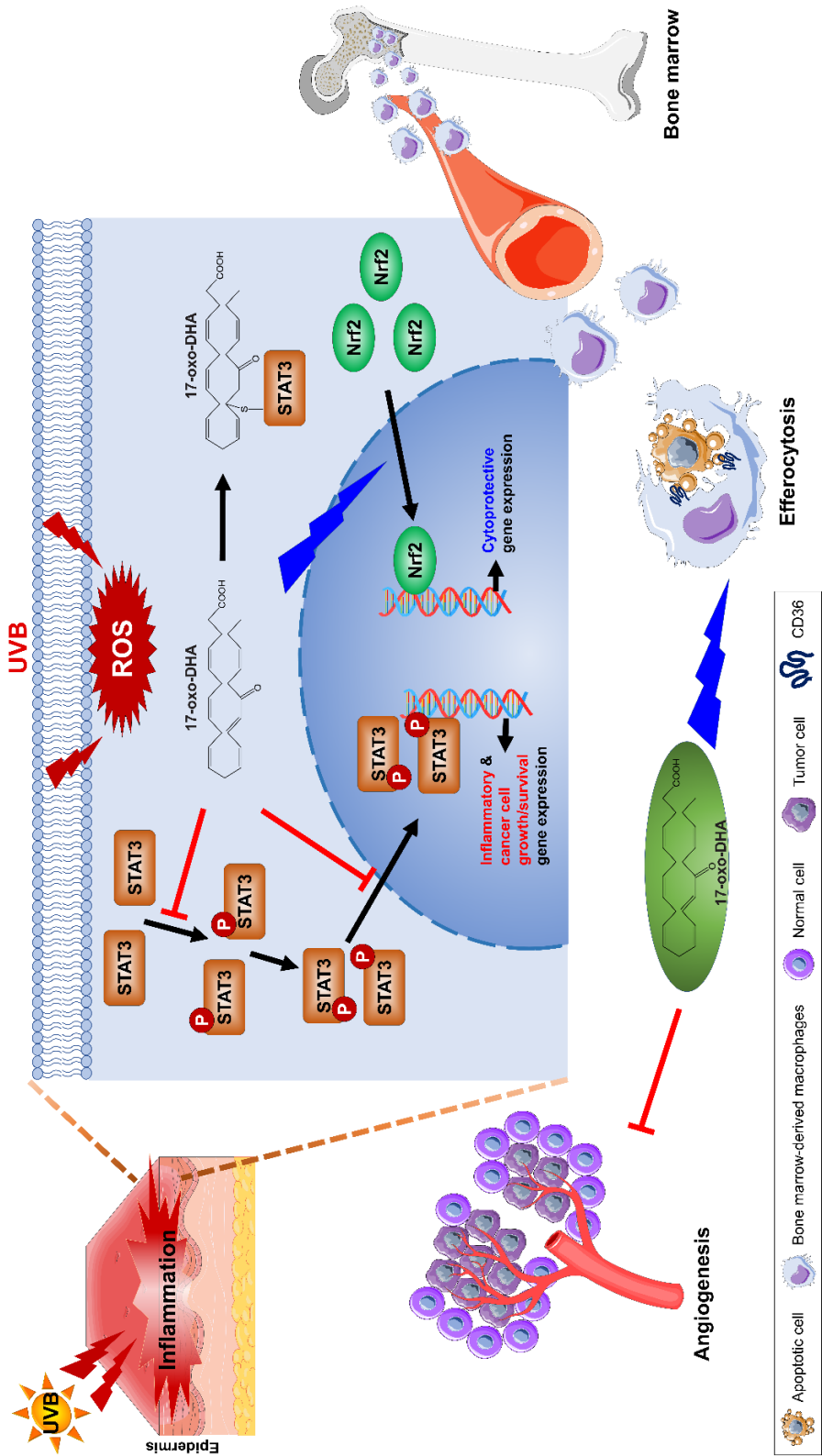
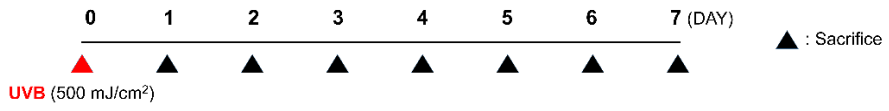
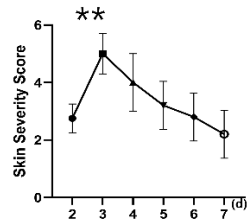
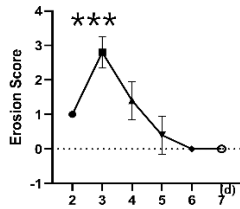
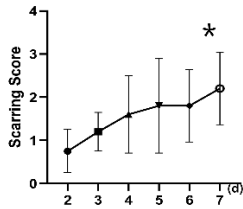


Figure 4-10. A schematic representation of the molecular mechanism underlying protective effects of 17-oxo-DHA against UVB-induced dermatitis and skin carcinogenesis.

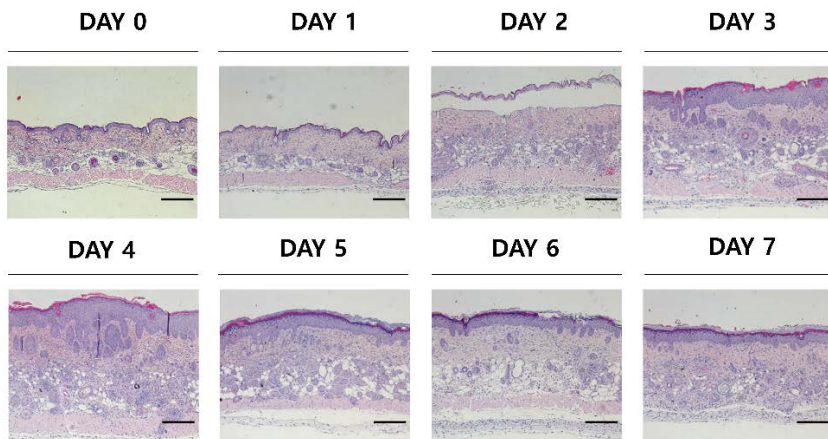
(A)



(B)

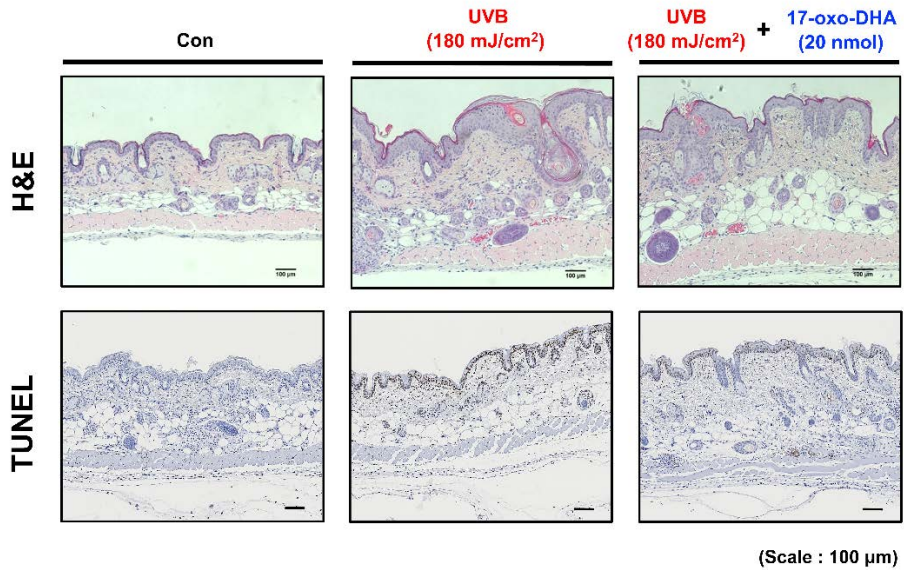


(C)



Supplementary Fig.1 The changes in inflammatory severity for 7 days after UVB irradiation.

(A) To confirm the severity change of the inflammation, mice were euthanized every day until the 7th day after UVB radiation (500 mJ/cm²). (B) The clinical skin score of mouse UVB-induced dermatitis which was evaluated by the sum of the main symptoms of inflammation. (C) Skin thickness was determined by H&E staining. Magnification $\times 100$. Scale bars correspond to 500 μm .

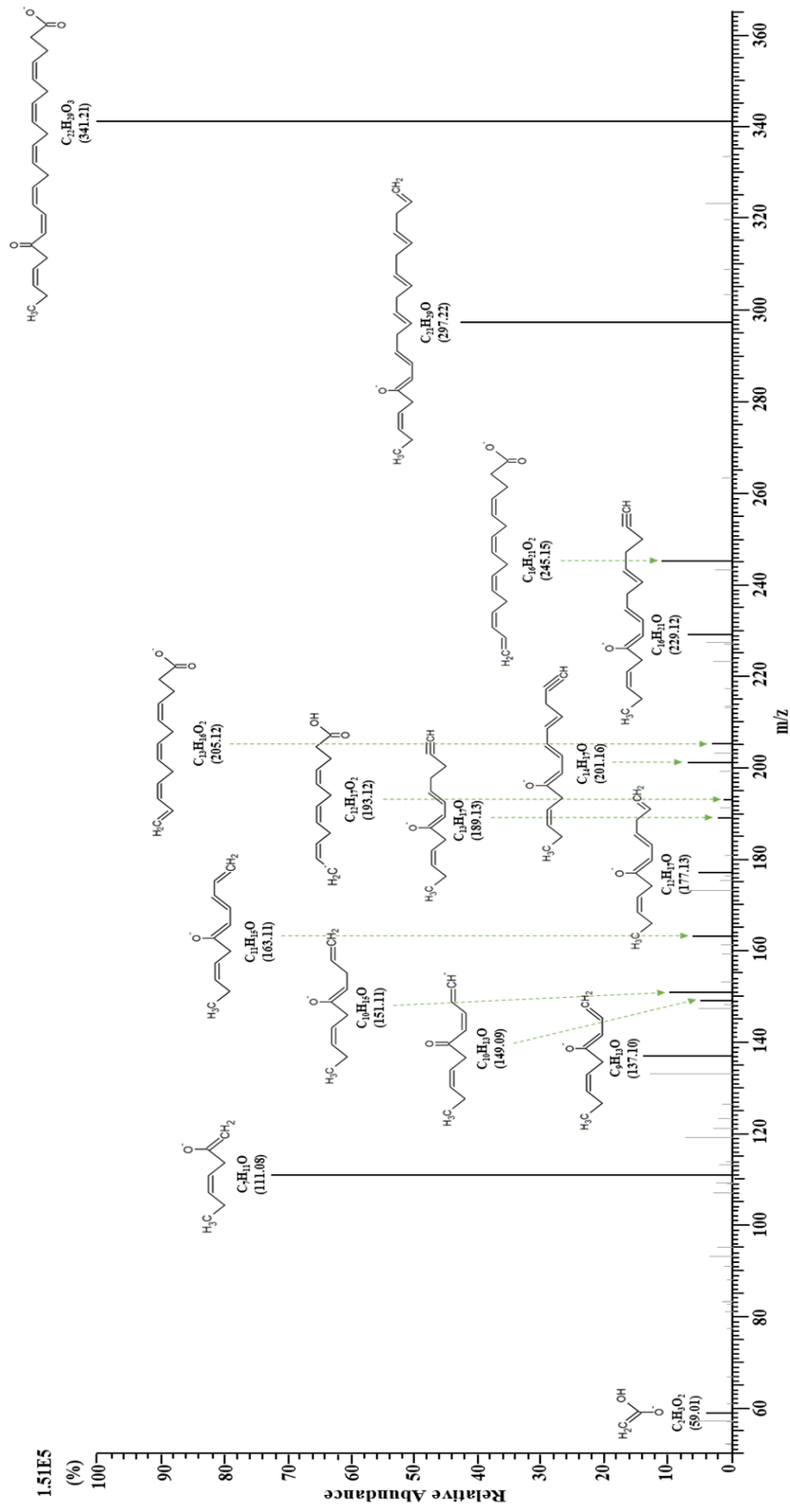


Supplementary Fig. 2. Attenuation of UVB-induced inflammation and apoptosis in mouse skin by topically applied 17-oxo-DHA.

After the UVB radiation (180 mJ/cm²), skin thickness and apoptotic cells in the skin epidermis were detected by H&E staining. The dorsal application of 17-oxo-DHA reduced the generation of TUNEL-positive apoptotic cells.

Magnification × 100. Scale bars correspond to 100 μm.

[M-H]⁻ = 341.2115



Supplementary Fig. 3. Cleavage information of 17-oxo-DHA was acquired by DIMS analysis.

MS/MS spectrum for direct infusion of 17-oxo-DHA. The fragment spectra of 17-oxo-DHA were scanned in negative ESI mode.

5. Discussion

The chemopreventive and anti-carcinogenic activities of DHA have been reported [30, 31]. In this study, we conducted a series of experiments focusing on UVB-induced dermatitis and carcinogenesis. Because the skin is composed of several layers that constitute a strong barrier to drug penetration, proper drug delivery to the skin is a major goal of pharmaceutical therapy, and penetration of topical drugs is essential for efficacy [32]. Fatty acids such as oleic acid, lauric, and capric acid have been demonstrated to enhance the penetrating effect by selectively acting on extracellular lipids constituting key regulatory channels [33]. Fish oils containing DHA can penetrate the cutaneous barrier and subsequently exert anti-inflammatory effects [34].

17-Oxo-DHA is an endogenous electrophilic derivative of DHA which is produced in activated macrophages via sequential enzymatic reactions catalyzed by COX-2 and dehydrogenase [23]. When DHA was topically applied onto mouse skin, 17-oxo-DHA as well as an intermediary metabolite 17-hydroxy-DHA was generated (S.-H. Kim & Y.-J. Surh, unpublished observation). Because of the electrophilic α,β -unsaturated carbonyl moiety, 17-oxo-DHA is anticipated to covalently bind to a sensor cysteine residue of Keap1, thereby activating Nrf2. In our previous study, 17-oxo-DHA was found to inhibit the Keap1-dependent ubiquitination of Nrf2 through modification of the Cys151 or Cys273 residues of Keap1 [35]. As a result, nuclear translocation and transcriptional activity of Nrf2 were enhanced,

followed by upregulation of HO-1 expression in murine epidermal cells.

Notably, direct topical application of 17-oxo-DHA exerted anti-inflammatory effects in UVB-irradiated mouse skin at much smaller dose than that of the parent compound, DHA [35].

Failure to resolve acute inflammation (unresolving inflammation) leads to chronic disorders, such as arthritis, asthma, psoriasis, and carcinogenesis [36-39]. The resolution of inflammation relates to the capacity of macrophages to use the substances derived from the phagolysosomal hydrolysis of apoptotic cells as the fuel of efferocytosis [40, 41]. Through this efferocytic ability, activated macrophages accelerate the resolution of inflammation, prevent cell destruction and release of toxic substances, and increase the production of anti-inflammatory cytokines, including IL-10 and TGF- β [42]. 17-Oxo-DHA suppresses the release of the proinflammatory cytokine, IL-1 β through inhibition of NLRP3 inflammasomes [25] and exerts antioxidant effects immune and structural cells [24]. Though *in vitro* studies using 17-oxo-DHA have been conducted, the anti-inflammatory response using the drug *in vivo* has not been reported yet.

Proinflammatory cytokines, chemokines and other mediators, such as IL-6 and TNF- α are involved in the inflammatory tumor microenvironment [43], and STAT3 is essential for regulating their expression [27, 44, 45]. The extrinsic inflammatory factors such as chemical carcinogens, pathogens and UVB can activate STAT3 via different pathways [46-49]. Thus, inhibition of

aberrant STAT3 activation is considered a practical therapeutic approach for achieving the prevention of carcinogenesis. Repression of STAT3 overactivation can be achieved not only through inhibition of upstream signaling pathways such as Janus kinase, epidermal growth factor receptor, and IL-6R [50], but also through direct covalent modification of specific cysteine thiol residues.

STAT3 contains 14 highly conserved cysteine residues of which nine are reported to be redox-sensitive and critical in controlling its transcriptional activity [51]. Previous studies in our laboratory demonstrated that the cysteine 259 residue of STAT3 was directly modified by the natural polyphenolic compound curcumin harbouring an α,β -unsaturated carbonyl moiety [52] or some electrophilic prostaglandin metabolites of arachidonic acid, which hampered the phosphorylation and consequently the activation of STAT3 [53, 54]. Unlike these compounds, however, 17-oxo-DHA was found to preferentially bind to the Cys718 residue of STAT3. To the best of our knowledge, this is the first demonstration of the posttranslational modification of STAT3 at this particular amino acid.

The STAT3 protein consists of 6 domains with different functions and roles [55]. Cys718 is present in the highly conserved but intrinsically disordered C-terminal transactivation domain (TAD) that is important for dimerization, nuclear translocation, and full transcriptional activity of STAT3 [56]. STAT3 activation is dependent on the Tyr705 residue, an essential site for

phosphorylation and dimerization of STAT3 [57]. We speculate that covalent modification of Cys718 by 17-oxo-DHA may induce a change in the structure of STAT3, which hinders accessibility to the upstream kinase, Janus kinase (JAK), thereby protecting the Tyr705 residue from phosphorylation. In support of this speculation, cysteine thiol modification in the TAD domain inhibited phosphorylation and nuclear localization of STAT3 without influencing the expression/activity of JAK1 and 2 [58]. Of note, Cys718 has been suggested to be involved in STAT3 dimerization and also in interaction with other proteins such peroxiredoxin-2 [59]. Further studies will be necessary to clarify the mechanisms underlying how Cys718 modification by 17-oxo-DHA can affect the STAT3 signaling.

Macrophages detect and engulf apoptotic cells through sequential mechanisms including the recognition of phosphatidylserine via scavenger receptors [60]. The association between CD36, one of the principal scavenger receptors present in macrophages, and resolution of inflammation has been continuously reported [61, 62]. In the present study, the role of Nrf2 in CD36-mediated efferocytosis was assessed by use of an Nrf2 inhibitor and Nrf2 knockout mice. BMDMs subjected to chemical inhibition and genetic deficiency of Nrf2 exacerbated efferocytic activity of macrophages, which was ascribed to repression of CD36 expression. HO-1, which is upregulated via the Nrf2 signal pathway, has been reported to potentiate the efferocytic

activity of macrophages by elevating the expression of scavenger receptors including CD36 and dectin-1 [63, 64].

In conclusion, the topical application of 17-oxo-DHA protects against UVB-induced dermatitis and carcinogenesis via suppression of the STAT3 pathway, and activation of the Nrf2/ARE signaling. Nrf2 activation promoted the resolution of skin inflammation through potentiation of efferocytic activity of macrophages phagocytosing apoptotic epidermal cells which was attributed to upregulated CD36 expression responsible for recognition and elimination of dead/dying cells. Therefore, 17-oxo-DHA can be suggested as a candidate for the chemoprotection/chemoprevention of UV-induced dermatitis and photocarcinogenesis.

6. References

- [1] C. Blanpain, E. Fuchs, Epidermal homeostasis: a balancing act of stem cells in the skin, *Nat Rev Mol Cell Biol* 10(3) (2009) 207-17.
- [2] E. Fuchs, Finding one's niche in the skin, *Cell Stem Cell* 4(6) (2009) 499-502.
- [3] K. Honda, D.R. Littman, The microbiota in adaptive immune homeostasis and disease, *Nature* 535(7610) (2016) 75-84.
- [4] M. Pasparakis, Regulation of tissue homeostasis by NF- κ B signalling: implications for inflammatory diseases, *Nat Rev Immunol* 9(11) (2009) 778-88.
- [5] V. Horsley, Skin in the game: stem cells in repair, cancer, and homeostasis, *Cell* 181(3) (2020) 492-494.
- [6] G.T. Bowden, Prevention of non-melanoma skin cancer by targeting ultraviolet-B-light signalling, *Nat Rev Cancer* 4(1) (2004) 23-35.
- [7] D.S. Rigel, Cutaneous ultraviolet exposure and its relationship to the development of skin cancer, *J Am Acad Dermatol* 58(5 Suppl 2) (2008) S129-32.
- [8] M. Pasparakis, I. Haase, F.O. Nestle, Mechanisms regulating skin immunity and inflammation, *Nat Rev Immunol* 14(5) (2014) 289-301.
- [9] A. Mantovani, M.A. Cassatella, C. Costantini, S. Jaillon, Neutrophils in the activation and regulation of innate and adaptive immunity, *Nat Rev Immunol* 11(8) (2011) 519-31.

- [10] G. Majno, I. Joris, *Cells, tissues, and disease: principles of general pathology*, 2nd ed., Oxford University Press, New York, 2004.
- [11] L.M. Coussens, Z. Werb, Inflammation and cancer, *Nature* 420(6917) (2002) 860-7.
- [12] M.R. Elliott, K.M. Koster, P.S. Murphy, Efferocytosis signaling in the regulation of macrophage inflammatory responses, *J Immunol* 198(4) (2017) 1387-1394.
- [13] E. Boada-Romero, J. Martinez, B.L. Heckmann, D.R. Green, The clearance of dead cells by efferocytosis, *Nat Rev Mol Cell Biol* 21(7) (2020) 398-414.
- [14] A.C. Doran, A. Yurdagul, Jr., I. Tabas, Efferocytosis in health and disease, *Nat Rev Immunol* 20(4) (2020) 254-267.
- [15] J.D. Hayes, A.T. Dinkova-Kostova, The Nrf2 regulatory network provides an interface between redox and intermediary metabolism, *Trends Biochem Sci* 39(4) (2014) 199-218.
- [16] M.B. Sporn, K.T. Libby, NRF2 and cancer: the good, the bad and the importance of context, *Nat Rev Cancer* 12(8) (2012) 564-71.
- [17] T. Bowman, M.A. Broome, D. Sinibaldi, W. Wharton, W.J. Pledger, J.M. Sedivy, R. Irby, T. Yeatman, S.A. Courtneidge, R. Jove, Stat3-mediated Myc expression is required for Src transformation and PDGF-induced mitogenesis, *Proc Natl Acad Sci USA* 98(13) (2001) 7319-24.

- [18] H. Yu, H. Lee, A. Herrmann, R. Buettner, R. Jove, Revisiting STAT3 signalling in cancer: new and unexpected biological functions, *Nat Rev Cancer* 14(11) (2014) 736-46.
- [19] C.N. Serhan, Pro-resolving lipid mediators are leads for resolution physiology, *Nature* 510(7503) (2014) 92-101.
- [20] M.C. Basil, B.D. Levy, Specialized pro-resolving mediators: endogenous regulators of infection and inflammation, *Nat Rev Immunol* 16(1) (2016) 51-67.
- [21] I. Tabas, C.K. Glass, Anti-inflammatory therapy in chronic disease: challenges and opportunities, *Science* 339(6116) (2013) 166-72.
- [22] H.W. Yum, J. Park, H.J. Park, J.W. Shin, Y.Y. Cho, S.J. Kim, J.X. Kang, Y.J. Surh, Endogenous omega-3 Fatty Acid Production by fat-1 Transgene and Topically applied docosahexaenoic acid protect against UVB-induced mouse skin carcinogenesis, *Sci Rep* 7(1) (2017) 11658.
- [23] A.L. Groeger, C. Cipollina, M.P. Cole, S.R. Woodcock, G. Bonacci, T.K. Rudolph, V. Rudolph, B.A. Freeman, F.J. Schopfer, Cyclooxygenase-2 generates anti-inflammatory mediators from omega-3 fatty acids, *Nat Chem Biol* 6(6) (2010) 433-41.
- [24] C. Cipollina, S. Di Vincenzo, S. Gerbino, L. Siena, M. Gjomarkaj, E. Pace, Dual anti-oxidant and anti-inflammatory actions of the electrophilic cyclooxygenase-2-derived 17-oxo-DHA in lipopolysaccharide- and cigarette

smoke-induced inflammation, *Biochim Biophys Acta* 1840(7) (2014) 2299-309.

[25] C. Cipollina, S. Di Vincenzo, L. Siena, C. Di Sano, M. Gjomarkaj, E. Pace, 17-oxo-DHA displays additive anti-inflammatory effects with fluticasone propionate and inhibits the NLRP3 inflammasome, *Sci Rep* 6 (2016) 37625.

[26] L. Siena, C. Cipollina, S. Di Vincenzo, M. Ferraro, A. Bruno, M. Gjomarkaj, E. Pace, Electrophilic derivatives of omega-3 fatty acids counteract lung cancer cell growth, *Cancer Chemother Pharmacol* 81(4) (2018) 705-716.

[27] H. Yu, D. Pardoll, R. Jove, STATs in cancer inflammation and immunity: a leading role for STAT3, *Nat Rev Cancer* 9(11) (2009) 798-809.

[28] C.L. Oeste, D. Perez-Sala, Modification of cysteine residues by cyclopentenone prostaglandins: interplay with redox regulation of protein function, *Mass Spectrom Rev* 33(2) (2014) 110-25.

[29] C.E. Paulsen, K.S. Carroll, Cysteine-mediated redox signaling: chemistry, biology, and tools for discovery, *Chem Rev* 113(7) (2013) 4633-79.

[30] L.A. Horrocks, Y.K. Yeo, Health benefits of docosahexaenoic acid (DHA), *Pharmacol Res* 40(3) (1999) 211-25.

[31] H.W. Yum, H.K. Na, Y.J. Surh, Anti-inflammatory effects of docosahexaenoic acid: Implications for its cancer chemopreventive potential, *Semin Cancer Biol* 40-41 (2016) 141-159.

- [32] M.E. Lane, Skin penetration enhancers, *Int J Pharm* 447(1-2) (2013) 12-21.
- [33] V.H. Mak, R.O. Potts, R.H. Guy, Percutaneous penetration enhancement in vivo measured by attenuated total reflectance infrared spectroscopy, *Pharm Res* 7(8) (1990) 835-41.
- [34] F.Q. Ames, F. Sato, L.V. de Castro, L.L.M. de Arruda, B.A. da Rocha, R.K.N. Cuman, M.L. Baesso, C.A. Bersani-Amado, Evidence of anti-inflammatory effect and percutaneous penetration of a topically applied fish oil preparation: a photoacoustic spectroscopy study, *J Biomed Opt* 22(5) (2017) 55003.
- [35] M.U. Jamil, J. Kim, H.W. Yum, S.H. Kim, S.J. Kim, D.H. Kim, N.C. Cho, H.K. Na, Y.J. Surh, 17-Oxo-docosahexaenoic acid induces Nrf2-mediated expression of heme oxygenase-1 in mouse skin in vivo and in cultured murine epidermal cells, *Arch Biochem Biophys* 679 (2020) 108156.
- [36] C.D. Buckley, D.W. Gilroy, C.N. Serhan, B. Stockinger, P.P. Tak, The resolution of inflammation, *Nat Rev Immunol* 13(1) (2013) 59-66.
- [37] G. Schett, D. Elewaut, I.B. McInnes, J.M. Dayer, M.F. Neurath, How cytokine networks fuel inflammation: Toward a cytokine-based disease taxonomy, *Nat Med* 19(7) (2013) 822-4.
- [38] I.B. McInnes, G. Schett, Pathogenetic insights from the treatment of rheumatoid arthritis, *Lancet* 389(10086) (2017) 2328-2337.

- [39] C. Nathan, A. Ding, Nonresolving inflammation, *Cell* 140(6) (2010) 871-82.
- [40] A. Hochreiter-Hufford, K.S. Ravichandran, Clearing the dead: apoptotic cell sensing, recognition, engulfment, and digestion, *Cold Spring Harb Perspect Biol* 5(1) (2013) a008748.
- [41] D.R. Green, T.H. Oguin, J. Martinez, The clearance of dying cells: table for two, *Cell Death Differ* 23(6) (2016) 915-26.
- [42] D. Korn, S.C. Frasch, R. Fernandez-Boyanapalli, P.M. Henson, D.L. Bratton, Modulation of macrophage efferocytosis in inflammation, *Front Immunol* 2 (2011) 57.
- [43] H. Yu, M. Kortylewski, D. Pardoll, Crosstalk between cancer and immune cells: role of STAT3 in the tumour microenvironment, *Nat Rev Immunol* 7(1) (2007) 41-51.
- [44] P.C. Heinrich, I. Behrmann, S. Haan, H.M. Hermanns, G. Muller-Newen, F. Schaper, Principles of interleukin (IL)-6-type cytokine signalling and its regulation, *Biochem J* 374(Pt 1) (2003) 1-20.
- [45] Z. Zhong, Z. Wen, J.E. Darnell, Jr., Stat3: a STAT family member activated by tyrosine phosphorylation in response to epidermal growth factor and interleukin-6, *Science* 264(5155) (1994) 95-8.
- [46] M. Gu, R.P. Singh, S. Dhanalakshmi, C. Agarwal, R. Agarwal, Silibinin inhibits inflammatory and angiogenic attributes in photocarcinogenesis in SKH-1 hairless mice, *Cancer Res* 67(7) (2007) 3483-91.

- [47] C.N. Landen, Jr., Y.G. Lin, G.N. Armaiz Pena, P.D. Das, J.M. Arevalo, A.A. Kamat, L.Y. Han, N.B. Jennings, W.A. Spannuth, P.H. Thaker, S.K. Lutgendorf, C.A. Savary, A.M. Sanguino, G. Lopez-Berestein, S.W. Cole, A.K. Sood, Neuroendocrine modulation of signal transducer and activator of transcription-3 in ovarian cancer, *Cancer Res* 67(21) (2007) 10389-96.
- [48] J. Arredondo, A.I. Chernyavsky, D.L. Jolkovsky, K.E. Pinkerton, S.A. Grando, Receptor-mediated tobacco toxicity: cooperation of the Ras/Raf-1/MEK1/ERK and JAK-2/STAT-3 pathways downstream of alpha7 nicotinic receptor in oral keratinocytes, *FASEB J* 20(12) (2006) 2093-101.
- [49] D.M. Bronte-Tinkew, M. Terebiznik, A. Franco, M. Ang, D. Ahn, H. Mimuro, C. Sasakawa, M.J. Ropeleski, R.M. Peek, Jr., N.L. Jones, *Helicobacter pylori* cytotoxin-associated gene A activates the signal transducer and activator of transcription 3 pathway in vitro and in vivo, *Cancer Res* 69(2) (2009) 632-9.
- [50] D.E. Johnson, R.A. O'Keefe, J.R. Grandis, Targeting the IL-6/JAK/STAT3 signalling axis in cancer, *Nat Rev Clin Oncol* 15(4) (2018) 234-248.
- [51] F.A. Zouein, R. Altara, Q. Chen, E.J. Lesnfsky, M. Kurdi, G.W. Booz, Pivotal Importance of STAT3 in protecting the heart from acute and chronic stress: new advancement and unresolved issues, *Front Cardiovasc Med* 2 (2015) 36.

- [52] Y.I. Hahn, S.J. Kim, B.Y. Choi, K.C. Cho, R. Bandu, K.P. Kim, D.H. Kim, W. Kim, J.S. Park, B.W. Han, J. Lee, H.K. Na, Y.N. Cha, Y.J. Surh, Curcumin interacts directly with the Cysteine 259 residue of STAT3 and induces apoptosis in H-Ras transformed human mammary epithelial cells, *Sci Rep* 8(1) (2018) 6409.
- [53] S.J. Kim, N.C. Cho, B. Han, K. Kim, Y.I. Hahn, K.P. Kim, Y.G. Suh, B.Y. Choi, H.K. Na, Y.J. Surh, 15-Deoxy-D^{12,14}-prostaglandin J₂ binds and inactivates STAT3 via covalent modification of cysteine 259 in H-Ras-transformed human breast epithelial cells, *FEBS Lett* 595(5) (2021) 604-622.
- [54] E.J. Lee, S.J. Kim, Y.I. Hahn, H.J. Yoon, B. Han, K. Kim, S. Lee, K.P. Kim, Y.G. Suh, H.K. Na, Y.J. Surh, 15-Keto prostaglandin E₂ suppresses STAT3 signaling and inhibits breast cancer cell growth and progression, *Redox Biol* 23 (2019) 101175.
- [55] S. Zou, Q. Tong, B. Liu, W. Huang, Y. Tian, X. Fu, Targeting STAT3 in cancer immunotherapy, *Mol Cancer* 19(1) (2020) 145.
- [56] J. Sgrignani, M. Garofalo, M. Matkovic, J. Merulla, C.V. Catapano, A. Cavalli, Structural biology of STAT3 and its implications for anticancer therapies development, *Int J Mol Sci* 19(6) (2018).
- [57] D.E. Levy, C.K. Lee, What does Stat3 do?, *J Clin Invest* 109(9) (2002) 1143-8.

- [58] X. Yu, L. He, P. Cao, Q. Yu, Eriocalyxin B Inhibits STAT3 signaling by covalently targeting STAT3 and blocking phosphorylation and activation of STAT3, *PLoS One* 10(5) (2015) e0128406.
- [59] M.C. Sobotta, W. Liou, S. Stocker, D. Talwar, M. Oehler, T. Ruppert, A.N. Scharf, T.P. Dick, Peroxiredoxin-2 and STAT3 form a redox relay for H₂O₂ signaling, *Nat Chem Biol* 11(1) (2015) 64-70.
- [60] G. Lemke, How macrophages deal with death, *Nat Rev Immunol* 19(9) (2019) 539-549.
- [61] M.S. Woo, J. Yang, C. Beltran, S. Cho, Cell surface CD36 protein in monocyte/macrophage contributes to phagocytosis during the resolution phase of ischemic stroke in mice, *J Biol Chem* 291(45) (2016) 23654-23661.
- [62] Y.M. Park, CD36, a scavenger receptor implicated in atherosclerosis, *Exp Mol Med* 46 (2014) e99.
- [63] S.H. Kim, X. Zhong, W. Kim, K. Kim, Y.G. Suh, C. Kim, Y. Joe, H.T. Chung, Y.N. Cha, Y.J. Surh, Taurine chloramine potentiates phagocytic activity of peritoneal macrophages through up-regulation of dectin-1 mediated by heme oxygenase-1-derived carbon monoxide, *FASEB J* 32(4) (2018) 2246-2257.
- [64] T. Ishii, K. Itoh, E. Ruiz, D.S. Leake, H. Unoki, M. Yamamoto, G.E. Mann, Role of Nrf2 in the regulation of CD36 and stress protein expression in murine macrophages: activation by oxidatively modified LDL and 4-hydroxynonenal, *Circ Res* 94(5) (2004) 609-16.

CONCLUSION

If the resolution of inflammation is not well achieved, it can cause chronic inflammation and metabolic syndrome, and if this state persists, there is a possibility of developing cancer. Before chronic inflammation occurs, appropriate and timely resolution of acute inflammation is required. Recent studies have unraveled the metabolome of endogenous molecules directly involved in the proresolving response. In addition, recent studies have focused not only on the inhibition of inflammation, but also on the resolution of inflammation. In this regard, evaluating the anti-inflammatory/proresolving effects of endogenous molecules and their potential ability to accelerate phagocytic capacity of macrophages, is worthwhile. In this thesis, I investigated the proresolving/anti-inflammatory as well as antioxidant effects of taurine chloramine and 17-oxo-DHA in the context of their chemopreventive potential against inflammation-associated cancer.

국 문 초 록

Taurine chloramine (TauCl)은 육류, 생선, 계란 및 우유를 포함한 일부 식품에서 발견되는, 준필수 황 함유 β -아미노산인 Taurine 에서 대사된 내인성 항염증 물질이다. 일반적으로 TauCl 과 Taurine 은 다양한 유형의 세포에서 조직 손상에 의해 유발되는 염증 매개체의 생성을 감소시킨다. 본 논문연구에서 실험적으로 유도된 대장염에 대한 TauCl 의 보호 효과를 확인하였다. 2,4,6-Trinitrobenzene sulfonic acid (TNBS)에 의해 유도된 대장염증은 TauCl 의 경구 투여에 의해 경감되었다. 또한 TauCl 의 투여는 TNBS 로 유도된 마우스의 대장 점막에서 세포자멸사를 감소시켰다. 이는 necrosis factor- α , interleukin-6 와 cyclooxygenase-2 (COX-2)를 포함하는 염증성 인자와 4-hydroxy-2-nonenal (4-HNE)을 포함하는 산화적 스트레스 인자의 억제를 통해 확인되었다. TauCl 은 또한 염증 신호전달을 매개하는 두 가지 주요 전사 인자인 nuclear factor kappa light chain enhancer of activated B cells (NF κ B) 및 signal transducer and activator of transcription 3 (STAT3)의 활성화를 억제하였다. 특히, TNBS 로 유도된 마우스의 대장에서 산화적 스트레스 및 염증에 대한 TauCl 의 보호 효과는 nuclear factor erythroid 2-related factor 2 (Nrf2)의 높은 활성화 및 heme

oxygenase-1 (HO-1), NAD(P)H:quinone oxidoreductase (NQO1)과 같은 표적 유전자의 발현 량 증가와 관련이 있음을 관찰할 수 있었다. 이러한 결과는 TauCl 이 Nrf2 에 의해 유도되는 항산화 유전자 발현의 상향조절을 통해 대장염에 대한 보호효과를 보임과 동시에, NF κ B 와 STAT3 에 의해 매개되는 염증성 신호를 억제함을 나타낸다.

태양광, 특히 자외선에 대한 과도한 노출은 광노화를 일으키며 피부염 및 피부암 발생의 주요 원인이다. 본 연구는 광손상으로부터 피부를 효과적으로 보호할 수 있는 후보 물질을 찾기 위해 염증 조직으로 집중된 대식세포의 Taurine 으로부터 생성되는 TauCl 을 사용하여 수행되었다. 180 mJ/cm² 강도의 Ultraviolet B (UVB) 조사는 마우스 표피에서 산화적 손상과 세포 사멸을 유발하였다. TUNEL-양성 표피 세포의 감소 및 세포사멸 억제 단백질인 Bcl-xL 의 발현량 증가, cleaved caspase-3 의 감소 및 4-HNE 의 억제에 의해 입증된 바와 같이 이러한 피부염증은 국소 도포 처리된 TauCl 에 의해 경감됨을 확인하였다. 또한 두 가지 주요 염증 효소인 COX-2 와 inducible nitric oxide synthase (iNOS) 의 발현은 TauCl 처리된 마우스에서 유의하게 낮음을 확인하였고, 염증성 사이토카인 (Tnf, Il6, Il1b, Il10) 의 전사 또한 유사한 경향성을 나타내는 것을 확인하였다. 또한 TauCl 의 항염증 효과는 STAT3 의 활성화 억제 및 Nrf2 의 활성화를 통한 HO-1, NQO1 과 같은 항산화 효소의 유도 와도 관련 있음을 확인하였다.

이러한 연구 결과들을 통해 대장염 및 피부염에 대한 TauCl의 화학적 암예방효과는 염증을 매개하는 표적 단백질들의 활성화를 경감시킴과 동시에 활성산소종의 제거와 관련된 항산화 단백질들의 증가된 발현을 통해 매개된다고 할 수 있다.

급성 염증은 조직 복구와 항상성 회복을 위한 자기 한정적 과정이다. 급성 염증이 적절하게 해소되지 않으면 염증 반응이 지속되어 천식, 관절염, 동맥경화증, 심지어 암 과도 같은 여러 만성 질환을 유발할 수 있다. 세포자연사는 조직의 염증 해소 단계에서 관찰되는 세포예정사의 가장 중요한 과정이다. 죽거나 죽어가는 세포의 축적은 지속적인 염증 반응을 일으키거나 악화시키기 때문에 세포 사멸 세포의 제거는 염증 조절에 필수적인 역할을 한다. 포식작용은 대식세포의 식세포 작용에 의해 죽거나 죽어가는 세포가 제거되는 과정이다. CD36을 포함한 다양한 식세포 수용체는 식균 작용을 하는 것으로 여겨지는 세포를 인식함으로써 이 과정에 관여한다. 포식작용은 염증을 해소에 기여함으로써 2차 피사, 염증의 심화, 그리고 만성 염증을 예방하는데 필수적인 역할을 한다.

외부 및 내부 염증 자극에 반응하여 항상성을 유지하는 가장 중요한 관문이자 기관으로서 피부의 중요성은 아무리 강조해도 지나치지 않는다. 표피에서 급성 염증의 해소가 제대로 이루어지지 않으면 염증의 중증도를 악화시킬 수 있다. Docosahexaenoic acid (DHA)는 오메가 3 불포화지방산 중 하나로, 대사과정을 거쳐

생물학적으로 활성화된 친전자성 대사체를 생성한다. 그 대사체중 하나인, 17-oxo-DHA 는 활성화된 대식세포에서 COX-2 와 탈수소효소에 의해 DHA 로부터 생성된다. STAT3 는 UVB 로 유도된 피부염증 및 피부암 발생에서 중요한 역할을 한다. STAT3 의 활성화에 필수적인 Tyr705 의 인산화는 17-oxo-DHA 로 처리된 무모 마우스에서 유의하게 감소하였다. 또한 UVB 조사로 인해 유도된 세포 사멸의 발생은 17-oxo-DHA 의 국소 도포로 인해 경감되었으며 이는 TUNEL-양성 세포의 비율 감소로 입증하였다. 17-oxo-DHA 의 처리는 또한 산화적 스트레스의 지표 단백질 발현을 감소시켰고, Nrf2 의 발현과 관련 항염증 및 항산화 단백질 발현을 증가시켜 염증성 사이토카인 생성을 약화시키고, 염증의 해소를 가속화하였다. 포식작용은 대식세포의 식균활동에 의해 수행되는 염증의 해소에 중추적인 역할을 한다. 이 실험에서 17-oxo-DHA 에 의한 골수 유래 대식세포의 포식작용 능력의 변화를 관찰하였고, 그 결과 17-oxo-DHA 의 처리에 의해 골수 유래 대식세포의 포식작용이 증가함을 확인하였다. 또한 이 결과는 스캐빈저 수용체인 CD36 및 Nrf2 의 발현량의 증가와 관련 있음을 Nrf2 knockout 마우스들을 통해 확인할 수 있었다. 결론적으로, 17-oxo-DHA 의 도포는 산화적 스트레스를 억제하고 대식세포의 포식작용 능력을 강화하여 염증의 해소 단계를 활성화시켜 UVB 에 의해 유도된 피부염 및 피부암으로부터 보호효과를 나타내었고, 이러한 효과는 Nrf2 의 활성화와 그에 따른 항산화 단백질 발현의

증가를 통해 확인되었다. 따라서 17-oxo-DHA 는 UVB 로 인한 피부 손상을 해결할 수 있는 치료제로서의 가능성이 있음을 시사한다.

주요어 (Keywords): Taurine Chloramine (TauCl); 17-oxo-docosahexaenoic acid (17-oxo-DHA); Nuclear factor erythroid 2-related factor 2 (Nrf2); Signal transducer and activator of transcription 3 (STAT3); Efferocytosis 포식작용

학번 (Student Number): 2016-21798